Regional atmospheric feedbacks over land and coastal areas

Herbert ter Maat

Regional atmospheric feedbacks over land and coastal areas

Hendrikus Wicher ter Maat

Thesis committee

Promotors
Prof. Dr A.A.M. Holtslag
Professor of Meteorology
Wageningen University

Prof. Dr P. Kabat
Director General and Chief Executive Officer at the International
Institute for Applied Systems Analysis, Laxenburg, Austria
Professor of Earth System Science
Wageningen University

Co-promotor
Dr R.W.A. Hutjes
Associate professor, Earth System Science Group
Wageningen University
Senior scientist, Climate Change and Adaptive land and Water
Management
Alterra, Wageningen UR

Other members
Prof. Dr B.J.J.M. van den Hurk, Utrecht University
Prof. Dr D. Jacob, University of Bergen, Norway
Prof. Dr R.A. Pielke Sr., Colorado State University, Boulder, United
States of America
Prof. Dr R. Uijlenhoet, Wageningen University

This research was conducted under the auspices of the Graduate School
WIMEK/SENSE

Regional atmospheric feedbacks over land and coastal areas

Hendrikus Wicher ter Maat

Regional atmospheric feedbacks over land and coastal areas

It used to rain
Dreary and grey
Most every day but not any more
We come out of our homes
We lie down
Under the cloud that never comes

We roll in the radiation
And we make love
Under the sun

The polar ice is melting
'Suits me fine
We go to the beach
On the Northern Line

We watch the sea
Comin' up the street
Under the sun

(Under the sun – Marillion)

Table of Contents

Regional atmospheric feedbacks over land and coastal areas

Chapter 1

General Introduction

This thesis deals with the impact of feedbacks between the earth surface (both at land and sea) and the atmosphere. Especially, the feedbacks between the surface and the local-to-regional state of the atmosphere are studied and their importance assessed. In this context a region is defined as an area of 300-500 km^2. Feedbacks between land cover and climate have been documented on a general level (Zhao et al. (2001), Pielke et al. (2007), Pielke et al. (2011), Mahmood et al. (2013)), but also focusing on different meteorological areas in the world, like semiarid environments (De Ridder et al. (1998)), tropical environments (Sampaio et al. (2007)) and temperate climates (Teuling et al. (2010), Nair et al. (2011)).

Each surface type has its own way of interacting with the atmosphere through the partitioning of available energy at the surface. The primary energy reaching the surface comes from solar radiation and from atmospheric radiation. At the surface solar radiation is partly reflected (albedo effect) and the surface also emits (longwave) radiation. The net available radiation energy at the surface is partitioned in various fluxes. The energy is partly used for evaporation (latent heat flux), for heating up the atmosphere (sensible heat flux) and for heating land (soil heat flux) or sea (storage). This partitioning depends on land use on vegetation and soil properties. Surfaces with a high albedo (e.g. concrete, snow) will reflect more solar radiation back into the atmosphere and surfaces with higher surface temperatures will emit more longwave radiation to the atmosphere. This will leave less energy at the surface than in cases with surfaces of low reflectivity and lower surface temperatures.

The sensible heat flux warms up the atmosphere from below, just as the latent heat flux will increase the amount of vapor in the atmosphere. The influence of the earth surface on the atmosphere is most apparent in the lowest 1-1.5 kilometer of the atmosphere in the, so called planetary boundary layer (PBL). The surface has a direct effect on the atmosphere through changes in temperature, vapor, boundary layer height, atmospheric circulations, cloud processes and precipitation (Figure 1.1). Changes in atmospheric circulation depend on variation in contrast between the various earth surface types. More heterogeneity leads typically to more contrasts and this leads to more changes in atmospheric circulation.
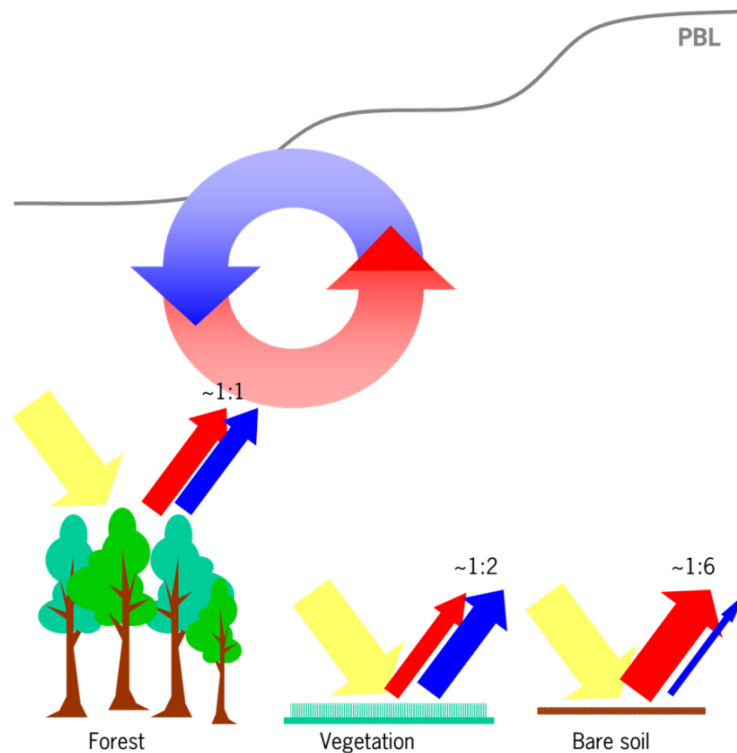
Figure 1.1: Graphical representation of the influence that land surface has on the dynamics of the atmosphere. Yellow arrows represent the incoming net radiation, red arrows: sensible heat flux, blue arrows: latent heat flux for 3 land surface types as indicated. The numbers near the arrows reflect the ratio between the sensible and latent heat fluxes.

1.1 Regional feedbacks

In a homogeneous environment it is expected that the atmospheric-earth surface interactions have a smaller impact on the regional climate than in a heterogeneous environment. The regional climate is, in a homogeneous setting, mostly determined by synoptically meteorological conditions. In a heterogeneous environment the surface plays its role in influencing the regional climate. The conditions which account for heterogeneity are for example topography, land cover, soil type, degree of urbanization. The effect that heterogeneity has on the atmosphere has been described by Wu et al. (2009).

Another important feedback between the surface and the atmosphere, which will be addressed in this thesis, deals with the exchange of chemical constituents. This thesis will focus on CO_2, which act as a non-reactive scalar. The importance that biospheric uptake and fossil fuel

emissions have on the amplitude and magnitude of diurnal and seasonal cyles of CO_2 concentration has been shown by Bakwin et al. (1995). The dispersion of CO_2 throughout the atmosphere is not only dependent on the processes at the surface but also on mixing in atmosphere through turbulent processes (de Arellano et al. (2004)). The role that the ocean plays in the carbon cycle is not part of this thesis because this role has a different timeframe than the diurnal variation that are witnessed near the land surface.

The sea-atmosphere interactions differ from land-atmosphere interactions due to the homogeneous setting of the sea and the heat capacity which is much greater than that of land. The feedbacks between the sea surface and the atmosphere are described by Sutton et al. (2005) who related the devastating summer heat wave of 2003 in main parts of Europe to basin-scale changes in the Atlantic Ocean. Other documented impacts of sea surface temperature (SST) on precipitation, which act on a smaller scale come, from studies in the Mediterranean Sea, Baltic Sea and North Sea (Lebeaupin et al. (2006), Kjellstrom et al. (2007), Lenderink et al. (2009)). These studies focus on a timescale which is still relatively large compared to the timescales in this thesis.

One of the challenges in present day atmospheric and climate sciences is to represent surface heterogeneity effectively and on the proper spatial and temporal scales. The need to derive meteorological data or climate data on a local level has increased over the last decades. Downscaling climate information from Global Climate Models (GCMs) to local level has gained high interest over the past decade. The disadvantage of these GCMs is the spatial scales that they represent (1-2 degrees) and, as a result, also the processes that they physically can solve. This led to the development of Regional Climate Models (RCMs) which can generate information on a much finer spatial resolution (0.25-0.5 degrees). The Fourth Assessment Report of the IPCC (IPCC AR4) states that "Global Climate Models remain the primary source of regional information on the range of possible future climates" (Christensen et al. (2007)). Higher resolution climate models are thought to provide more regionally detailed climate predictions and better information on extreme events as spatial and temporal details are better resolved. However, an increased understanding of climate processes and feedbacks is still necessary to reduce the uncertainty in climate projections (e.g. Holtslag et al. (2013)). Atmospheric models are one of the tools to fill this gap, even though the gap between climate models and atmospheric models is big.

Atmospheric models have the ability to simulate physical processes on a very fine resolution (1-2 km). This level of detail is still not present in an

14

RCM due to limitation in the equations used to describe all involved physical processes. Of course, this is justified by the timeframe over which a RCM intends to generate information. A mesoscale model can act as a complementary model to the RCM in a way that it can and will provide extra climate information for a certain region on a local level. The degree of complexity of the physical processes is of a higher order and also the spatial variability can be better solved. This means that realistic and complex land surface processes can be included.

This thesis presents four different cases in order to increase our understanding of the processes and feedbacks. All four cases are executed using a regional atmospheric model coupled to a sophisticated land surface model that represent the surface correctly. The weaknesses of a regional atmospheric model are also discussed as each case has its own difficulties in understanding the feedbacks between the earth surface and the atmosphere

1.2   Research tools

To study the feedbacks between the earth's surface and the atmosphere, a proper combination of observations and models is needed. Models are necessary and useful tools to upscale point observations and to obtain information on a more local to regional level. Also 1D land surface models (LSMs) are instrumental in understanding earth surface-atmospheric interactions (e.g., Pitman (2003), Ek et al. (2004) among many others) . A LSM calculates the feedbacks between the land surface and the atmosphere and are therefore an essential boundary condition for regional atmospheric models. The regional atmosphere provides on its turn the boundary conditions to the LSM through atmospheric variables (e.g. temperature, relative humidity, wind speed, incoming radiation, precipitation). Land surface models have evolved from over the last decades from simple models to highly-detailed models in which not only fluxes of water, momentum and heat are calculated but also fluxes of constituents like CO_2 and in which vegetation is dynamically prescribed.

The quantity of most of the fluxes is parameterized in a LSM. One example of a parameterized variable is the stomatal conductance that control the opening and closing of the stomata in the leaf and the stomata on its turn influence the evaporation (Jarvis (1976), Jacobs et al. (1996)). Another example is the assimilation and respiration of CO_2 on plant/tree level, both variables are parameterized (Collatz et al. (1992)) To derive the right values of the parameters measurements are essential. These measurements are used to optimized the

parameterization in order that the fluxes are well simulated using a set of formulas and parameters. A common strategy is that parameters are optimized for a certain land-use type or plant functional type (PFT) (Knorr (2000)). Subsequently, it is assumed that these parameters are representative for the same PFT in any part of the world.

In this thesis two flavors of land surface models are used. The LSM used in chapters 2 and 3 is SWAPS-C and the LSM in chapters 4 and 5 is LEAF. SWAPS-C has a carbon extension that LEAF is missing and SWAPS-C is therefore essential in quantifying the carbon fluxes in chapter 3. The parameters of SWAPS-C were optimized for the Dutch situation as observational records were available to perform optimizations. The strength of SWAPS-C (Ashby (1999)) is that it comprises a one- or two-layer evaporation and energy balance model, detailed soil moisture calculations, and a module to simulate carbon fluxes between the land surface and the atmosphere. Land surface and atmosphere interact through fluxes of water, heat, and momentum, which are controlled by a set of parameters.

LEAF is the LSM included in the regional atmospheric model (RAMS) used in this thesis and is executed with the parameters incorporated in the model. LEAF has been documented by Walko et al. (2000). Both LSMs are configured in such a way that a grid cell can be divided into various so-called patches. Each patch represents a land cover type and fluxes for each grid cell are calculated using an area-weighted expression to sum all possible fluxes. Within the study area of chapter 5 (Saudi Arabia) a meteorological station was not present that also observed latent heat flux to optimize the parameters for the stomatal conductance. Chapter 4 investigates the influence of sea surface temperature (SST) and thus optimized parameters were expected not to influence the results of this chapter much with the focus on changing the sea surface.

This LSM component is embedded in a mesoscale model, which is called Regional Atmospheric Modelling System (RAMS). Orlanski (1975) defined the mesoscale as all meteorological processes between the 2 km and 2000 km, and thus ranging from thunderstorms and urban effects (mesoscale-γ) to fronts and hurricanes (mesoscale-α). The focus in this thesis is on the small scale effects that belong to the mesoscale-γ classification. The impacts, that are explored in this thesis, are of scales of several kilometres. Therefore, a mesoscale model is an ideal model to quantify the regional feedbacks between the earth's surface and the atmosphere. It gives the option to work on a fine grid scale (1-2 km), but it also quantifies the feedbacks to a more local or regional level.

16

In this thesis a fully, online coupled model, basically consisting of the Regional Atmospheric Modelling System (RAMS,Cotton et al. (2003), Pielke et al. (1992)) is used and coupled with the above mentioned LSMs. RAMS is a 3D, non-hydrostatic model based on fundamental equations of fluid dynamics and includes a terrain following vertical coordinate system. One of the advantages of the model is the ability to perform simulations at high grid increments and the subsequent representation of microphysics and precipitation processes. RAMS allows for passive atmospheric transport of any number of scalars and this has been implemented for CO_2 in chapter 4. To study regional scale feedbacks it is important to use land surface descriptions of appropriate complexity, that include the main controlling mechanisms and capture the relevant dynamics of the system, and to represent the real-world spatial variability in soils and vegetation.

1.3   Research questions and outline

This thesis explores the effect of a better representation of the land and sea surface on regional climate. To quantify the important feedbacks between the earth's surface and the atmosphere the following research questions are formulated:

- What is the regional atmospheric climate effect of land cover on precipitation and carbon dynamics in a heterogeneous environment in a temperate climate?

- What role plays the sea surface temperature on precipitation in coastal areas in temperate and desert environments?

- What are the differences in impacts of land use change on the regional climate between a temperate and a desert environment?

For the temperate climate the Netherlands and its surroundings are taken as a case study. The impacts of land-use change on the desert climate are investigated using a case study in the coastal area of the Arabian Peninsula close near the Red Sea.

Chapter 2 deals with the effects of land cover and topography on precipitation maxima in the Netherlands. This precipitation maxima can be found at the Veluwe, which is an elevated area (maximum elevation of 100 meters) mainly covered with a forest. Chapter 3 continues the

analysis of the central part of the Netherlands, while looking at the influence of the land surface on carbon dynamics (e.g. uptake of carbon by the forest, emissions of carbon by the cities). In chapter 4 the focus shifts towards a second precipitation maximum in the Netherlands, which is located in the coastal area of the country. The effect that the sea surface has on the precipitation is being explored. Chapter 5 shows the effect that the earth surface has on the local meteorology in Saudi Arabia taking into account changes in the land use and also addressing the effect that the sea surface has on the local meteorology.

Regional atmospheric feedbacks over land and coastal areas

Chapter 2

Exploring the impact of land cover and topography on rainfall maxima in The Netherlands

abstract

The relative contribution of topography and land use on precipitation is analysed in this paper for a forested area in The Netherlands. This area has an average yearly precipitation sum which can be 75-100 mm higher than the rest of the country. To analyse this contribution different configurations of land use and topography are fed into a mesocale model. We use the Regional Atmospheric Modelling System (RAMS) coupled with a land surface scheme simulating water vapour, heat and momentum fluxes (SWAPS-C). The model simulations are executed for two periods which cover varying large scale synoptic conditions of summer and winter periods.

The output of the experiments leads to the conclusion that the precipitation maximum at the Veluwe is forced by topography and land use. The effect of the forested area on the processes that influence precipitation is smaller in summertime conditions when the precipitation has a convective character. In frontal conditions the forest has a more pronounced effect on local precipitation through the convergence of moisture. The effect of topography on monthly domain-averaged precipitation around the Veluwe is, in the winter 17 % increase and in summer 10% increase, which is quite remarkable for topography with a maximum elevation of just above 100 meter and moderate steepness. From our study it appears that the version of RAMS using Mellor-Yamada turbulence parameterization simulates precipitation better in wintertime, but that the configuration with the MRF turbulence parameterization improves the simulation of precipitation in convective circumstances.

2.1   Introduction

Over the past decades feedbacks between land use and land cover change and climate have been widely documented. Not only on a general level (Zhao et al. (2001), Pielke et al. (2002), Kabat et al. (2004) Pielke et al. (2007)), but also focussing on certain areas in the world, like semi-arid environments (De Ridder and Gallee (1998), Ter Maat et al. (2006), Sogalla et al. (2006)), tropical environments (Sampaio et al. (2007)) and more temperate climates (Teuling et al. (2010), Nair et al. (2011), Kala et al. (2011)). A substantial subset of this literature focuses on the influence and/or impact of a land cover change on precipitation under various atmospheric conditions in different regions of the world.

The basic mechanism behind atmospheric impacts of land cover change is that land cover determines the surface roughness, the radiation balance and the subsequent partitioning of available energy over sensible or latent heat fluxes. Their relative importance may vary spatially and in time depending on the synoptic meteorological situation.

Differences in the heat, moisture and momentum fluxes at the land surface interface can lead to altered heat and moisture content of the atmospheric boundary layer (ABL) (e.g. Ek and Holtslag (2004), van Heerwaarden et al. (2009)). Changes in temperature and humidity in the ABL affect convective heating, total diabatic heating, subsidence and moisture convergence. This in turn can affect, through a chain of microphysical and cloud processes, precipitation which activates additional potential feedbacks, acting on increasingly longer timescales, through soil moisture stores, vegetation growth and phenology and eventually ecosystem changes.

These feedbacks have been studied at relatively large spatial scales (e.g. Koster et al. (2004)). To unravel the feedbacks between land cover and regional meteorology, however, high resolution studies are required (Pielke et al. (1991)). The feedbacks between changes in land use and topography and their impacts at the regional scale may directly affect processes which drive and change mesoscale circulations. Studies in other parts of the world have shown that forest can also contribute to this phenomenon described by Noilhan et al. (1991), van der Molen et al. (2006), and, more recently, Dyer (2011). In a global setting, Fraedrich et al. (1999) showed that land use change has certain potential to affect the climate.

Climate change is another factor which can have its impact on regional weather patterns. Christensen et al. (2007) found "that an increase in

the amount of precipitation that exceeds the 95th percentile is very likely in many areas of Europe, despite a possible reduction in average summer precipitation over a substantial part of the continent". Koning and Franses (2005) discussed the possible consequence of global warming for The Netherlands: more rainy days throughout the year and higher levels of precipitation.

The Netherlands may also be strongly affected by global change as the deltas of two main European rivers (Rhine and Meuse) cover a large part of the country, and their discharges will change (Pfister et al. (2004)). It is expected that in the coming decades, besides an increase in urban areas, agricultural lands will be abandoned and replaced by forests (Verburg et al. (2009)). This land use change may have impacts on the discharge regime of the river Rhine adding to the already mentioned first order consequences of global warming.

Wieringa and Rijkoort (1983) analysed the effect of topography on the wind in The Netherlands and concluded that only two areas, amongst these the Veluwe area, can potentially influence the local wind climate. Interestingly, the Veluwe exhibits an average yearly precipitation sum which can, locally, be 75-100 mm higher than the rest of the country, a difference of 10-15% per year (see Figure 2.1, KNMI (2011)). The distribution of rainfall throughout the year is reasonably uniform with an average monthly precipitation sum at the Veluwe of 72 mm.

From Figure 2.1 we can also discover a second precipitation maximum in the western part of the Netherlands. It is thought that both these maxima have different sources of origin. The precipitation maximum in the western part is mostly thought to be caused by the sea surface temperature and is expected to increase over the next decades as sea surface temperatures increase Lenderink et al. (2009). The Veluwe precipitation maximum is hypothesized to be caused by topography and land cover as a major part of the Veluwe is covered by trees. To investigate the reason behind this precipitation maximum of the Veluwe we address the following main question: What is the relative sensitivity of regional precipitation, evaporation and other meteorological variables to topography and land cover on and around the Veluwe?
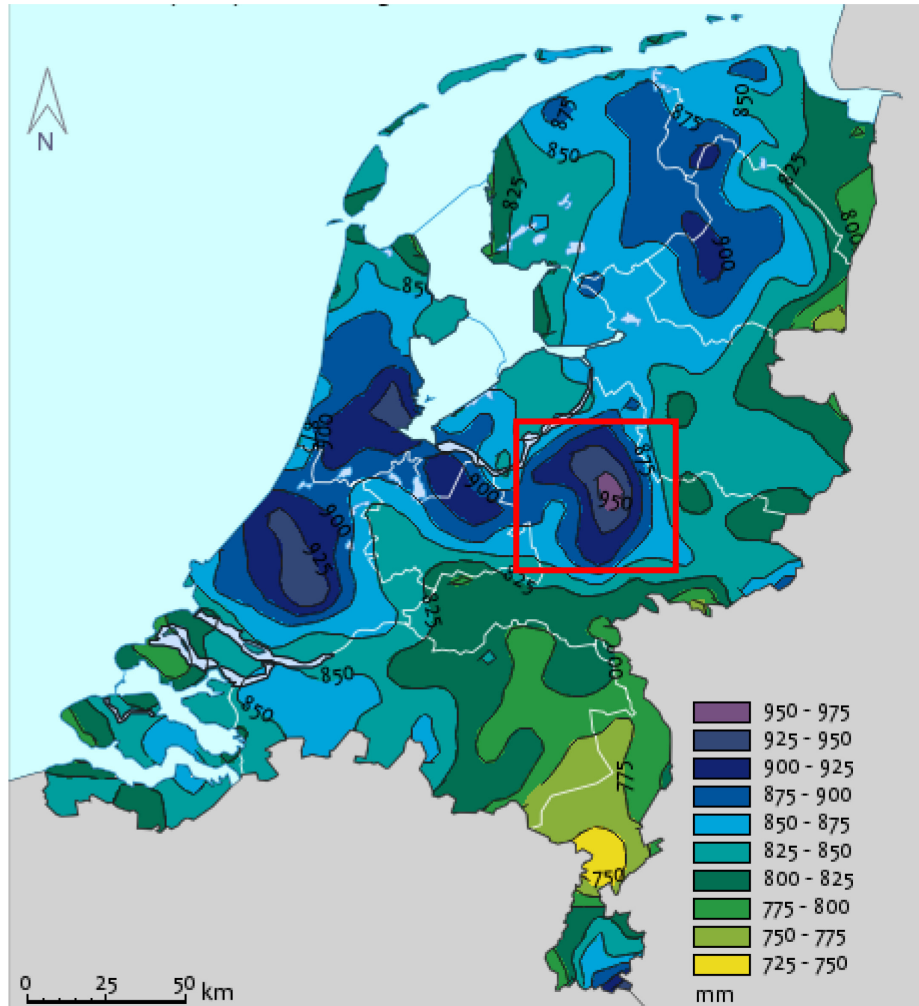
Figure 2.1: Yearly precipitation sum (mm) as a climatological mean (1981-2010). The red square is approximately the area of interest for this paper

We use the RAMS model (Regional Atmospheric Modelling System, Pielke et al. (1992), Cotton et al. (2003)) for different configurations to analyse the relative contribution of topography and of land use change on precipitation. The configurations used in this study are highly idealized but are designed in such a way that the possible reasons behind the precipitation maximum can be unravelled, which is the main question to be answered in this study. One configuration is to remove the forest to investigate the impact of forest on precipitation. The other configuration is to remove the topography to investigate what the effect

is of topography on precipitation. The model will be validated using actual vegetation and topography in a control simulation.

The paper is organized as follows. First, we will describe the Veluwe area followed by a description of the modeling system together with the various databases and configurations which are incorporated and used in the simulations within the atmospheric model. Also, the criteria will be described which we use to select the simulation periods. Consequently, the output of the validation simulations will be described together with the results of the configuration simulations. Subsequently, we will discuss the differences between the simulations and how these relate to the rainfall maximum of the Veluwe.

2.2   Description of the Veluwe

The Veluwe is a densely forested and elevated area of approximately 625 km^2 with a maximum altitude of just over 100 meter in an otherwise flat surrounding. The area is covered with glacial deposits, but in the early 20th century it was decided that the area would be afforested to reduce wind erosion that was threatening the surrounding agricultural area and produce construction wood for the mines. As most forested areas in the Netherlands the Veluwe is an important infiltration regions for groundwater bodies.

To increase the amount of available groundwater, proposals were made to convert the predominantly dark and dense coniferous forests to deciduous forests or even deforest complete areas and replant them with among others heather. Stuurgroep Grondwaterbeheer Midden (1992). This discussion was stimulated by reports that indicated high interception losses for forests Evers et al. (1991). The main forest type studied at that time was Douglas fir. The interest in Douglas fir forests was because the main objective was to study acid rain and dry deposition. Both entities being high as Douglas fir is among the trees with the highest leaf area index (up to $LAI = 11$ m²m^{-2}) and the highest water storage capacity (2.5 mm). According to common use, the benefits and effects were translated directly into economic values. Water supply companies became interested and were willing to compensate forest owners for changing the tree species from coniferous with a high interception storage to a land cover with a presumed much lower water loss, such as deciduous forest or grassland. At present these changes have only been taking place at a very small scale and primarily to remove exotic species.
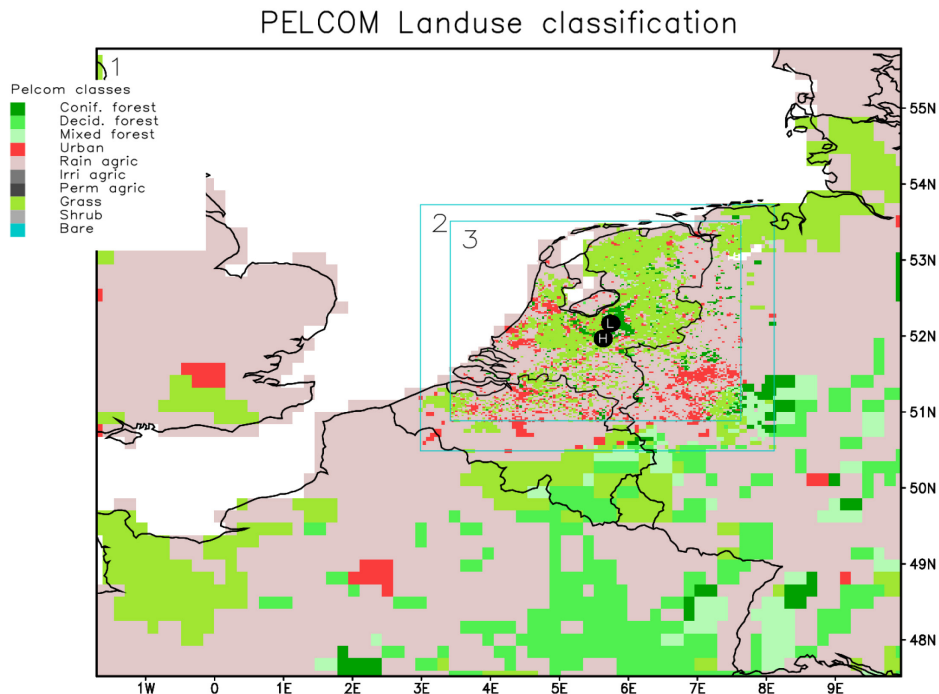
Figure 2.2: Current land use derived from PELCOM classification and projected on the complete modelling domain of the simulation (dark green: coniferous forest, light green: deciduous forest, green: grassland, gray: rainfed agricultural land, red: urban). The location of the observational stations are also given: H – Haarweg, Wageningen, L - Loobos

The main vegetation is coniferous forest as can be seen from Figure 2.2, where the land use of the complete modelling domain is given. The land use in this picture is derived from the PELCOM classification which has been described in detail by Mücher et al. (2001) and which is also used as input within the RAMS model. PELCOM has a grid increment of approximately 1 km and compared to other land cover database the forest of the Veluwe is well represented.

The topography of the Veluwe area and surroundings is given in Figure 2.3. From this map it is evident that The Netherlands is a low lying and flat country with only the area of the Veluwe showing significant topography besides the more sloping area in the south-eastern tip of the country. The topography is derived from the Digital Elevation Model of the USGS (GTOPO30) which has approximately a 1 by 1 kilometre grid increment.
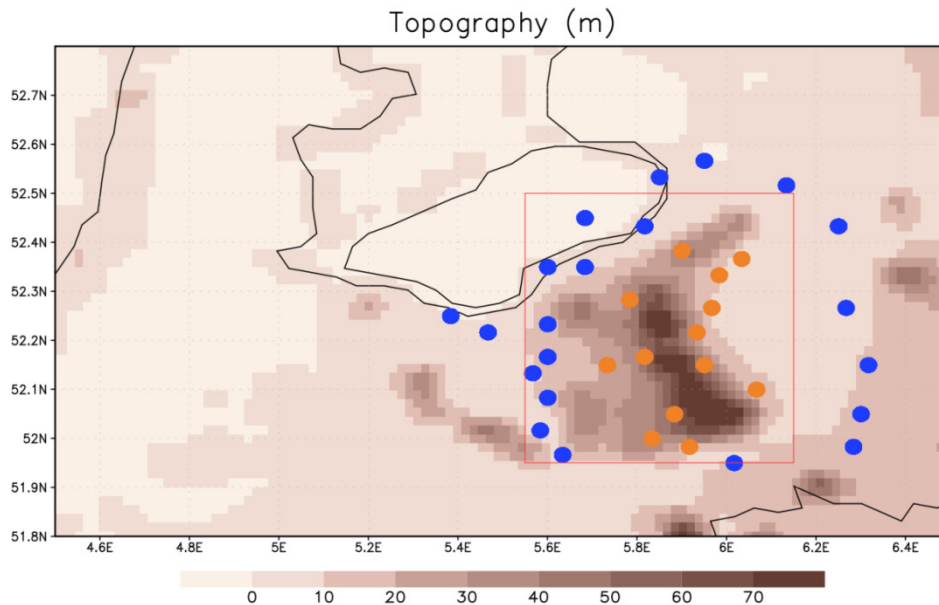
Figure 2.3: Topography (meters) projected on part of the finest grid increment in RAMS. The location of the rainfall observation sites are also displayed as dots (blue - sites around the Veluwe, orange - stations at the Veluwe. The Veluwe is enclosed by the red square.

The Netherlands and the Veluwe exhibits a maritime temperate climate. Annual average temperature is 9.7 °C, average maximum temperature 13.8 °C and minimum is 5.5 °C. Annual precipitation ranges from 850-975 millimeters in the domain; annual evaporation ranges from 560-580 millimeters in this domain. Wind speed averages 4 m s^{-1} with a preference for southwestern directions. These figures are based on the KNMI Climate Atlas KNMI (2011) in which a climatological analysis is made for the period 1981-2010.

The most important variable of interest in this study is precipitation. Figure 2.3 shows the various stations from the national rainfall and precipitation network in and around the Veluwe where rainfall is measured. Figure 2.4 shows the difference between the averaged monthly sums of rainfall at stations on and around the Veluwe as a percentage over a year. This graph shows that the differences between precipitation on and around the Veluwe change seasonally with larger values in the winter months (maximum difference of 14.5 %, 10.8 mm; yearly total difference is 65 mm). Given these seasonal differences and
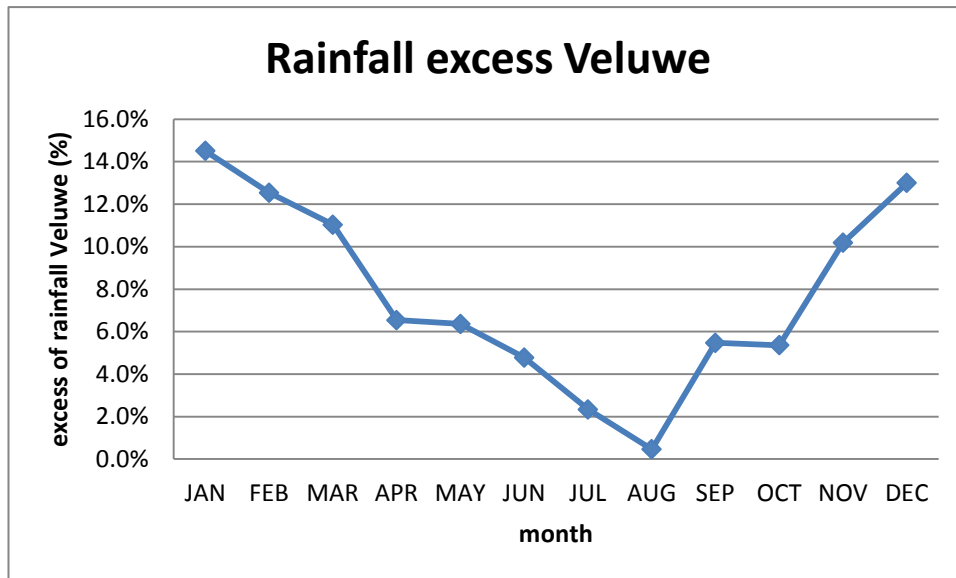
Figure 2.4: Relative difference (%) in monthly averaged precipitation sums between stations on and around the Veluwe. This analysis is based on KNMI Climate Atlas in which a climatological analysis is made for the period 1981-2010

the fact that synoptic systems differ between winter and summer, both these seasons will be simulated to address the feedback between the land and the atmosphere and the patterns which do arise from a change at the land-atmosphere interface.

2.3   Description of the model

RAMS (version 4.3) is used to quantify the relative contributions of topography and land use to the precipitation maximum of the Veluwe. The model is a 3D, non-hydrostatic based on fundamental equations of fluid dynamics and includes a terrain following vertical coordinate system. One of the advantages of RAMS is the possibility to perform simulations on high resolution and its representation of microphysics and precipitation processes. Table 2.1 shows the various options/parameterizations which are used in RAMS for this study. The setup of the model followed the setup which has been earlier used and described by Ter Maat et al. (2010). A two-way nested grid configuration was used Walko et al. (1995), in which parent (18 km), regional (6 km), and fine grid (2 km), respectively, covered the Benelux countries including parts of neighboring countries, The Netherlands and

Table 2.1: Configuration of RAMS4.3

grids	1	2	3
dx, dy	18 km (50x54)	6 km (60x62)	2 km (149x149)
dt	20 s	20 s	6.7 s
dz	25 – 1000 m (35)		
Radiation	Harrington (1997)		
Topography	GTOPO30 (~1 km grid increment)		
Land cover	PELCOM (1 km grid increment, Mücher et al. (2001))		
Land surface	SWAPS-C (Ashby (1999), Hanan et al. (1998))		
Diffusion	Mellor/Yamada (Mellor et al. (1982))		
Microphysics	Full microphysics package (Meyers et al. (1997))		
Forcing	ECMWF		
Nudging	lateral: 1800 s (only on grid 1)		
Period	1 February 2000- 29 February 2000 (Winter) 9 May 2005 – 7 June 2005 (Summer)		

a 300 km by 300 km domain centered around the Veluwe. The nudging extends inwards from the lateral boundary region of the coarser grid by 5 gridpoints. Note that the grid is stretched vertically to obtain high vertical grid increments (25 m) near the ground and lower vertical grid increments (1000 m) at higher levels with a total of 35 vertical levels. The convective scheme is not switched on in the three grids and is explicitly solved by the full microphysics package which is part of RAMS and described by Flatau et al. (1989).

RAMS is forced by analysis data from the European Centre for Medium-Range Weather Forecasts (ECMWF) global model. The grid spacing of the forcing data is 0.5° by 0.5° and available every 6 hours. Monthly sea surface temperatures have been extracted from the Met Office Hadley Centre's sea ice and sea surface temperature (SST) data set, HadISST1 Rayner et al. (2003) and are linearly interpolated during the simulation period. Soil properties were derived from the IGBP-DIS Soil Properties database (Global Soil Data Task Group 2000) which has a grid mesh of approximately 10 km.

This study does not only require a detailed map of the land surface but also a land surface model which is able to simulate the relevant differences in energy partitioning between land cover and soil classes. In this study the land surface model, SWAPS-C, is used and has been coupled to the numerical core of RAMS. The strength of SWAPS-C Ashby (1999), is that it comprises a one- or two-layer evaporation and energy balance model, detailed soil moisture calculations and a module to simulate carbon fluxes between the land surface and the atmosphere. Land surface and atmosphere interact through fluxes of water, heat and momentum which are controlled by a set of parameters. Each land

Table 2.2: Important parameters for calculating the latent heat flux and partitioning of the available energy, classified by land use. $g_{s,max}$: maximum surface conductance (mm s-1), z_0: roughness length (m), α: albedo (-)

	$g_{s,max}$ (mm s^{-1})	z_0 (m)	α (-)
Coniferous forest	33.4	0.9	0.1
Deciduous forest	51.0	0.9	0.18
Grass	25.9	0.02	0.2
Agricultural land	25.0	0.1	0.25

surface type has its own parameter set. Table 2.2 shows the most important parameters for the four dominant land use classes in the domain. SWAPS-C is not the default land surface model in RAMS, but has been coupled successfully to RAMS in earlier studies Ter Maat et al. (2010). This is the major reason to leave this coupled modelling system intact as it is, even though newer versions of RAMS are available.

To validate the results of the control simulation surface observations are used. The observations from the sites of Haarweg (grassland south of Veluwe, Jacobs et al. (2009)) and Loobos (coniferous forest on the Veluwe, Dolman et al.(1998), Moors (2012)) are used. At these sites standard meteorological parameters are measured together with observations of exchange fluxes of radiation, heat, moisture, CO_2 and momentum.

Besides the control simulation (CTRL), the following configurations are evaluated (see Figure 2.5):
- NoForest (NF): The dominant forest type (coniferous forest) has been replaced by grassland in a rectangular box around the Veluwe (top right graph in Figure 2.5) for the current topography. This change leads to a change in aerodynamic roughness (z_0) from 0.9 meter to 0.02 meter, a change in LAI from 1.8 m^2 m^{-2} to 3.0 m^2 m^{-2} and a change in albedo from 0.10 to 0.20 (dimensionless);
- NoTopo (NT): The topography of the Veluwe has been brought back to sea level in a rectangular box around the Veluwe (bottom left graph in Figure 2.5);
- No Topo/No Forest (NFT): Combination of the configurations NoForest and NoTopo.
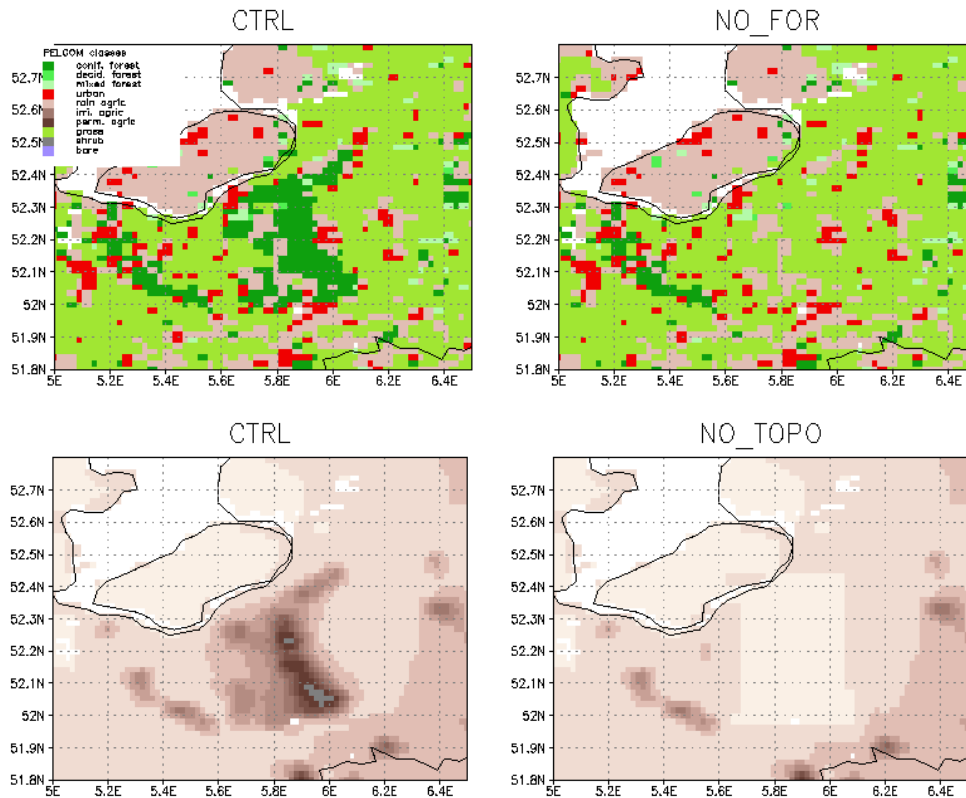
Figure 2.5: Graphical representation of the various configurations used in the simulations. Top left: actual land use; Bottom left: actual topography; top right: land use in the NF-and NTF-configuration; bottom right: topography in the NT- and NTF-configuration

All model runs (CTRL, NF, NT and NFT) are executed for the same time periods, i.e. summer (9 May – 8 June 2005, called SUM from now on) and one month in winter (1 February – 29 February 2000, called WIN). The SUM period has recorded various interesting periods which are representative of summer periods in the Netherlands with days of warm weather followed by rainy days. The amount of precipitation in this period is comparable with climatological means. For the WIN period we searched for a winter month with an average amount of rainfall and with a noticeable difference between precipitation on and around the Veluwe, so that the processes between this difference can be studied. This was also one of the conditions to choose the May/June period for the SUM simulation, although this was harder than for WIN as the difference between on and around the Veluwe is much smaller as was shown in Figure 2.4.

The selected periods cover varying large scale atmospheric dynamics that are representative synoptic conditions of summer and winter months, with convective conditions prevailing under warm conditions. Winter precipitation is mostly part of low pressure systems with accompanying frontal precipitation under westerly conditions. Next to this difference in synoptic conditions, Table 2.3 also shows for these two seasons the differences in observed rainfall between stations on the Veluwe and around the Veluwe. In both seasons a considerable amount of precipitation has been observed so that the effect of the various configurations can be quantified. The SUM period of May/June in 2005 was overall characterized by normal temperatures, normal amounts of rainfall and more than average incoming solar radiation. However according to the Royal Netherlands Meteorological Institute (KNMI, www.knmi.nl), the rainfall was not distributed evenly with the eastern part of The Netherlands being wetter. Also, intensive areas of rainfall crossed the country, especially the northern part of the country, at 14 May and 3 June.

The weather in the WIN period of February 2000 was characterized by an almost constant westerly flow with which warm maritime air was transported. This led to a higher temperature than normal, more rainfall, but also higher amounts of incoming solar radiation which can be explained by the fact that the showers mostly passed the Netherlands during the night. The temperature in the first and last decade of the month was high compared to climatology. Also the amount of incoming solar radiation was high as the showers mostly passed during the nighttime. Due to the strong westerly flow, lots of showers passed frequently over The Netherlands leading to a wetter than normal month.

2.4   Control run and model validation

The control run (CTRL) is compared against observations of meteorological parameters and of fluxes of heat and water. As precipitation is the most important variable our focus will mostly be on precipitation in both spatial and temporal sense. Observations of precipitation are taken from the database of the Royal Netherlands Meteorological Institute (KNMI). These observations are collected every day at 8:00 UTC for the past 24 hour period. We only took the observations from the locations nearest to the Veluwe (see Figure 2.3 for the geographic distribution of these stations). Both observations and simulations are averaged over a box around the Veluwe (see Figure 2.3) which ranges from 5.55 °E to 6.15 °E and from 51.95 °N to 52.5 °N. Figure 2.6 shows these results as time series over the simulation periods WIN-CTRL and SUM-CTRL.

WIN-CTRL shows that the simulated precipitation compares satisfactorily to the measured precipitation. The simulated precipitation expressed as the averaged accumulated sum i.e. 97 mm, is close to the observed value of 103 mm (RMSE=2.7 mm). The observed temporal pattern is also closely resembled by the model. The observed peaks in daily precipitation are mostly captured by the model, except for 5 February (overestimation of 6.5 mm) and 25 February (underestimation of almost 9.3 mm). These differences between model and observations show the inability of the current set-up of the model on these days to simulate the areas of intensive precipitation rates at the exact location. The observations from the KNMI database confirm these spatial differences in precipitation amounts at such a short distance, as stations in a certain area of the domain give different rainfall rates than in a other parts of the domain. For example, the observed rainfall rates on 5 February 2000 in the southeastern part of the Veluwe are on a daily basis 5 millimeters lower than in the more northern parts of the Veluwe. As not all KNMI rainfall stations are located in the domain which is used for the averaging these differences are not cancelled out.

The difference in monthly rainfall sum over the Veluwe between model and observations is larger in the SUM-CTRL simulation and the model mostly overestimates the rainfall rates (bottom Figure 2.6). Especially, in the first days of June at the end of the simulation RAMS overestimates precipitation. This period is characterized by frontal systems (both warm and cold) above and around The Netherlands which dominate the weather. During this period, the timing of frontal systems is simulated well by the model for the summer simulation when compared to surface analyses and satellite images of these days (not shown). However, the current set-up of RAMS has problems with the exact location of the rainfall maxima. This results in an overestimation of rainfall rates at 21 May, 31 May and 1 June as in all three cases the heaviest rainfall is simulated more inland whereas the observations tend to locate the heaviest rainfall more in the coastal provinces. As a result, RAMS is overestimating the rainfall in the summer simulation by a factor 2 (simulated: 145 mm, observed: 60 mm, RMSE: 6.6 mm).
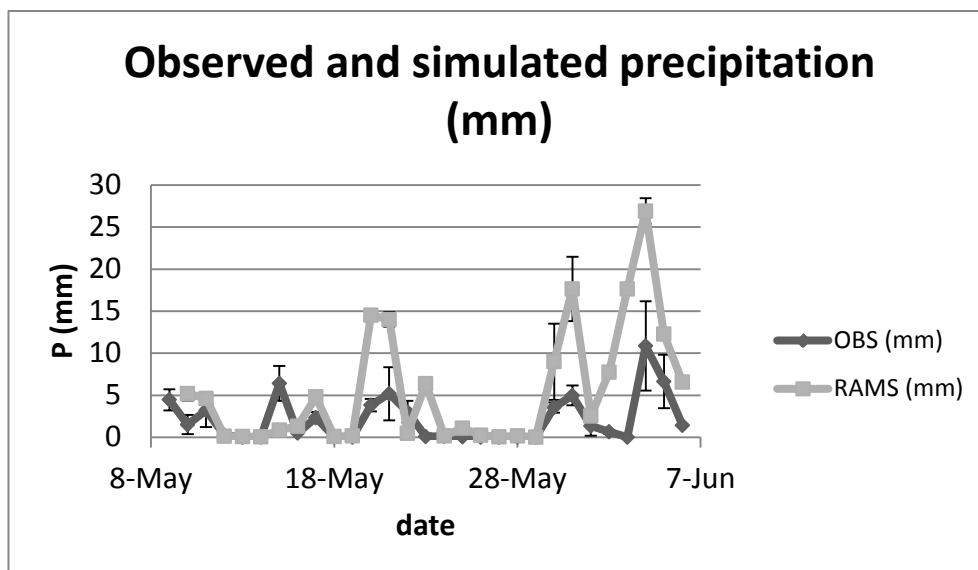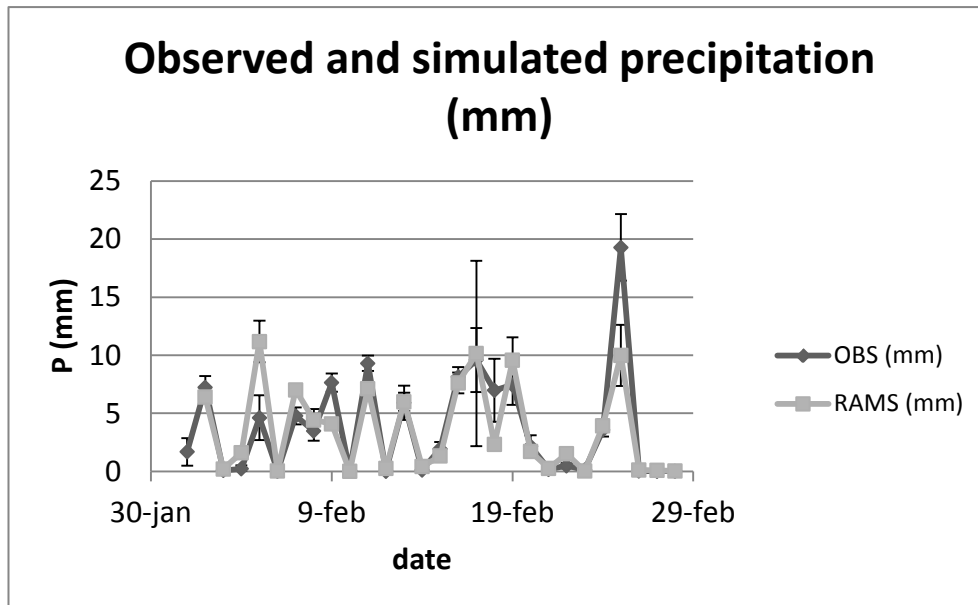
Figure 2.6: Time series of precipitation (mm) and accompanying error bars for WIN-CTRL (top) and SUM-CTRL (bottom). Black line: observations KNMI; gray line: RAMS

Table 2.4: Precipitation Skill scores for WIN-CTRL and SUM-CTRL. POD:Probability of Detection, GSS: Gilbert Skill Score.

Simulation	Bias	POD	GSS
WIN-CTRL	1.20	0.97	0.34
SUM-CTRL	1.46	0.97	0.24

Next to the analysis of the precipitation depth we also looked at various precipitation skill scores, namely bias score, probability of detection (POD) and the Gilbert Skill Score (GSS, also known as Equitable Threat Score, ETS). These values are displayed in Table 2.4 for both summer and winter simulation. The skill scores are averaged over all rainfall stations in the domain. The bias score is in both simulations higher than 1 which means that rainfall events are overestimated. However, the POD shows for WIN-CTRL (0.97) and SUM-CTRL (0.97) that most observed events are simulated by the model. Next to that, the GSS shows that the model has skill in simulating precipitation events. The values are in agreement with Vedel et al. (2004) who used precipitation skill scores to evaluate a numerical weather prediction model for Europe.

To gain insight in the causes for the simulated differences the next step in the validation process is the comparison between simulated and observed radiation fluxes at station level. The analysis of shortwave radiation is split into 1) an analysis on daily sums for the simulated period for both WIN-CTRL and SUM-CTRL (Tabel 2.5), and 2) a more detailed comparison for only SUM-CTRL and the observations (Figure 2.7).

Table 2.5: Statistical analysis of radiation components and surface temperature at station level (Loobos, Haarweg) for both WIN-CTRL and SUM-CTRL (MAE: Mean Absolute Error, RMSE: Root Mean Square Error, r^2: square of correlation coefficient)

Simulation	MAE	RMSE	r^2
Incoming Shortwave Radiation			
Loobos-WIN	159.0	211.7	0.54
Haarweg-WIN	165.5	207.5	0.51
Loobos-SUM	477.9	652.7	0.58
Haarweg-SUM	429.6	587.5	0.57
Incoming Longwave Radiation			
Loobos-WIN	133.1	182.8	0.45
Loobos-SUM	308.6	360.0	0.65
Surface Temperature			
Loobos-WIN	1.668	2.035	0.66
Loobos-SUM	2.725	3.331	0.67

(a)
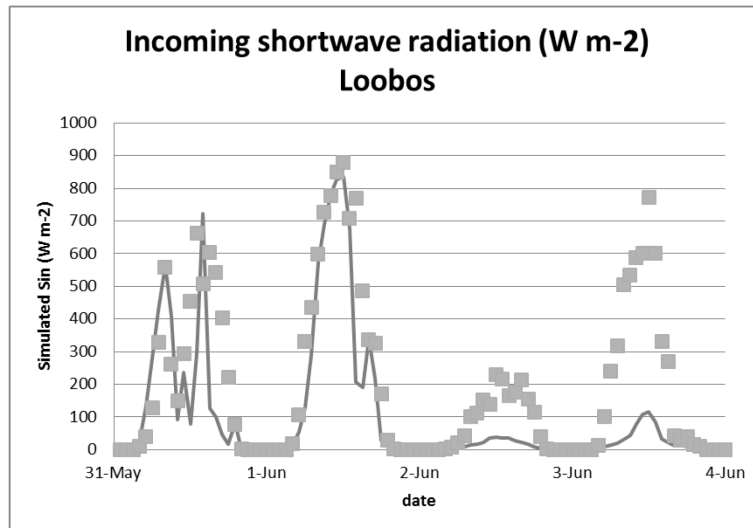
(b)
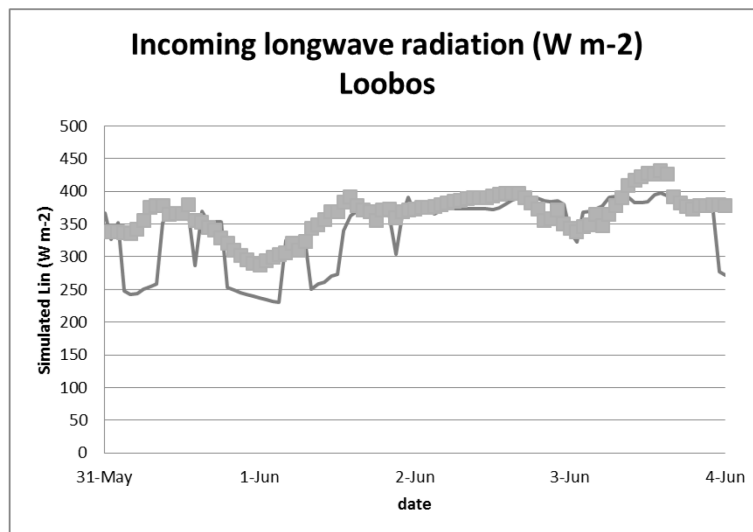
Figure 2.7: Time series of (a) incoming shortwave radiation (W m^{-2}) and (b) incoming longwave radiation (W m^{-2}) at Loobos for SUM-CTRL. Line: model; gray dots: observations

The daily sums of shortwave radiation for WIN-CTRL are underestimated by the model with almost 15% (Loobos, $r^2=0.54$) and 31% (Haarweg, $r^2=0.51$). From the graphs these underestimation is caused by: i) certain days where RAMS simulates clouds over the Veluwe where in reality these were just west or east of the Veluwe, and ii) on cloudy days RAMS has a tendency to simulate cloudy layers that block the incoming shortwave radiation more than they do in the observations.

Sunny days are reasonably well simulated by the model. This holds also true for the SUM-CTRL simulation. Days with more than 1500 J cm^{-2} for the daily sum of incoming radiation are better simulated by the model than days with lower values of incoming shortwave radiation. On average the model is overestimating the daily incoming radiation by 8% (Loobos) and 5% (Haarweg), both r^2=0.58. While zooming in on a couple of days in SUM-CTRL for Loobos station we try to illustrate the signals of the model better. The end of the SUM-CTRL is characterized by a period with clear days which are followed by cloudy days (see Figure 2.7a). This figure clearly shows that the observations are closely simulated by the model on clear days (1 June) and this holds even true for days when the weather is more unsettled with alternating cloudy and clear spells (31 May). However, on completely cloudy days the model is underestimating the radiation. Figure 2.7b shows for this same period the longwave radiation and from this figure we can conclude that the model is simulating the cloudy days much better than the less cloudy and sunny days.

If we analyse the differences between observed and simulated temperature we come to the same conclusion. On days when the simulated shortwave radiation is underestimated the temperature seems to be underestimated as well as a direct effect of solar radiation on the temperature. Overall the temperature at Loobos is captured better by the model in wintertime than in summertime with lower RMSE and bias (see Table 2.5). The r^2 for both periods are higher than those for the radiation (WIN: 0.66; SUM: 0.67).

From the radiation analyses we conclude that the model is generating dense clouds in summertime conditions that block the shortwave radiation more than the observations justify. To justify this hypothesis a closer look has been taken at the vertical profiles of the water vapour mixing ratio (not shown). These profiles show that at days when the shortwave radiation is underestimated the water vapor content in the planetary boundary layer is overestimated and that low-altitude cumulus clouds are simulated whereas the observations don't justify the formation of these low-altitude clouds.
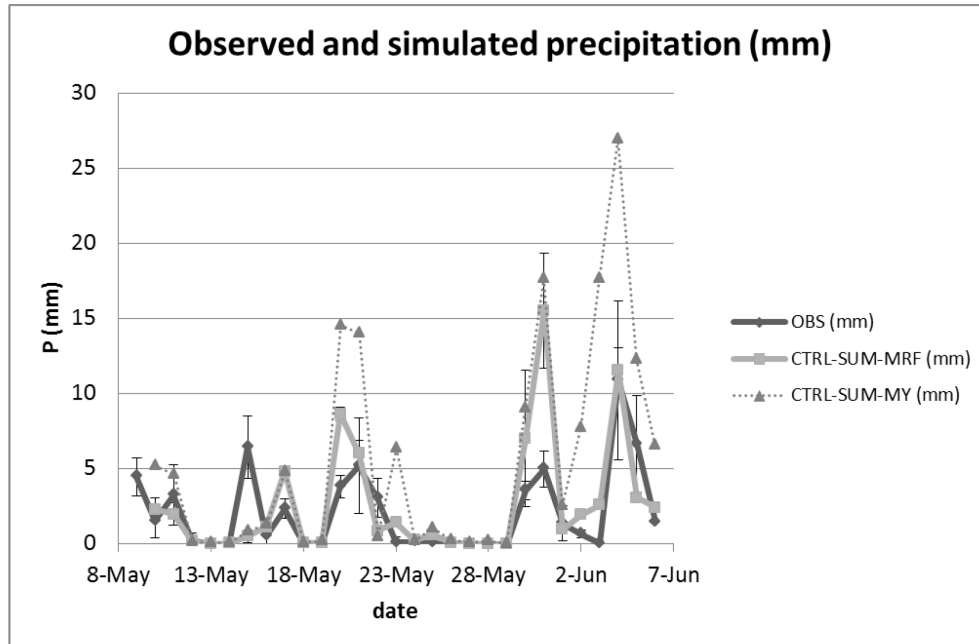
Figure 2.8: Time series of precipitation (mm) and accompanying error bars for SUM-CTRL (bottom) with the MRF turbulence parameterization. Black line: observations KNMI; gray line: RAMS. As a comparison the simulation with the MY-parameterization is included as well (dashed)

2.4.1 Sensitivity of CTRL to turbulence parameterization

One of the issues which needed attention was the choice of turbulence parameterization. Our initial choice was for the Mellor-Yamada parameterization (MY, Mellor and Yamada (1982)) which has been widely used by the RAMS community. However, Steeneveld et al. (2011) already noted the importance that PBL schemes play in simulating the boundary layer and its effect on the boundary layer heat budget. Steeneveld et al. (2008) compared the various PBL schemes in a range of mesoscale models and concluded that the model forecasts are sensitive to the choice of the PBL scheme both during day and night. Therefore, we investigated the effect that another PBL scheme may have on the simulation of the total precipitation. The PBL scheme that we implemented in the RAMS system was the MRF-scheme documented by Hong and Pan (1996) as this parameterization has also been widely used in the mesoscale modelling and climate community Holtslag et al. (1993). We find that the representation of precipitation in the summertime is improved and especially the rainy days at the end of the simulation period are much better simulated (see Figure 2.8, and

compare this by Figure 2.6). This is caused by a more realistic distribution of water vapour and temperature through the boundary layer which subsequently impacts on the convection (not shown). It appears that the vapour and heat are better mixed throughout the PBL. The simulated PBL height is more in agreement with PBL heights that are normally observed in the Netherlands. The precipitation in the wintertime was well simulated by the model with the MY parameterization. However, in wintertime the results with the MRF scheme deteriorated even further.

Even though, based on these control runs some details in the modeling system could be improved, for comparison purposes we decided to leave the control simulation as it is. The anticipated results of the impact assessment studies and the differences between the various configurations and the control simulations are thought not to be affected much by these model biases.

2.5 Impact assessment of land use and topography configurations

This section deals with the difference between the control run (CTRL) and the various land configurations This section deals with the difference between the control run (CTRL) and the various land configurations (NF, NT, NFT). All simulations use the same meteorological initial and boundary conditions. The idea is that changes in land cover leads to changes in evaporation and turbulence which has its direct impact on the boundary layer height and the process which form clouds and precipitation. The topography has its effect on wind pattern and convergence of vapour which feeds through the mxing in the boundary layer to cloud formation and precipitation.

The analyses will first focus on the differences in simulated precipitation. This is followed by the simulated effects of the configurations on the energy balance and the partitioning of energy over the various heat fluxes. Correlating the changes at the land surface with simulated changes in atmospheric variables completes the analysis. The hypothesis is that changes in precipitation in the various configurations are caused by changes in vertical windspeed, vapour convergence and evaporation which is, on its turn, caused by changes in the partitioning of energy at the land surface.
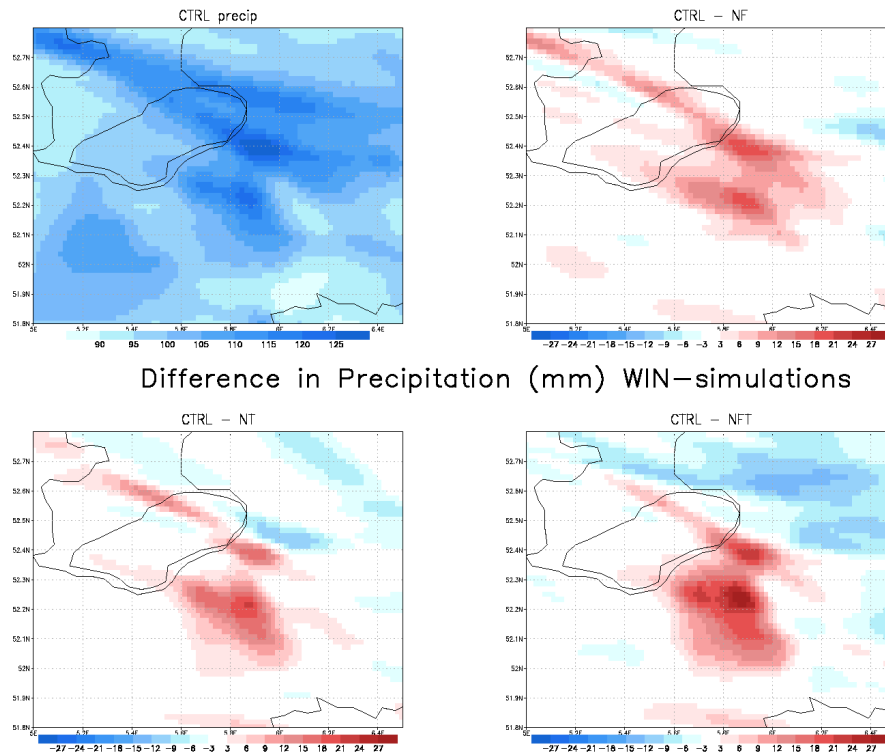
Figure 2.9: Top left graph: simulated cumulative precipitation (mm) at the end of the WIN-simulation; top right: difference between simulated precipitation between CTRL and NF (P_{CTRL}-P_{NF}); bottom left: difference between simulated precipitation between CTRL and NT (P_{CTRL}-P_{NT}); bottom right: difference between simulated precipitation between CTRL and NFT (P_{CTRL}-P_{NFT})

2.5.1 Precipitation

Figures 2.9 and 2.10 display, besides the simulated monthly precipitation sum in the control simulation, the spatial differences in precipitation between the configuration simulations and the control simulation for respectively the winter and summer period. For both periods the configuration simulations show a decrease in precipitation for the Veluwe region compared to the control simulation. This signal is stronger in winter than in summer time with the model simulating for all configurations less rainfall in winter than in the summer simulation compared to the control simulations.

Difference in Precipitation (mm) SUM−simulations
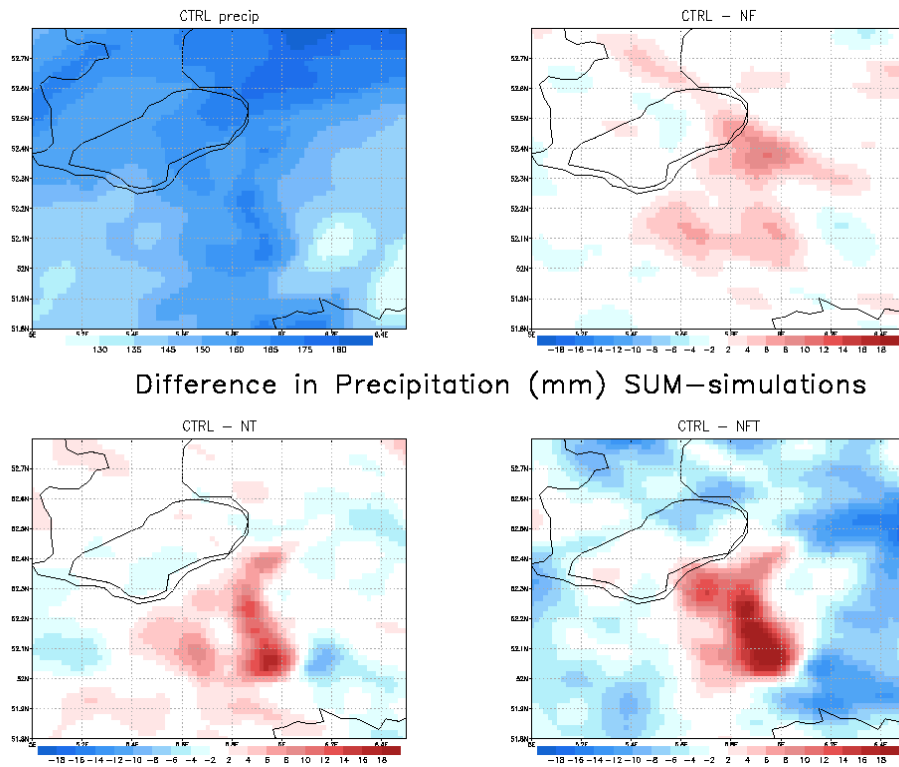
Figure 2.10: Top left graph: simulated cumulative precipitation (mm) at the end of the SUM-simulation; top right: difference between simulated precipitation between CTRL and NF (P_{CTRL}-P_{NF}); bottom left: difference between simulated precipitation between CTRL and NT (P_{CTRL}-P_{NT}); bottom right: difference between simulated precipitation between CTRL and NFT (P_{CTRL}-P_{NFT})

The spatial differences between the configuration simulations and the control simulation are clearly visible. Figure 2.9 shows that a decrease in precipitation in the winter simulation is simulated more to the north/northwest of the Veluwe. This has mainly to do with the passage of a strong depression on 17 February which crosses The Netherlands from the northwest. Due to the change in land use and topography this depression takes a slightly different route. Consequently, this results in a difference in precipitation upstream of the Veluwe which is ordered in bands with a north-western orientation. The spatial differences in the summer simulations show that the differences are more limited to the Veluwe area. The difference in precipitation between NT and CTRL is limited to the area where the topography has been removed and is located in the same location for both winter and summer simulation. The

Table 2.6: Accumulated simulated precipitation (mm) for winter and summer simulations. The abbreviations are referred to in the text

Period	CTRL	NF	NT	NFT
Feb 2000	106.4	100.2	101.7	98.3
May 2005	155.7	152.5	152.4	151.1

difference in precipitation between NF and CTRL does not show such a clear spatial pattern, but shows a more diffuse view of the difference in precipitation.

Table 2.6 shows the average of precipitation that is simulated by the model in the box, which has been defined earlier in this paper (see also Figure 2.3). As a larger area is included the differences are not as pronounced as the more local differences mentioned above.

As already mentioned before the differences between the configurations and the control is largest in the winter situation. The signal is almost the same in both NT and NF-configuration (maximum difference of respectively 17.5% and 18.6%) and in the NTF-configuration the signal is even stronger (maximum difference: 26.3%). In the summer simulation the difference is much smaller between the control simulation and the configuration simulations (NT:10.2%, NF: 6.4%, NTF: 12.4%) and the change in topography seems to have a larger effect than the change in land use. Note that the areas surrounding the Veluwe show an increase in precipitation in NT, NF and NTF. This is a direct result of a redistribution of vapour in the model domain as the amount of vapour, originating from the input files, does not change.

2.5.2 Radiation balance

To explore the causes of the effects in the differences of precipitation between the configurations, we will first take a look at the incoming shortwave radiation, S_{in}. Table 2.7 shows, amongst others, for the configurations the difference in monthly average S_{in} in W m^{-2} between NT/NF and CTRL for both SUM and WIN. In NF S_{in} is higher in winter and summer. In NT we see a reversed signal with higher S_{in} in both winter and summer. In absolute terms the signal is smaller in wintertime than in summertime. Through the albedo this will also have an effect on the outgoing shortwave radiation, S_{out}.

The other term in the radiation balance which determines the net radiation, is the longwave radiation. The outgoing longwave radiation, L_{out}, only shows a signal in both NF configurations. This is a result of the surface temperature being influenced by the removal of the forest. In

Table 2.7: Differences between NT/NF and CTRL for S_{in} (W m^{-2}), L_{in} (W m^{-2}), L_{out} (W m^{-2}), latent heat flux (W m^{-2}, LHF), vapour convergence (VC, kg m^{-2} s^{-1}), w at ~1100 m (1/100 m s^{-1}). The differences are averaged over a box on the Veluwe (see figure 3)

	NT-SUM	**NF-SUM**	**NT-WIN**	**NF-WIN**
S_{in}	1.44	-2.96	0.76	-0.78
L_{in}	-1.46	0.28	-0.10	0.80
L_{out}	-0.058	-0.61	0.13	0.70
LHF	0.69	7.21	0.70	3.10
VC	-0.20	-0.0073	-0.13	0.03
w	-0.49	0.020	-0.61	0.0079

SUM the surface temperature is warmer in NF as the soil heats faster in a grassland than in a forest. The opposite is true in WIN when bare soil cools faster than forest-covered soil leading to colder surface temperatures in NF-WIN.

In NT-SUM we see a higher incoming longwave radiation, L_{in}, than in CTRL-SUM which is caused by more clouds in the atmosphere. The lower S_{in} in NT-SUM is also explained by this. In other configurations the effect on L_{in} is almost non-existing. The net radiation only shows strong difference between CTRL and the NF-simulations. Especially in summertime, the net radiation is for a large part of the Veluwe around 15 W m^{-2} higher in the CTRL simulation. This is caused by the outgoing shortwave radiation which is much higher in the NF simulation due to the albedo effect. The albedo changes namely from 0.1 (CTRL) to 0.2 (NF), i.e. the vegetation changing from pine forest to grassland.

The next step in the radiation balance is to analyse how the changes in the shortwave and longwave radiation components are reflected in the partitioning of the radiation into latent and sensible heat fluxes. The most obvious signal can be seen in the monthly averaged difference in latent heat flux decreasing between CTRL and NF in both summertime and wintertime (Figure 2.11). During daytime these differences can lead up to 5.8 % (SUM) and 10.5 % (WIN) of the averaged latent heat flux (CTRL). The resulting higher surface temperatures generate higher sensible heat fluxes when the Veluwe forest is removed (not shown). The largest differences in latent heat flux between CTRL and NF are in the early morning and late afternoon. The differences in the energy balance have its impact on the local temperature as well. In the summertime the monthly averaged temperature at 11 GMT increases with almost 0.5 °C when the forest is removed and decreases by just over 0.5 °C in the evening, which was also mentioned in Noilhan et al. (1991).
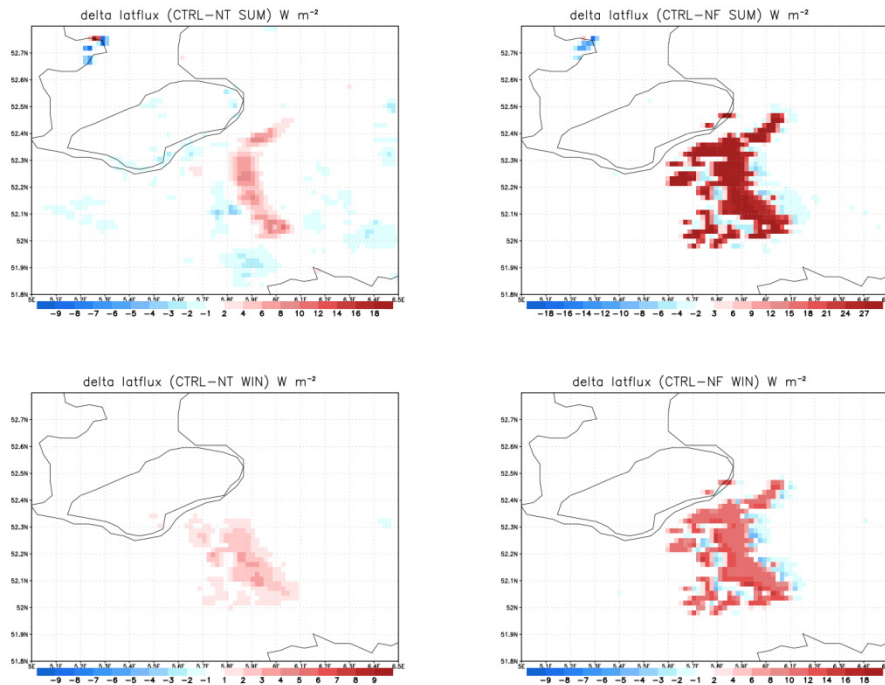
Figure 2.11: Top left graph: difference in simulated monthly averaged latent heat flux (W m^{-2}) between CTRL and NT for SUM-simulation; top right: difference in simulated monthly averaged latent heat flux (W m^{-2}) between CTRL and NF for SUM-simulation; bottom left: difference monthly averaged latent heat flux (W m^{-2}) between CTRL and NT for WIN-simulation; bottom right: difference in monthly averaged latent heat flux (W m^{-2}) between CTRL and NF for WIN-simulation

The difference in sensible and latent heat flux between CTRL and NT are not as pronounced but on the eastern side of the area where the topography has been removed the latent heat flux is lower in the NT simulation than in the CTRL simulation. This is largely explained by the lower availability of the net radiation in the NT simulation.
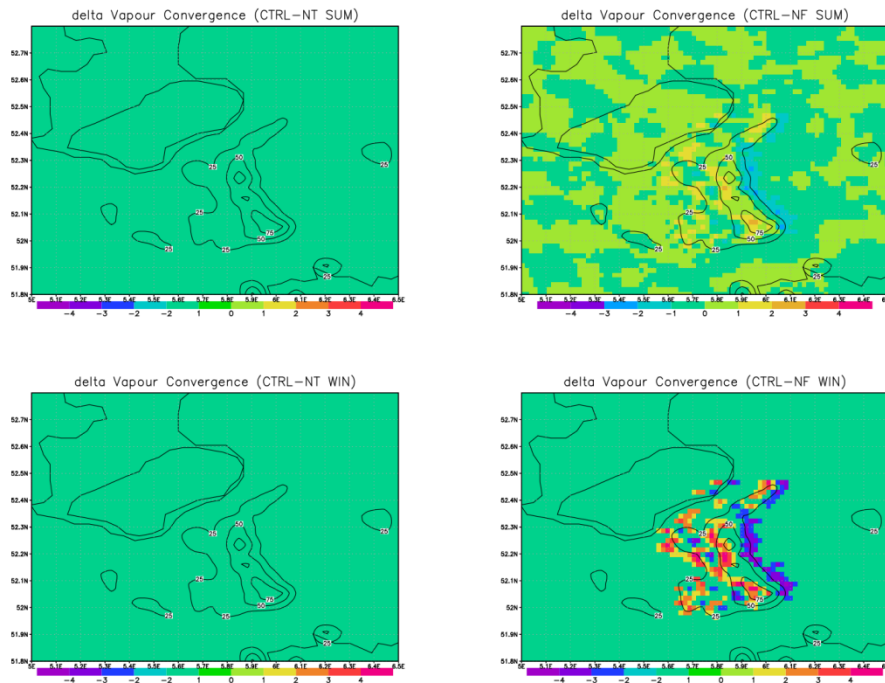
Figure 2.12: Same as Figure 2.11 for simulated monthly averaged vertically integrated vapour convergence (kg m-2 s-1) from the surface to the 850 mbar level.

2.5.3 Atmospheric dynamics

Figure 2.12 shows the effect of the removal of the topography and the forest on the vapour convergence. In both summertime and wintertime the vapour convergence in the NF simulations is lower in the area where the deforestation has taken place. This is a direct result of a change in the roughness length which leads in NF to a more gradual transition between the area which has been deforested and the surrounding area. The deforested area has mostly the same land cover characteristics (grass) as the surrounding area. Figure 2.12 and Table 2.7 also shows that the difference in vapour convergence between CTRL and NF is a factor 2 to 3 higher in wintertime. This is related to the character of the weather systems which influence the distribution of vapour in the atmosphere and the wind vectors (frontal vs convection). The difference in vapour convergence between CTRL and NT is also present but only at the leeside of the Veluwe area. The absence of downward motion in NT does also mean that divergence is likely to occur in the lower parts of the atmosphere.

In the CTRL simulation the vertical windspeed is downward at the eastern side of the Veluwe (Figure 2.13), which is in most cases also the leeside of the Veluwe as most of the weather is coming from the western direction. This downward motion prohibits to a certain extent the formation of clouds. In the NT simulation the vertical velocity is not influenced by any topographical features and therefore does not obstruct the formation of clouds in the eastern part of the Veluwe in the NT configurations. Table 2.7 shows that in both NT-configurations the net effect is that the vertical windspeed is suppressed by removing the topography.

The removal of vegetation also has its effect on the vertical velocity in the lower atmosphere as is displayed in Figure 2.13 although the effect is smaller than in NT. The only effect that can be seen is that the location of the positive windspeeds and negative windspeeds on respectively the windward side and leeward side. Under influence of the change in land use both are shifted more to the east (downstream). The presence of the forest would lead to smooth-rough transitions between grassland and forest and which, according to Andre et al. (1989), would lead to increased turbulence at these transitions. In wintertime the
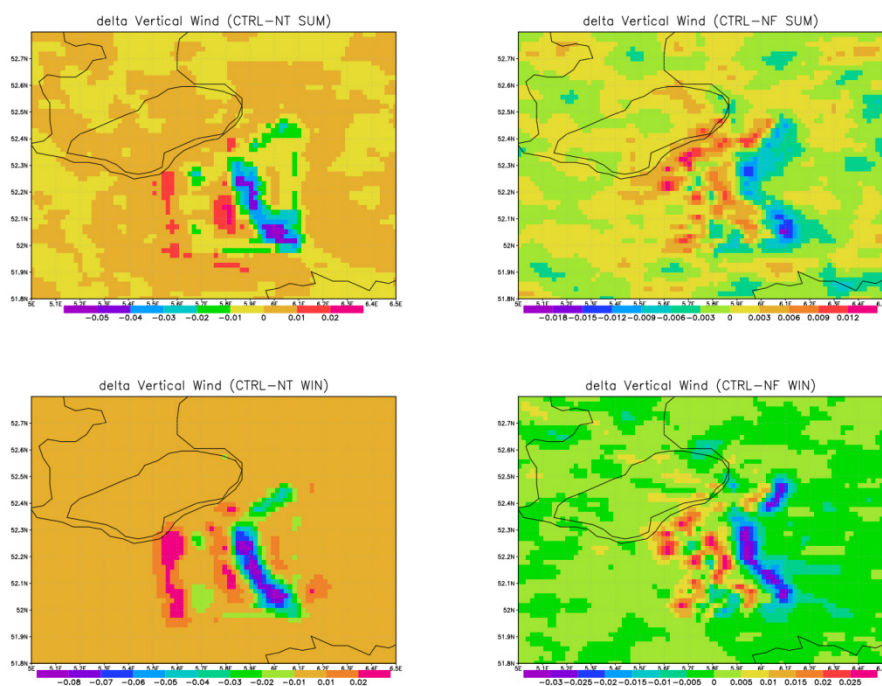
Figure 2.13: Same as Figure 2.11 for simulated monthly averaged vertical windspeed at 1100 m (m s^{-1})
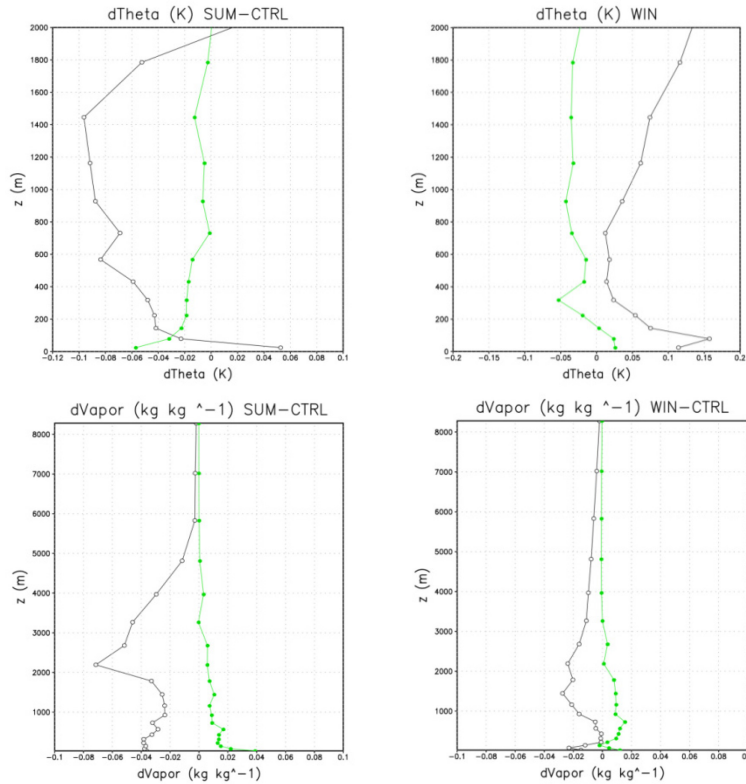
Figure 2.14: Vertical profiles of differences between potential temperature (upper two panels) and mixing ratio (lower two panels). The difference is evaluated as CTRL-NT (black lines) or CTRL-NF (green lines).

difference in vertical motions between NF and CTRL is stronger than in summertime. The influence of land use on the passage of frontal systems is stronger with regards to vertical windspeed than in more convective circumstances.

Figure 2.14 shows vertical profiles of the potential temperature, θ (K), and of the vapour mixing ratio (kg kg^{-1}). This figure shows an average of all vertical profiles at 12:00 GMT during the simulation period for the Loobos site. These graphs show that in summertime both NT and NF configuration are warmer than the CTRL throughout the PBL and that the NT configuration is remarkably wetter. From our analysis we can conclude that in convective condition the boundary layer in NF is higher than in CTRL. The effect of NT on the depth of the PBL is hardly noticeable in the summer simulations, although the PBL is wetter in NT than in CTRL. It is expected that NF is drier as the Veluwe forest is a major source of moisture in the CTRL simulation. In the winter simulation the NF is also drier and NT is wetter, but less pronounced

than in SUM. The effect of NT on the vertical distribution of vapour has all to do with the aforementioned absence of downward vertical motion which is drier air.

2.6 Discussion and conclusions

In this paper we analysed the relative contribution of topography and land use on a precipitation maximum at the Veluwe in The Netherlands. This analysis was performed with a regional atmospheric model using different land surface configurations for two different seasons. The setup of the model followed the setup which has been earlier described by Ter Maat et al. (2010) with some minor modifications. The overall analyses suggest that the precipitation maximum at the Veluwe can only be explained by taking into account both the topography and land use. The effect of the Veluwe forest on the processes that influence precipitation is smaller in summertime conditions when the precipitation has a more convective character. In frontal conditions the forest has a more pronounced effect on local precipitation through the convergence of moisture. The effect of topography is, in the winter 17 % maximum and in summer 10%, which is quite remarkable for topography with a maximum elevation of just above 100 meter and a gradual steepness.

A regional atmospheric model, is an essential tool to study the mesoscale processes and feedbacks discussed in this paper. However, there are some shortcomings of the model in correctly simulating the summertime precipitation. The main conclusion from the sensitivity tests with the changing turbulence parameterization is that the choice for turbulence parameterization should be based on the event that needs to be modelled. From our study it appears that the selected version of RAMS using MY is doing a better job in simulating precipitation in the wintertime (frontal situation), but that the configuration with MRF is doing a better job in simulating precipitation in convective circumstances. Further research is necessary to develop a parameterization which combines the properties and skill for winter and summer. This was also concluded in a study conducted by Steeneveld et al. (2011) in which MRF and MY where compared with a special focus on the representation of the physical processes in the atmospheric boundary layer. Thus, users of regional atmospheric models should take extra care when applying a certain PBL-scheme for their simulation. It is important to note that the choice of PBL-scheme has no influence in the signal between the various configurations and the CTRL-simulations.

However, the mismatch between model and observations in the radiation terms which is still present while using both PBL-schemes

means that the effect of various radiation parameterization still needs to be quantified and that more detailed radiative transfer schemes might be necessary to realize a more realistic performance. Extra care should also be taken with the representation of the land surface (e.g. land use, topography) in regional atmospheric models.

This paper investigated the feedbacks between the land surface and the atmosphere and the effect of land use and topography on local meteorology (energy heat fluxes, total precipitation, wind flow) for an area in The Netherlands. For this location it was shown that land use and topography are boundary conditions which should be well validated before they can be implemented in a mesoscale modelling system. This does not only mean that land use classes are located correctly, but also that parameterization of these land use classes within the modelling system should be well validated. This conclusion is also valid for the representation of soils and soil moisture content within The Netherlands, or even broader on an European scale. Schar et al. (1999) already demonstrated that summertime European precipitation in a belt 1000 km wide between the wet Atlantic and the dry Mediterranean climate heavily depends upon the soil moisture content. This soil moisture feedback was not the objective of this paper but it could be taken into consideration in future work. Another important phenomenon in the area of The Netherlands is the influence of the sea surface temperature and to investigate to what extend the sea influences the precipitation processes in the coast provinces of The Netherlands. It is hypothesized that the precipitation maximum in the western part of the Netherlands is a direct result of its location close to the sea. Lenderink et al. (2009) showed the importance of sea surface temperatures on coastal rainfall with a coarse resolution model. Mesoscale modelling may give additional information on the processes which on a regional scale influence precipitation. The relative fine resolution on which mesoscale atmospheric models can be executed also means that land use and topography can be represented on this fine resolution. This means that the regional atmospheric models are a perfect platform to develop and test descriptions of processes not well described currently in regional atmospheric models.

Regional atmospheric feedbacks over land and coastal areas

Chapter 3

Simulating carbon exchange using a regional atmospheric model coupled to an advanced land-surface model

abstract

The study in this chapter is a case study to investigate what the main controlling factors are that determine atmospheric carbon dioxide content for a region in the centre of The Netherlands. We use the Regional Atmospheric Modelling System (RAMS), coupled with a land surface scheme simulating carbon, heat and momentum fluxes (SWAPS-C), and including also submodels for urban and marine fluxes, which in principle should include the dominant mechanisms and should be able to capture the relevant dynamics of the system. To validate the model, observations are used that were taken during an intensive observational campaign in central Netherlands in summer 2002. These include flux-tower observations and aircraft observations of vertical profiles and spatial fluxes of various variables.

The simulations performed with the coupled regional model (RAMS-SWAPS-C) are in good qualitative agreement with the observations. The station validation of the model demonstrates that the incoming shortwave radiation and surface fluxes of water and CO2 are well simulated. The comparison against aircraft data shows that the regional meteorology (i.e. wind, temperature) is captured well by the model. Comparing spatially explicitly simulated fluxes with aircraft observed fluxes we conclude that in general latent heat fluxes are underestimated by the model compared to the observations but that the latter exhibit large variability within all flights. Sensitivity experiments demonstrate the relevance of the urban emissions of carbon dioxide for the carbon balance in this particular region. The same tests also show the relation between uncertainties in surface fluxes and those in atmospheric concentrations.

3.1 Introduction

A large mismatch exists between our understanding and quantification of ecosystem atmosphere exchange of carbon dioxide at the local scale and that at the continental scale. In this paper we address some of the complexities emerging at intermediate scales.

Inverse modelling with global atmospheric tracer transport models has been used to obtain the magnitude and distribution of regional CO_2 fluxes from variations in observed atmospheric CO_2 concentrations. However, according to Gurney et al. (2002) no consensus has yet been reached using this method and more recent 'progress' in inversion modelling developments paradoxically has led to more divergent estimations. Gerbig et al. (2003) suggests that models require a horizontal resolution smaller than 30 km to resolve spatial variation of atmospheric CO_2 in the boundary layer over the continent.

At the local scale, eddy-flux observation sites throughout the world are trying to estimate the carbon exchange of various ecosystems within reasonable accuracy (e.g. Valentini et al. (2000), Janssens et al. (2003)). These surface fluxes show a large variability over various vegetated areas. Together with the vertical mixing in the atmosphere, these surface fluxes vary diurnally and seasonally, leading to the rectifier effect, which is difficult to capture in large scale transport models (Denning et al. (1995), Denning et al. (1999)). Earlier studies (e.g. Bakwin et al. (1995)) showed also the importance of processes like fossil fuel emission and biospheric uptake on the amplitude and magnitude of diurnal and seasonal cycles of CO_2 concentration ($[CO_2]$)

The hypothesis is that the uncertainties mentioned before can be reduced at the regional level if a good link between local and global scale can be established. A critical role at the regional level is played by the planetary boundary layer (PBL) dynamics influencing the transport of CO_2 away from the biospheric and anthropogenic sources at the surface. PBL processes that influence the local CO_2 concentration are: entrainment of free tropospheric CO_2 (de Arellano et al. (2004)); subsidence; lateral advection of air containing CO_2 and convective processes leading to boundary layer growth (Culf et al. (1997)). Local and global scales can be linked experimentally through a monitoring campaign of a certain region in spatial and temporal terms (Gioli et al. (2004), Dolman et al. (2006) and Betts et al. (1992)), preferably combined with model analyses using regional atmospheric transport models of high resolution. (Perez-Landa et al. (2007), Perez-Landa et al. (2007), Sarrat et al. (2007))

This paper will focus on modelling the regional carbon exchange of a certain region in an attempt to quantify CO_2 fluxes from various sources at the surface. The following question will be addressed: What are the main controlling factors determining atmospheric carbon dioxide concentration at a regional scale as a consequence of the different surface fluxes?

To study this regional scale interaction it is important to use land surface descriptions of appropriate complexity, that include the main controlling mechanisms and capture the relevant dynamics of the system, and to represent the real-world spatial variability in soils and vegetation. In this study we use a fully, online coupled model, basically consisting of the Regional Atmospheric Modelling System (RAMS, Pielke et al. (1992); Cotton et al. (2003)) coupled with a land surface scheme carrying carbon, heat and momentum fluxes (SWAPS-C, Soil Water Atmosphere Plant System-Carbon, Ashby (1999); Hanan et al. (1998); Hanan (2001)). Area of interest is The Netherlands where in 2002 an intensive, two week measurement campaign was held , as part of the EU-financed project RECAB ("Regional Assessment and monitoring of the CArbo Balance within Europe"). The ensuing database has been used to calibrate and validate the models used in the present study.

First, a description of the modelling system will be given, together with the various databases (e.g. anthropogenic emissions) that are incorporated in the atmospheric model and how some of these databases are downscaled in time and space. A short description of the measurement campaign will also be provided, detailing the various observations taken and followed by a summary of the synoptic weather during the campaign.

Next, the results of the coupled model will be presented and compared with the observations. This paper will conclude with a discussion of these results in terms of the factors that control the carbon dioxide content at a regional scale.

3.2 Description of methods/ observations

3.2.1 Modelling system

The forward modelling system used in this study is the RAMS model version 4.3. The model is 3D, non-hydrostatic, based on fundamental equations of fluid dynamics and includes a terrain following vertical coordinate system. Together with its nesting options these allow it to be
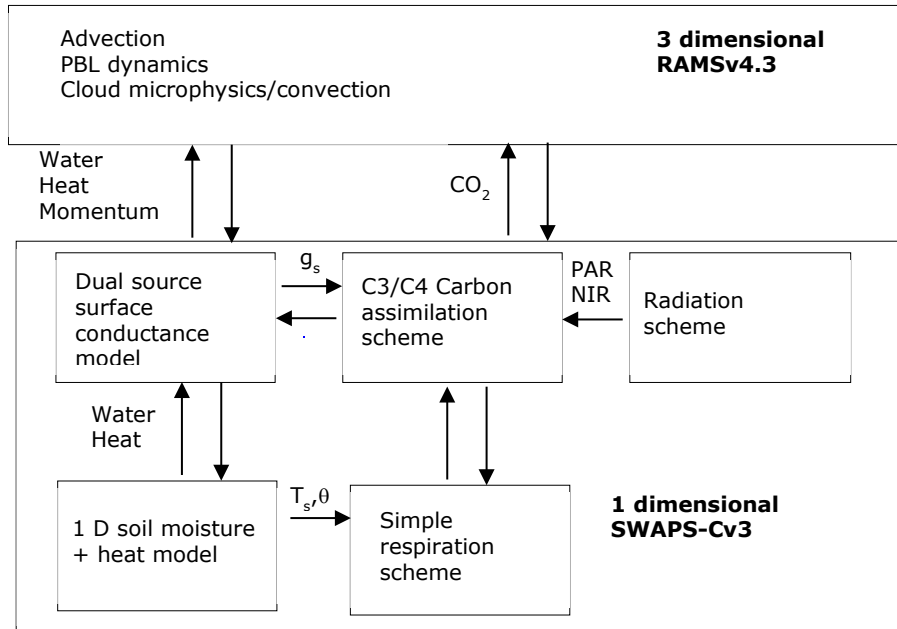
Figure 3.1: Schematic of the coupling between RAMS and SWAPS-C. The main interactions between submodels is also given together with the variables with g_s – surface conductance, T_s – surface temperature, θ – soil moisture, PAR – photosynthetically active radiation, NIR – near infrared radiation

used in high resolution modes. RAMS allows for passive atmospheric transport of any number of scalars and this has been implemented for CO_2. Amongst other reasons we therefore coupled RAMS to SWAPS-C that simulates CO_2 fluxes from assimilation and respiration. The land surface scheme uses the tile-approach for treating subgrid variability in vegetation and soils, in our implementation 4 tiles per grid box (1 water tile and 3 land tiles). The coupling has been implemented in such a way that both models retain full functionality (Figure 3.1). The standalone version of SWAPS-C allows easy calibration of its parameters on measured flux datasets.

Surface layer turbulent mixing follows the standard formulation in RAMS and uses identical diffusion parameterisations for all three scalars (temperature, humidity and CO_2). Unlike the other scalars, temperature and water vapour, atmospheric CO_2 fields in this implementation are not nudged to some pre-determined large scale analysis during long model integrations. Instead a different approach was followed using the interactive nesting routine in RAMS. The smallest domain has been nested in two larger domains and the atmospheric [CO_2] fields at the boundary are obtained from the parent grid (see Figure 3.2). Thus, CO_2 concentrations are free to develop, after the initial horizontal

homogeneous initialisation from (aircraft) observed concentration profiles. We assume that the spatial differences in $[CO_2]$ in the smallest domain, resulting from emissions and/or uptake at the surface, are larger than the spatial differences in background $[CO_2]$ for the smallest domain. Higher $[CO_2]$, as a result of CO_2-emissions originating from cities outside the smallest domain (e.g. London and major cities in the Ruhr Area in Germany), will also be fed back into the smallest domain through the interactive nesting routine. Observations at the observatory in Mace Head at the west coast of Ireland demonstrate the small differences in background $[CO_2]$ in relative clean air masses under Northern Hemispheric background conditions (Derwent et al. (2002)). Since our analysis focuses on the smallest domain we assume that reasonable realistic horizontal gradients and associated advective fluxes develop along its edges, as a result of flux variability at the largest scales. The typical RAMS configuration used in this study is given in Table 3.1.
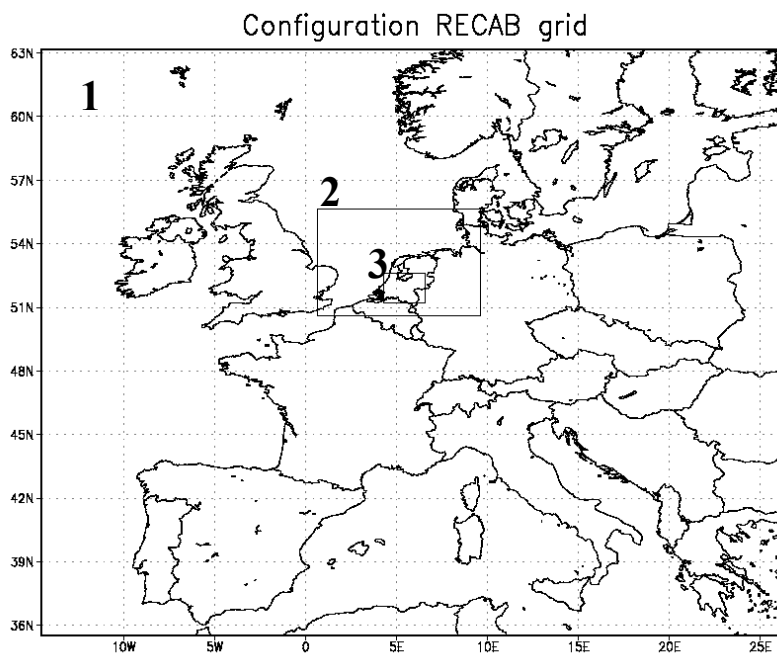
Figure 3.2: Configuration of the modelling domain. Boxes and numbers illustrate the three nested grids.

Table 3.1: RAMS4.3 configuration used in this study

Grids	1	2	3
dx, dy	48 km (83x83)	16 km (41x38)	4 km (42x42)
dt	50 s	16.7 s	16.7 s
dz	25 – 1000 m (35)		
Radiation	Harrington (1997)		
Topography	GTOPO30 (~1 km grid increment)		
Land cover	PELCOM (Mücher et al. (2001))		
Land surface	SWAPS-C (Ashby (1999), Hanan et al. (1998))		
Diffusion	Mellor/Yamada (Mellor et al. (1982))		
Convection	Full microphysics package (Meyers et al. (1997))		
Forcing	ECMWF		
Nudging period	Lateral 1800 s		

RAMS is forced by analysis data from the European Centre for Medium-Range Weather Forecasts (ECMWF) global model. The grid spacing of the forcing data is 0.5 by 0.5 degree and data is available every 6 hours. Monthly sea surface temperatures (SST) have been extracted from the Met Office Hadley Centre's sea ice and sea surface temperature data set, HadISST1 (Rayner et al. (2003))

CO_2 surface fluxes come from either of three sources:
- Terrestrial biospheric fluxes simulated by SWAPS-C
- Marine biospheric fluxes computed from large scale observed partial CO_2 pressures in the marine surface layer
- Anthropogenic CO_2 emissions

Each of these will be described in the following sections

3.2.2 Terrestrial biospheric fluxes

The land surface model SWAPS-C was extended with a carbon assimilation and respiration routine. The strength of SWAPS-C (Ashby (1999)), is that within the model above- and below-ground processes are represented in similar physical details and that in earlier studies it has been shown that the model simulates energy fluxes and long-term soil moisture (Kabat et al. (1997)) very well. The model allows for three different canopy architectures with a mean canopy flow regulating interaction of fluxes from upper and lower layers (Dolman (1993)). Photosynthesis and respiration are parameterised using the equations used by Collatz et al. (1992), Hanan et al. (1998) and Lloyd et al. (1995). Although these equations were originally developed for leaf scale, in SWAPS-C they are applied at canopy scale assuming the Table

3.2: Parameters for calculating the surface conductance and the net ecosystem exchange, classified by land use. $g_{s,max}$: maximum surface conductance (mm s^{-1}), $V_{m,ref}$: maximum catalytic capacity for Rubisco at canopy level (μmol m-2 s-1) and α the intrinsic quantum use efficiency [-].

	$g_{s,max}$ (mm s^{-1})	$V_{m,ref}$ (μmol m^{-2} s^{-1})	α (-)	
Coniferous forest	33.4	55.8	0.0384	Optimized
Deciduous forest	51.0	41.0	0.0084	Ogink-Hendriks (1995), Knorr (2000)
Grass	25.9	91.96	0.0283	Optimized
Agricultural land	25.0	39.0	0.0475	Soet et al. (2000), Knorr (2000)

canopy can be described as a 'big leaf'. Model parameters for each land use class were either objectively optimized against observed flux data (coniferous forest, grasslands) or taken from literature (deciduous forest and croplands, from e.g. Ogink-Hendriks (1995), Spieksma et al. (1997), Van Wijk et al. (2000), Soet et al. (2000), Knorr (2000), see Table 3.2). The parameters were optimized by minimizing the sum of squares of differences between model predictions and measurements using a Marquardt-Levenberg algorithm for optimization (Marquardt (1963)).

The land use map used in the model is extracted from the 1 kilometer PELCOM database (Mücher et al. (2001), Figure 3.3). Soil properties were derived from the IGBP-DIS Soil Properties database (Global Soil Data Task Group (2000)) that has a grid mesh of approximately 10 kilometers (Figure 3.4). In RAMS overlays are generated using vegetation and soil maps and then for each grid box the most frequently occurring soil-vegetation combinations are determined, which are then assigned to the number of sub-grid tiles effective in that particular implementation.

3.2.3 Marine biospheric fluxes

The exchange of carbon between ocean and atmosphere has been based on the global compilation of the partial pressure of CO_2 (pCO_2) by Takahashi et al. (1997). The reference year of this climatological database is 1990 and its grid mesh is 5 by 4 degrees on a monthly basis (see Figure 3.5). The prominent peak in October is in line with the findings of Hoppema (1991), who attributed this peak mainly to mixing of fresh water and saline North Sea water. From this seasonally varying
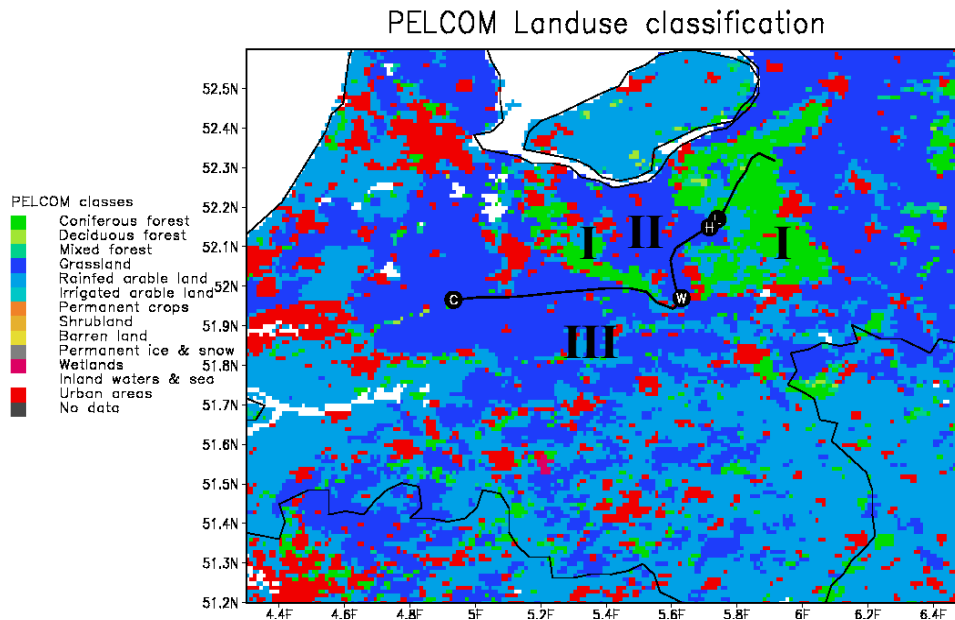
Figure 3.3: Land cover classification (based on PELCOM) for the smallest grid in the domain. Along the flight track (black line) the location of the observational sites are also given: C- Cabauw; W – Wageningen; H – Harskamp; L – Loobos. The roman numbers correspond to the areas described in the text.
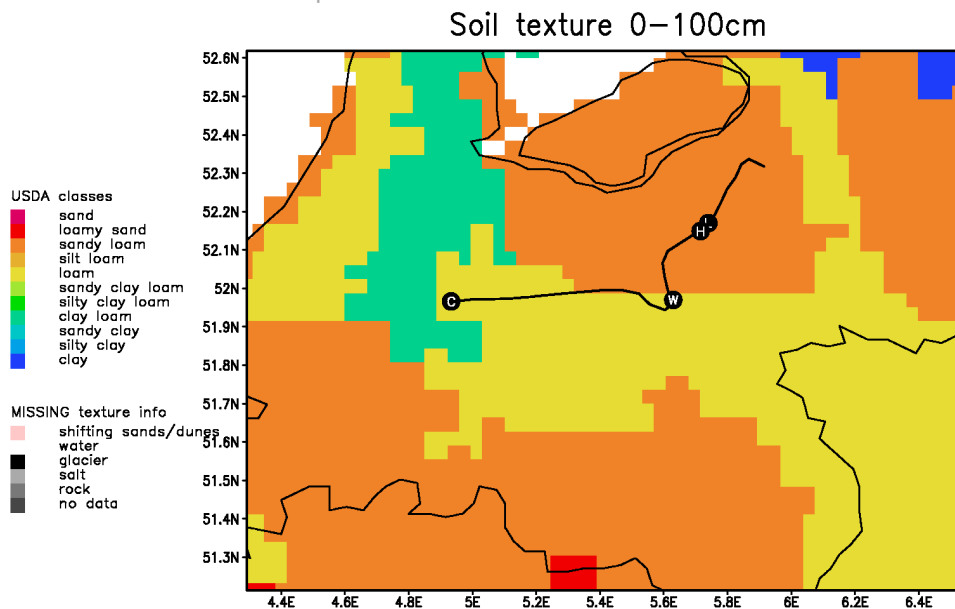
Figure 3.4: Soil classification (depth 0-100 cm) for the smallest grid in the domain. Along the flight track (given as a black line) the location of the observational sites are also given: C- Cabauw; W – Wageningen; H – Harskamp; L – Loobos.
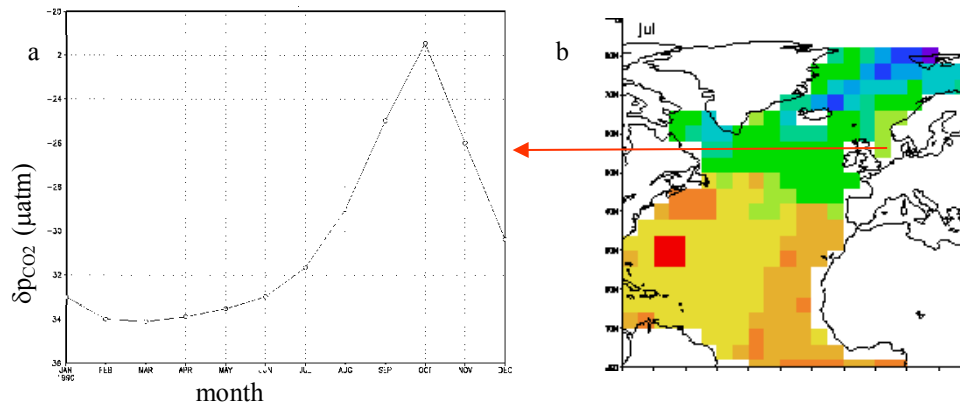
Figure 3.5: a) Monthly dynamics of δpCO_2 (μatm; 1 atm=1.01325 Pa) as a time series for a pixel in the North Sea (left panel), **b)** Spatial representation of δpCO_2 for the Atlantic Ocean.

partial pressure we derive the CO_2-flux depending also on (simulated) wind speed and to a lesser degree on SST following Wanninkhof (1992) and Weiss (1974). To prevent unrealistic sharp flux jumps at grid increments higher than the original 5 by 4 degrees, we downscaled the dataset to 1 degree grid mesh by simple linear interpolation.

3.2.4 Anthropogenic CO2 emissions

Anthropogenic emissions from road transport, power generation and air traffic are important CO_2 sources in our domain. The emission inventory implemented in the RAMS/SWAPS-modelling system is the EDGAR 3.2 database (Olivier et al. (2001)). The grid mesh of this database is 1 degree and annual emissions of CO_2 are available for 1995 (see Figure 3.6). Emissions over the oceans from shipping and upper-air emissions from air traffic are neglected in this process.

To get a better spatial representation of anthropogenic emissions, these emissions are downscaled in space. This is done by equally distributing the emissions of a particular 1 by 1 degree grid box over all the 1 by 1 kilometer urban pixels in the land cover map. Mismatches due to differing land-sea masks at different grid increments have been solved by distributing the emission of an EDGAR pixel found over sea over its neighbouring land pixels following knowledge of the local situation.

The emissions are also disaggregated in time and here a distinction is made between the 'mobile' emissions (mostly road transport) and non-
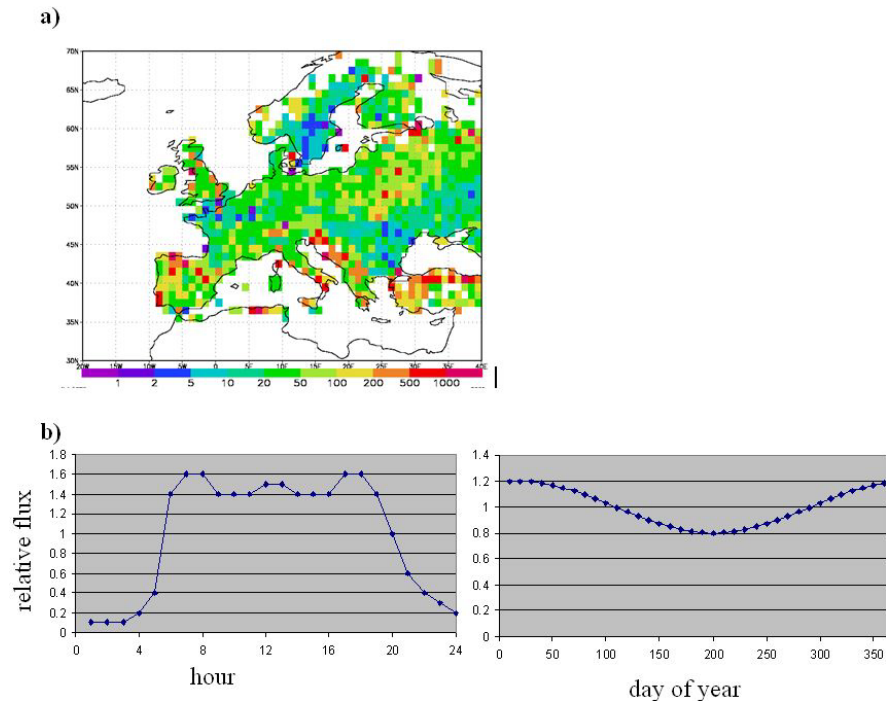
Figure 3.6: a) Anthropogenic CO_2 flux (terrestrial only) in μmol m^{-2} s^{-1} from EDGAR database version 3.2, **b)** Temporal disaggregation of these emissions: mobile emissions (left) vary diurnally, non-mobile emissions (right) vary seasonally. Note that the emission is per m^2 urban area per pixel.

mobile emissions (industry, energy and small combustion and residential). For mobile emissions a diurnal cycle is assumed with no seasonal cycle where as for the non-mobile emissions a seasonal cycle is assumed with no diurnal cycle. Both graphs in Figure 3.6 show the relative contribution of that category to the emission. In the mobile emissions clearly a higher emission value can be seen during rush hours in the morning and evenings and almost no emission during night time. The shape of this graph is based upon work done by Wickert (2001) and Kuhlwein et al. (2002). For the non-mobile emissions a different pattern can be seen with higher emissions for Europe during wintertime as a result of higher heating rates.

3.2.5 Region

The simulations are performed for the RECAB summer campaign which was held between 8 and 28 July 2002. The experimental region comprises a big part of the centre of The Netherlands, measuring 70 km

diagonally between the flux tower of Loobos and the tall tower of Cabauw. Figures 3.3 and 3.4 both show the location of both towers together with other observational sites (Haarweg-site in Wageningen and Harskamp) which were used during the campaign. These figures also show the land use cover and the soil map of the area. On these maps four major landscape units can be distinguished (Roman numbers on Figure 3.3):

- hilly glacial deposits of coarse texture mainly covered by various forest types (evergreen needle leaf, deciduous broadleaf and mixed); maximum altitude 110 meters above mean sea level (area I)
- agricultural land dominated by a mixture of grassland and maize crops on mostly sandy soils in between the hilly glacial deposits (area II)
- very low lying, wet grassland on clay and/or peat soils, mostly along the major rivers to the south of the line Wageningen – Cabauw. (area III)
- urban areas (bright red areas in Figure 3.3)

The region has a maritime temperate climate. During the campaign the local weather was rather unstable, cloudy and slightly colder and wetter than average. The maximum temperature dropped to values well below 20 °C at three days in the campaign and only in the final days of the campaign the temperature started to rise strongly to maximum values of 25-30 °C. The prolonged period of cold weather was accompanied with cloudy circumstances from time to time, leading to precipitation. At Loobos a total of 14.2 mm was measured during this period. During this colder period it was impossible for the aircrafts to do proper measurements and therefore flying days were limited to the starting days and ending days of the campaign.

3.2.6 Observations

Campaignwise observations have been made of:

- fluxes of CO_2 between land and atmosphere deploying permanent (3) and mobile (1) eddy-correlation flux towers (see Table 3.3). aircraft fluxes of momentum, latent and sensible heat, and CO_2 performed with the eddy covariance technique, using a low-flying aircraft (Sky Arrow ERA). Flight altitude was 80 m above ground

Table 3.3: Description of observational sites during the RECAB campaign

Site	Location	Landuse	
Loobos	5.7439E, 52.1667N	Coniferous forest	fluxes of H,LE,CO_2; weather
Harskamp (mobile)	5.7157E, 52.1491N	Maize (Agricultural land)	fluxes of H,LE,CO_2; weather
Wageningen	5.628E, 51.977N	Grassland	fluxes of H,LE,CO_2; weather
Cabauw	4.927E, 51.971N	Grassland	fluxes of H,LE,CO_2; weather; concentrations of CO_2 and other GHGs

        level. The methodology and the validation of such measurements against flux towers can be found in Gioli et al. (2004).
- convective boundary layer (CBL) concentrations of CO_2 and other greenhouse gases, deploying flask-and continuous sampling from an aircraft (Piper Cherokee), and continuous sampling from the tall tower at Cabauw.

3.2.7 Aircraft fluxes uncertainty estimation

Aircraft eddy fluxes typically show a high variability, that is related to random flux errors like those induced by large convective structures, spatial heterogeneity, and transient processes like mesoscale motions. To estimate such contributions to observed variability and derive uncertainty figures, multiple passes over the same area in stationary conditions can be used (Mahrt et al. (2001)), but such an approach is possible only for small areas that can be adequately sampled in short amount of time. The experimental strategy used in RECAB was instead to fly and sample large areas comparable to regional model domains, with a small number of repetitions.

To partially overcome this limitation in characterizing uncertainty, fluxes have been computed on a 2 km spatial length, then groups of four consecutive windows over homogeneous landscape units have been averaged to derive 8 km fluxes, that are still comparable with model grid mesh. The standard deviation of such averaging process is related to random flux errors, surface heterogeneity within the 8 km length, and non stationarity of fluxes on larger time scales. This latter effect can generally be ruled out because of the short amount of time that separates the averaged 2 km windows, up to few minutes. Thus an

uncertainty estimation, mostly related to random flux error and surface heterogeneity, is derived and used to interpret the observations.

Flying days during the campaign were on 15, 16, 23, 24, 25, 26 and 27 July with the last day in the best meteorological conditions. On 15, 16, 24 and 27 July two return flights from Loobos to Cabauw were performed with the low-flying eddy-correlation flux aircraft and on 15,16 and 27 July vertical profiles were taken in the morning and in the afternoon with the aircraft performing CBL measurements. This paper will focus on the first period of the summer campaign as for these days multiple reliable observations are available to test the model.

3.3   Results and analyses

The results of the model have been compared to observations carried out during the RECAB summer campaign. First, a comparison will be made between station observations and simulated results focussing on the various fluxes between the land surface and atmosphere. Second, the observations carried out by the aircrafts are compared with model results. These will be divided into comparisons of vertical profiles of CO_2 concentrations and temperatures on one hand and comparisons of latent heat, sensible heat and CO_2-fluxes along paths flown by the low-flying flux aircraft on the other. Model output is stored every hour and only output from the smallest 4 kilometer grid increment is presented. For comparison with the observational tower data, model output was taken from the grid point nearest to the observational site. Aircraft data was compared against interpolated model output using bilinear interpolation in a horizontal rectangular grid in space followed by a linear interpolation in time.

3.3.1 Validation against station observations

In the first set of graphs we compare simulated fluxes at grid and patch level with observed fluxes at the tower sites. Each grid box of a model can represent more than one land use class in the so-called tile-approach for sub-grid variability. We compare fluxes for the grid box nearest to the tower-site, and for the land cover class most resembling the land cover at the tower site. For the grid cell including the Loobos pine forest site we find the following distribution of land use classes 44% forest, 44% grassland and 11% agriculture. The same grid cell also covers the nearby Harskamp maize site. The grid cell containing the Cabauw grass site contains 100% grassland. The Wageningen

(grassland in reality) grid cell contains 56% grassland, 33% agriculture and 11% urban area.

Figure 3.7 shows a comparison of observed and simulated incoming shortwave radiation (W m^{-2}) for the Loobos and Cabauw sites, statistics are given in Table 3.4. For a number of days the agreement is very good

a)

b)
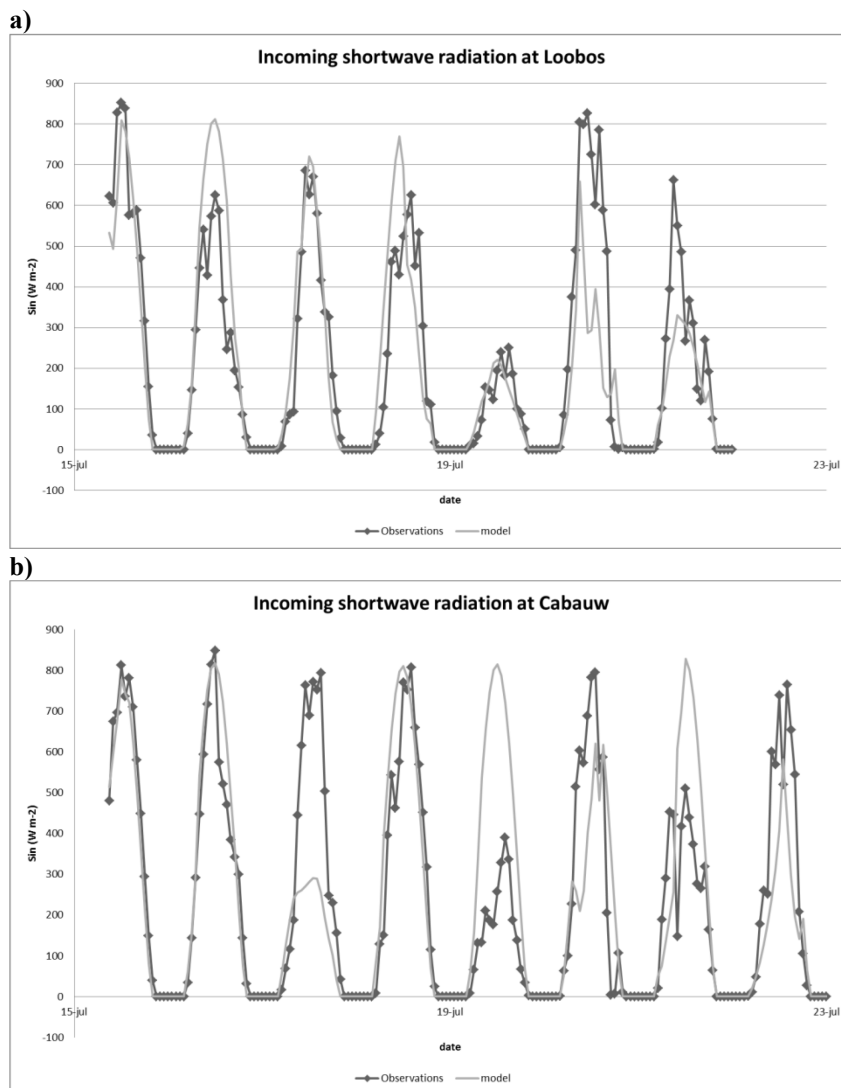
Figure 3.7: Comparison of observed and simulated incoming shortwave radiation fluxes (W m^{-2}) at the Loobos and Cabauw sites. Diamonds and dotted lines: observed values. Black lines simulated at a grid point nearest to the Loobos site and representing the appropriate tile. Tick marks are placed at 0:00 hours, same for figure 8, 9 and 14.

Table 3.4: Statistical analysis of simulated against observed shortwave incoming radiation (W m-2), latent heat flux (W m-2) and net ecosystem exchange (μmol m-2 s-1). These statistics are based on hourly observations and simulated results for the period 15 July 2002 – 29 July 2002

Incoming shortwave radiation			
Site	**RMSE**	**Slope**	**r^2 (corr coeff)**
Loobos	138.492	0.792	0.708
Cabauw	187.443	0.778	0.591
Wageningen	158.728	0.739	0.621
Latent heat flux			
Site	**RMSE**	**Slope**	**r^2 (corr coeff)**
Loobos	53.693	0.704	0.578
Cabauw	56.783	0.618	0.485
Wageningen	78.536	0.470	0.584
Harskamp	64.053	0.821	0.693
Net ecosystem Exchange			
Site	**RMSE**	**Slope**	**r^2 (corr coeff)**
Loobos	5.249	0.583	0.648
Cabauw	4.515	0.530	0.707
Wageningen	5.070	0.452	0.702

at both sites, but for other days the model underestimates the global radiation. This is mostly due to a misrepresentation of the exact location and timing of the passage of various simulated cloud systems., As mentioned before the local weather was rather unstable. For example, the second day in the simulation (16 July) was a day with clear conditions in most of The Netherlands except for the eastern part. This is reflected in the observations at Loobos compared to the observed incoming shortwave radiation at Cabauw. However, the model simulates clear conditions not only for the western part but also for the eastern part of The Netherlands with cloudy conditions simulated approximately 50 kilometers east of Loobos site. Comparisons with other sites show similar results. Overall the incoming shortwave radiation is underestimated by 20-25 % at Loobos, Cabauw and Wageningen with a correlation coefficient (r^2) varying between 0.591 and 0.708 (Table 3.4).

Since largely determined by available solar energy, similar patterns can be found in the comparison between observations and model for the latent heat flux (W m^{-2}). Figure 3.8 shows the observed and simulated

latent heat flux for the three main land use types: needle leaf forest (Loobos), grassland (Wageningen) and agricultural land (Harskamp). In general, evaporation is underestimated by 20-35 %, much like shortwave radiation. Only for the Wageningen grassland site the evaporation is underestimated by twice as much as the driving radiation is.

a)

b)

c)
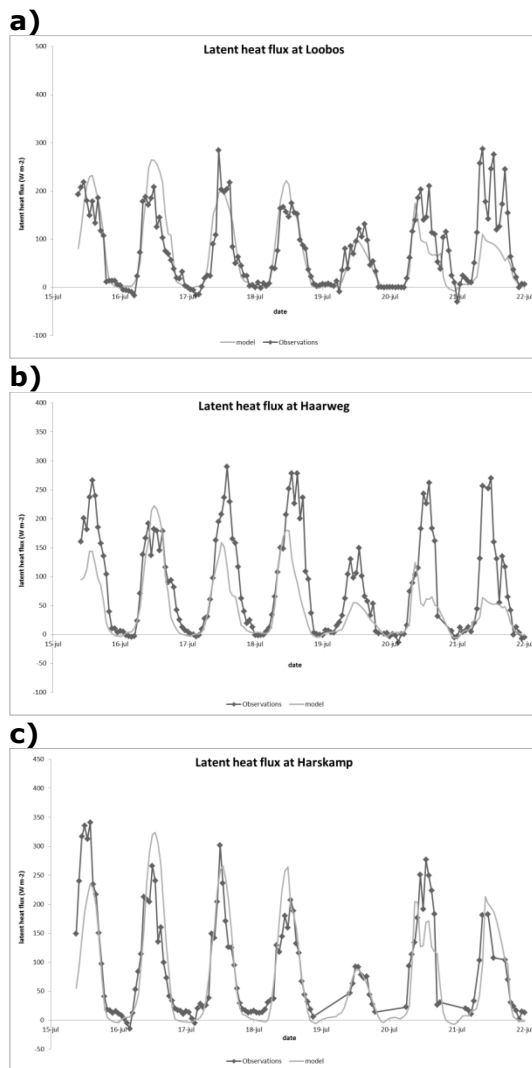
Figure 3.8: Comparison of observed and simulated latent heat fluxes (W m^{-2}) for Loobos (a., forest site), Wageningen (b., grass site) and Harskamp (c., maize site). Black: observed values; grey: simulated at a gridpoint nearest to the observational site and representing the appropriate tile.

66

a)

b)

Figure 3.9: Comparison of observed and simulated CO_2 fluxes (μmol m^{-2} s^{-1}) for Loobos (a.) and Wageningen (b.). Diamonds and dotted lines: observed values; black lines simulated at a gridpoint nearest to the observational site and representing the appropriate tile.

Simulated CO_2 fluxes (μmol m^{-2} s^{-1}) are compared with observations in Figure 3.9. Only the Loobos and Wageningen sites are displayed here, as the CO_2 observations of the Harskamp site were limited in this period due to problems with the measurement instrument. However, for this

site from the few data available we can conclude that the simulated CO_2 uptake of the maize is underestimated as a result of the generic parameter values obtained from literature (Knorr (2000)). This lack of observational data made it impossible to derive correct parameter values for the maize-site in Harskamp. Another complication is that PELCOM does not discriminate between specific crops in the PELCOM classes of rain fed or irrigated arable land (see Figure 3.3). The simulated net ecosystem exchange (NEE, μmol m^{-2} s^{-1}) is simulated well for Loobos and to a lesser degree for Wageningen. At Loobos, except for some unexplained midday peaks, the simulated assimilation is quantitatively in accordance with the observations. At 19 and 20 July assimilation is underestimated by the model. During these days the model simulates for both sites a weaker photosynthesis than the observations show. Especially, 19 July is characterized by a shortwave radiation which is limited by cloud cover in both simulations and observations (see Figure 3.7). The effect of reduced shortwave radiation on the CO_2 flux appears stronger in the model than in the observations. The daytime NEE at Wageningen is on average underestimated by 2-3 μmol m^{-2} s^{-1} which is a result of an underestimation of incoming shortwave radiation by the model. Due to simulated clouds, the model simulates incoming shortwave radiation values which are 100-400 W m^{-2} lower than the observations. At the grass-sites of Wageningen and Cabauw (another grass site, not shown), the model has clearly difficulties in simulating night time respiration, but for the forest site the respiration is simulated better . The simulated respiration at Loobos is of the same order of magnitude although the model has difficulty in simulating the apparent morning respiration peak at 16 July and 19 July. Statistics displayed in Table 3.4 show that overall the absolute NEE is underestimated at Wageningen by more than 50 % which is largely explained by a structural underestimation of especially respiration.

3.3.2 Validation against aircraft observations

Figures 3.10 and 3.12 respectively show spatially explicit simulated latent heat and carbon fluxes in comparison with those observed from the flux aircraft, for 16 July around 7 AM UTC and 11 AM UTC (9 AM and 1 PM local time). The top panel of both figures show the spatial patterns of the simulated fluxes combined with an overlay of the flight track. The lower panel shows a comparison between simulated and observed fluxes in terms of both their absolute values and anomalies of the flux, defined as the deviation from the average of the total flight track. These are also normalized by the standard deviation of the data points

a)

b)
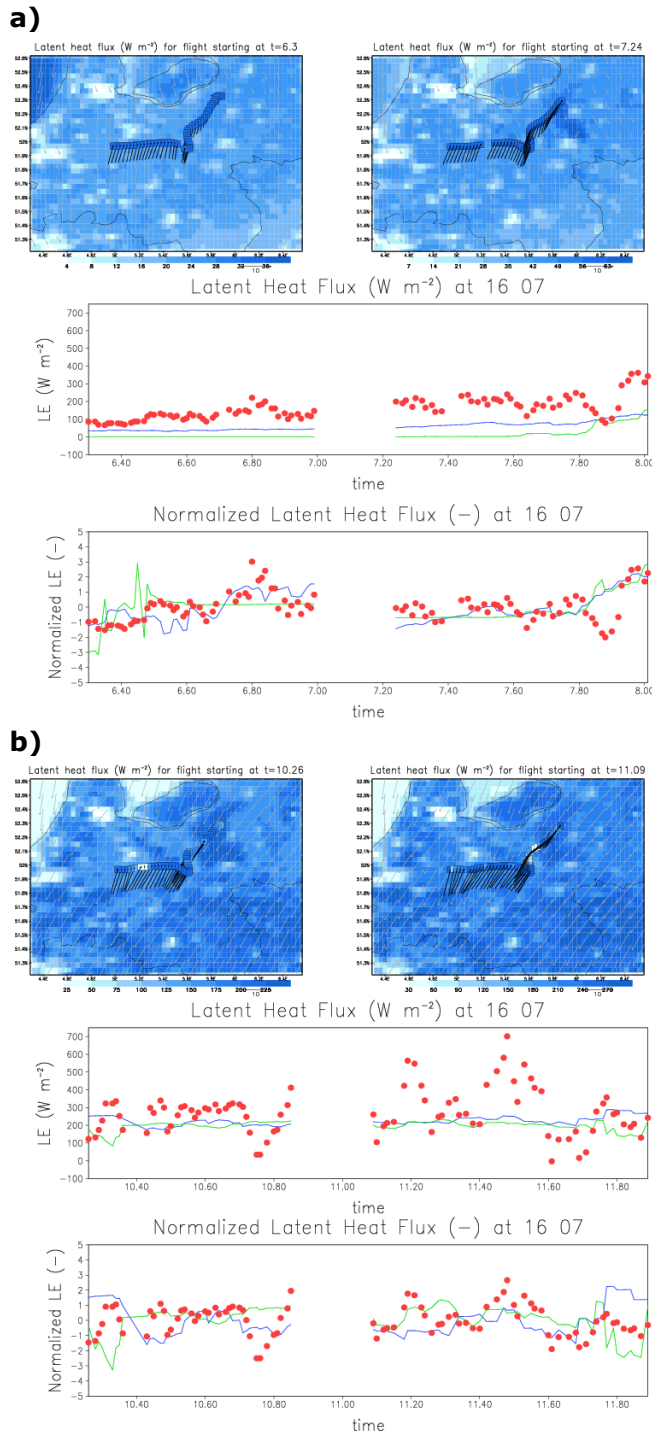
Figure 3.10: Spatial comparison of latent heat fluxes (W m^{-2}) against aircraft observations, for the flights on 16 July 2002 (a.: 6.28 UTC, 7.22 UTC; b.: 10:25 UTC, 11:07 UTC). The maps show simulated latent heat flux at the surface and wind vectors (gray). Superimposed on that is the flight track with observed fluxes (squares) in the same colour coding as the background map, plus aircraft observed windvectors (black). The lower plots in a. and b. show the aircraft observed fluxes (red dots), simulated fluxes at the surface (dark blue) and at flying altitude (green) in terms of both their absolute values and anomalies of the flux which is defined as the deviation from the average of the total flight track divided by the standard deviation. Simulated fluxes have been interpolated from model grid to exact location and time of flight overpass. The early flight moves from NE to SW, the return flight from SW to NE. So in the scatter plot the left side is the NE the middle the SW and the right side NE again.

Table 3.5: Landscape averaged latent heat fluxes (W m^{-2}) along the flightpath for both flights on 16 July 2002. The three landscapes (see text) are referred to according to their roman number in figure 3. *flux atm* represents the simulated flux at the same level as the flightpath, whereas *flux sfc* represents the simulated flux at the land surface below the flightpath

16/07 1st flight	I	II	III	flightpath
average obs	141.7	140.7	179.1	163.3
average flux atm	43.4	14.0	1.5	12.4
average flux sfc	73.7	60.6	53.6	59.5
16/07 2nd flight	I	II	III	flightpath
average obs	185.4	199.6	243.4	219.0
average flux atm	155.6	173.3	181.9	174.8
average flux sfc	249.6	216.1	217.9	223.2

$$F' = \frac{F - \overline{F}}{\sigma} \qquad\qquad [3.1]$$

Figures 3.10 and 3.12 demonstrate that the wind direction and speed (displayed as wind vectors) are simulated in accordance with the observations from the aircraft. Comparing spatially explicit simulated and observed fluxes shows that in general simulated latent heat fluxes are lower than observed (Figure 3.10). Table 3.5 presents the average latent heat flux per major landscape unit (I, II and III in Figure 3.3) for both flights on 16 July. The difference between observed and simulated fluxes for all landscape units is notably larger for the early morning flight on 16 July with fluxes underestimated on average for the whole flight track by almost 150 W m^{-2}. If the uncertainty is taken into account, this underestimation is reduced. However, the fact remains that the simulated flux at flight level is near zero due to a lack of turbulent diffusion. This is probably a result of a stable boundary layer in the early morning which is simulated too shallow. The discrepancy in latent heat flux between model and airplane is not in line with the validation on station level (see Figure 3.8) where latent heat flux is reasonably simulated by the model on 16 July. The average simulated latent heat flux for the second flight on 16 July is more in line with observation with a simulated latent heat flux of 174.8 W m^{-2} compared to an observed flux of 219.0 W m^{-2}. This underestimation is detected in all landscape units but is most apparent for landscape unit III (wet grassland along the river). We can also see that simulated flux divergence with height can be considerable (green and blue lines in the Figure 3.10, *flux atm* vs *flux sfc* in the Table 3.5). For the second flight

a)

b)
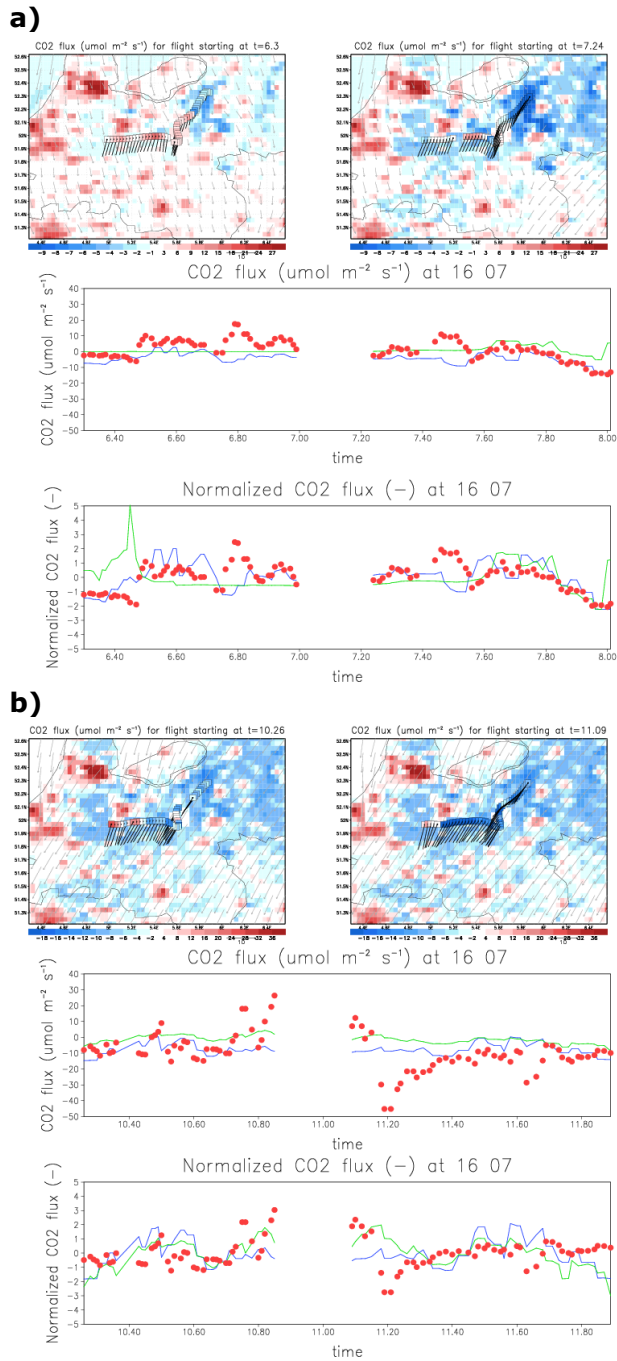
Figure 3.12: Spatial comparison of carbon fluxes (μmol m-2 s-1) against aircraft observations, for the flights on 16 July 2002 (top: 6.28 UTC, 7.22 UTC; bottom: 10:25 UTC, 11:07 UTC). Explanation of the maps is given in the caption accompanying Figure 3.10

observed values fall in between the flux magnitudes simulated at the surface and at flight altitude. However, uncertainty in observed latent heat fluxes is very large (average uncertainty of 110 W m^{-2} for first flight; 137 W m^{-2} for second flight) making it almost impossible to draw firm conclusions. This is true especially for the afternoon flight of July 16, where high variability in incoming radiation is also present, possibly inducing non stationary conditions even within the relatively small averaging lengths, and holds for other latent heat flux observations of aircraft measurements during the observational campaign. Especially mid-day flights around local noon often exhibit an uncertainty estimation that can be larger than the flux itself. For morning and afternoon flights the variation is generally somewhat reduced. Figure 3.11 shows the typical uncertainty in aircraft observed latent heat and CO_2 flux graphically for both flights at 16 July 2002 .

The spatially simulated CO_2-fluxes are compared in Figure 3.12 with the observations from the aircraft. From the comparison between simulated trends in results and observations a similar pattern can be seen, with a

Airborne observations of CO_2 Flux (μmol m^{-2}s^{-1}) at 16 July 2002
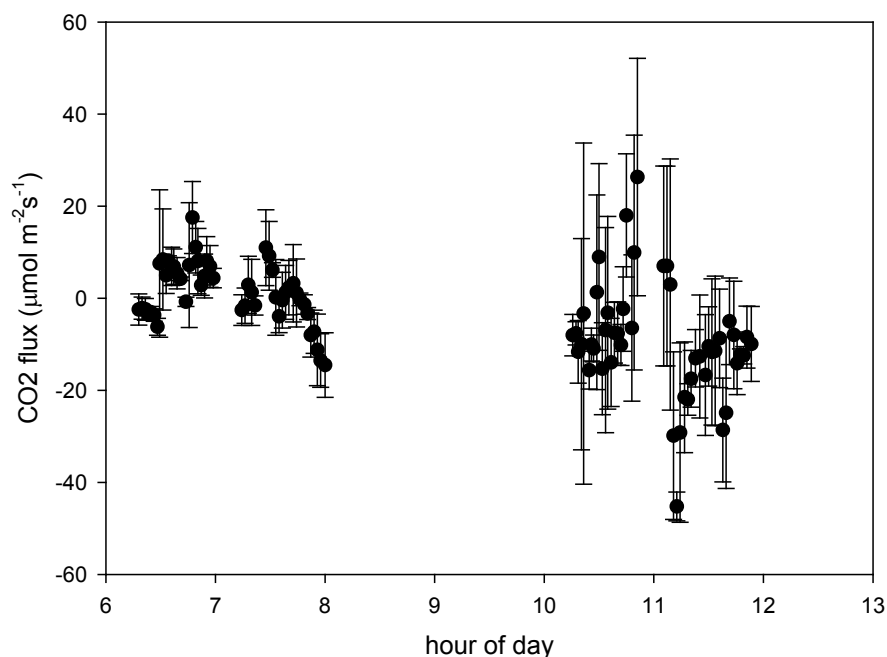
Figure 3.11: Airborne observations of latent heat flux (W m^{-2}) and CO_2 flux (μmol m^{-2} s^{-1}) for 16 July 2002. The error bars represent the 95% confidence interval

larger uptake for the Veluwe area (beginning and ending of the graph in the lower panel of Figure 3.12). The top panel of both figures show absolute values of CO_2 fluxes where the blue colour coding reflects the uptake of CO_2 by the vegetation and the red colour the release of CO_2 through emission or respiration. Simulated spatial variation in CO_2-fluxes is dominated by the contrast between anthropogenic sources over urban areas and biospheric sinks over rural areas. Since the aircraft flight path was obligatory avoiding build-up areas (for safety reasons), it could not capture the largest contrasts in this environment. The landscape feature that is rather consistently resolved in both model and observations and in both latent heat and CO_2 fluxes is the large forest area of the Veluwe, located in the eastern part of the domain. Averaged along the flight track (Table 3.6) we see that the simulated CO_2 flux is comparable with the observed flux for the early morning flight. The observations show only a stronger downward flux of CO_2 compared to the simulated values above the forested area. This is partly compensated by a stronger simulated downward flux of CO_2 above the wet grassland along the rivers. Due to the near-absence of turbulent diffusion in the early morning at levels above the surface both latent heat and CO_2 fluxes at flight level are underestimated by the model as is shown by the line graphs in both figures 3.10 and 3.12. Looking at the trends of CO_2-fluxes along the flight path the model captures the various landscape elements with negative fluxes simulated at the end of the return flight of the airplane.

During the field campaign profiles of various variables were measured using an aircraft. Figures 3.13 and 3.14 show the comparisons between, respectively, potential temperature (K) and CO_2 concentration (ppm) for four timeslots during 16 July when the profiles were measured. The profiles are measured at various locations in central-Netherlands. Comparing potential temperature profiles we can observe that the fit between simulated and observed profiles is improving during the day.

Table 3.6: Averaged CO_2 fluxes (μmol m^{-2} s^{-1})along the flightpath for both flights on 16 July 2002. As in table 5.

16/07 1st flight	I	II	III	flightpath
average obs	-7.56	0.19	3.23	0.39
average flux atm	-0.59	1.45	0.71	0.70
average flux sfc	-8.74	-3.07	-3.51	-4.27

16/07 2nd flight	I	II	III	flightpath
average ob	-7.85	-9.16	-8.40	-8.44
average flux atm	-4.51	-1.77	0.05	-1.32
average flux sfc	-10.92	-5.10	-6.98	-7.23

The profiles measured in the vicinity of Cabauw (red – morning and blue – afternoon) show that in the morning the lower part of the atmosphere is simulated with lower potential temperature than observed. This is also true for the morning profile measured near the Loobos observational tower. The afternoon profile near Cabauw shows that the potential temperature in the lower atmosphere is simulated in accordance with measurements. The model tends to underestimate potential temperature by 1-2 K higher up in the planetary boundary layer (PBL). Simulated PBL height on 16 July stays somewhat behind reality - respectively 1200m vs. 1500m maximum. This has its direct effect on simulated $[CO_2]$ with a lower PBL height leading to higher $[CO_2]$. Although the concentration is in general overestimated by the model for this particular day, the temporal trends are simulated well by the model with a typical early morning $[CO_2]$ profile (CO_2 trapped in the lower part of the atmosphere) developing into a well-mixed profile in the afternoon.
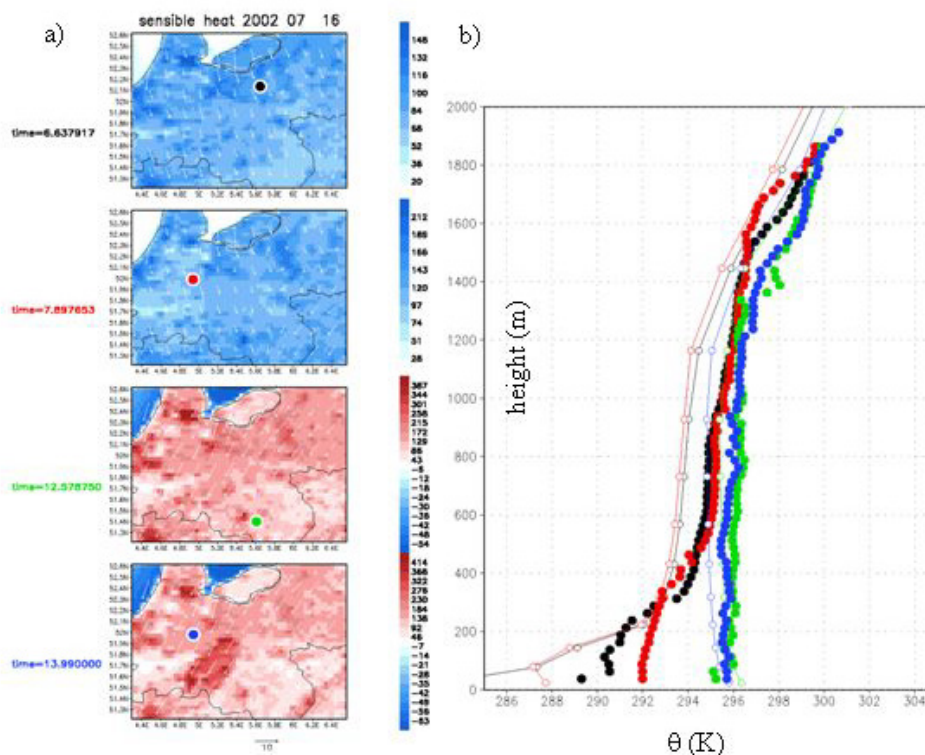
Figure 3.13: Comparison of simulated profiles of potential temperature (K) against aircraft observations. a) simulated surface sensible heat flux field at time of profile flight, with profile flight locations (coloured dots). b): observed profiles (filled dots) and simulated profiles (open circles and lines). Note that the time sequence of the profiles is black, red, green and blue.

74
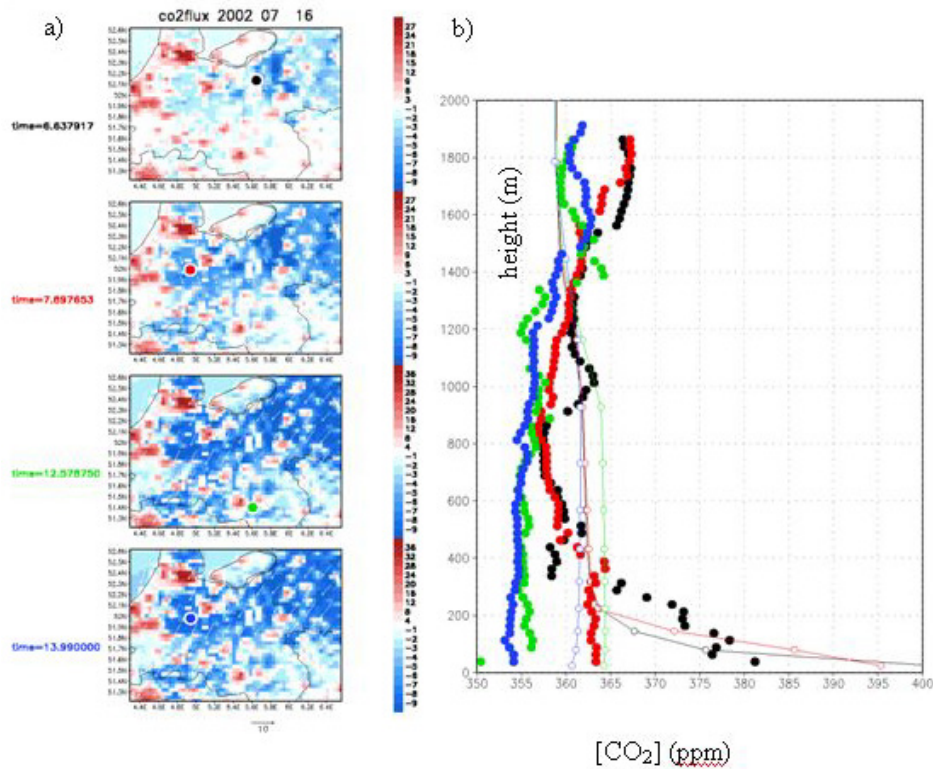
Figure 3.14: Comparison of simulated profiles of CO_2 concentration (ppm) against aircraft observations. a) simulated surface CO_2 flux at the time of the profile flight, with profile flight locations (coloured dots), b) observed profiles (filled dots) and simulated profiles (open circles and lines). Note that the time sequence of the profiles is black, red, green and blue.

Figure 3.15 shows the time series of the observed and simulated $[CO_2]$ at the 60 meter level at Cabauw. In general the model captures $[CO_2]$ dynamics well (i.e. the diurnal range), but on a number of days the simulated $[CO_2]$ is lower in the simulations than observed, on 17th and 18th mostly during night time, later on more so during daytime. Also on some days a phase lag seems to exist between simulated and observed $[CO_2]$. These discrepancies may partly be a result of an underestimated night time respiration by the model, but more likely result from the turbulence parameterization used in the model (Mellor-Yamada). The CO_2 concentration near the surface at 17 July is simulated well (not shown here) which does imply that the nighttime and early morning boundary layer is simulated too shallow by the model. The building up and the breaking down of the PBL most probably also leads to the aforementioned phase lag.

CO2 concentration at Cabauw
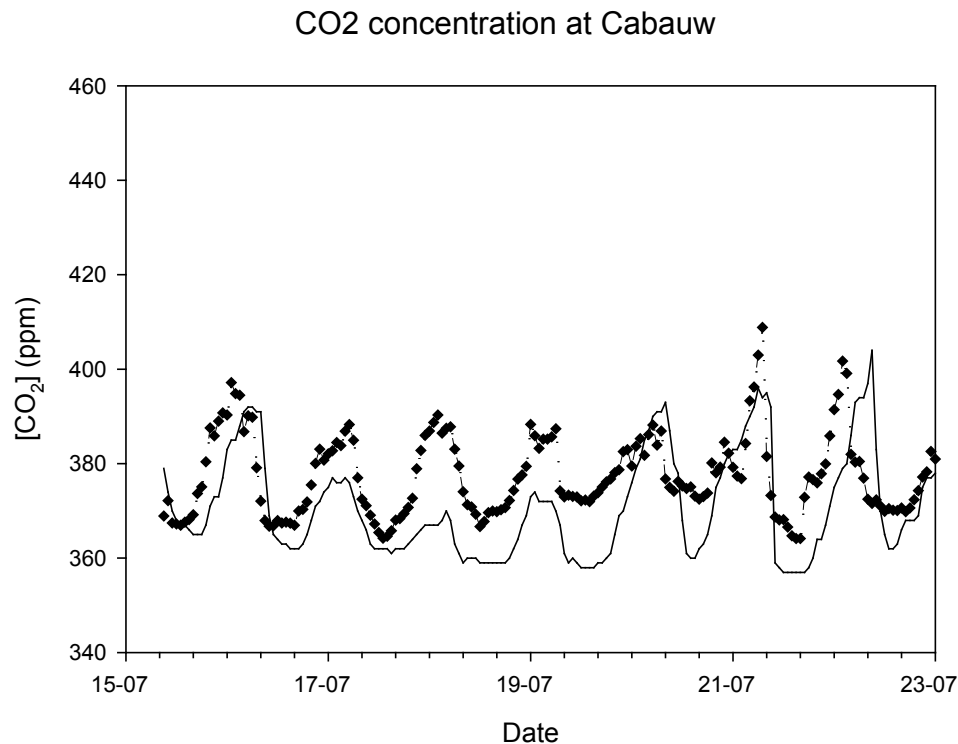
Figure 3.15: Comparison of observed and simulated [CO$_2$] (ppm) at 60 meters for Cabauw. Diamonds and dashed lines: observed values; black lines simulated at a grid point nearest to the observational site

3.3.3 Sensitivity experiments

To explore some of the controlling factors that determine [CO$_2$] two sensitivity experiments were performed for the first three days of the period. In the first simulation anthropogenic (urban) fluxes were increased by 20 % and in the second simulation a 20 % increase was given to the biogenic (all vegetation classes) fluxes. Both increases are applied on the absolute values of the fluxes. Results of both sensitivity experiments were subsequently compared with the standard experiment. This analysis suggest that the densely populated western part of the Netherlands, is more sensitive to the 20 % change in anthropogenic emissions leading to a change of more than 8 ppm in [CO$_2$] near the surface in the anthropogenic sensitivity experiment (Figure 3.16). The model simulates this change only close to the surface, limiting the impact to the lower 200 meter of the atmosphere.

The relative contribution of the biogenic sources (maximum change: 1.6 ppm, not shown) is smaller than the relative contribution of the anthropogenic emissions. The reason for this is that the anthropogenic emissions influence the concentration strongly during night-time, when accumulation is relatively strong due to low PBL heights, while biogenic uptake only takes place during day-time when PBL heights are relatively large and contributions are relatively low. Night-time anthropogenic emissions under the footprint of the tower are strong compared to the biogenic emissions. For the eastern part (surroundings of the Veluwe) the results are different. In the vicinity of the Loobos tower it appears that a 20 % change in both anthropogenic and biogenic fluxes account for an equal change in $[CO_2]$ of about 2.5 ppm during night time resulting from higher anthropogenic emissions and higher respiration of the forest (Figure 3.17). During daytime the change in $[CO_2]$ at Loobos resulting from different emissions is smaller than at Cabauw. Higher uptake of the forest reduces $[CO_2]$ as the contribution of a more assimilating forest outweighs that of the few cities on and around the Veluwe.
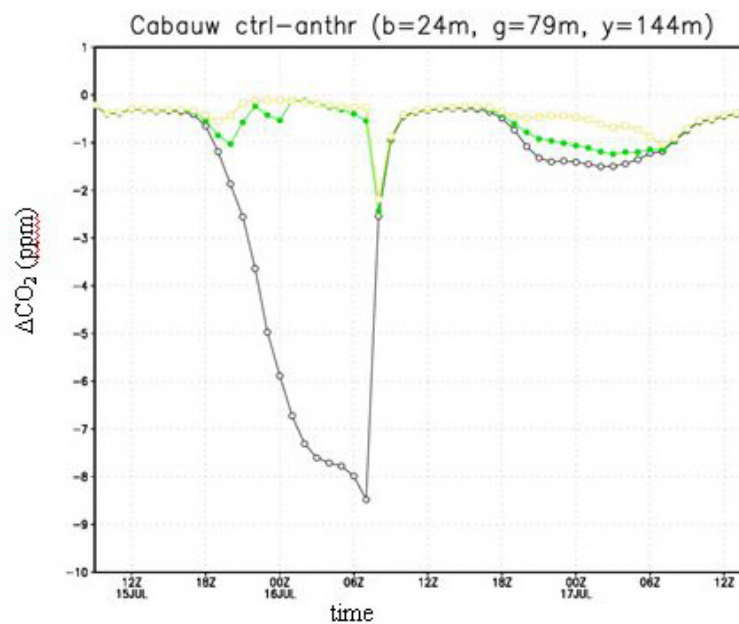
Figure 3.16: Difference in simulated $[CO_2]$ (ppm) at Cabauw between the control simulation and the simulation with an increase of 20 % in anthropogenic emissions for three heights: Black: 24 meter, green: 79 m, yellow: 144 m
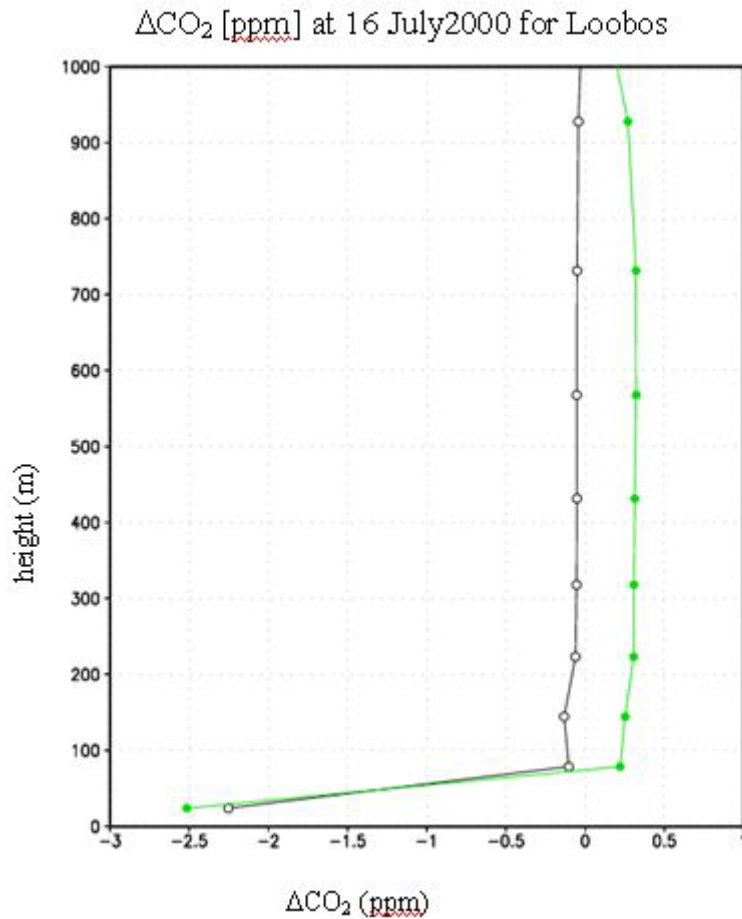
Figure 3.17: Vertical profile at Loobos (16 July 2002 0:00 GMT) of the difference in simulated $[CO_2]$ (ppm) between control simulation and a 20% increased anthropogenic emissions simulation (black) and between the control simulation and 20% increased biogenic fluxes simulation (green).

Figure 3.18 shows the important role that cities play in determining the $[CO_2]$ in The Netherlands and especially in the western part of the country. It also shows the transport of carbon dioxide in the atmosphere when western winds dominate the regional weather. This figure shows the dispersion of $[CO_2]$ rich plume originating from the cities over The Netherlands.
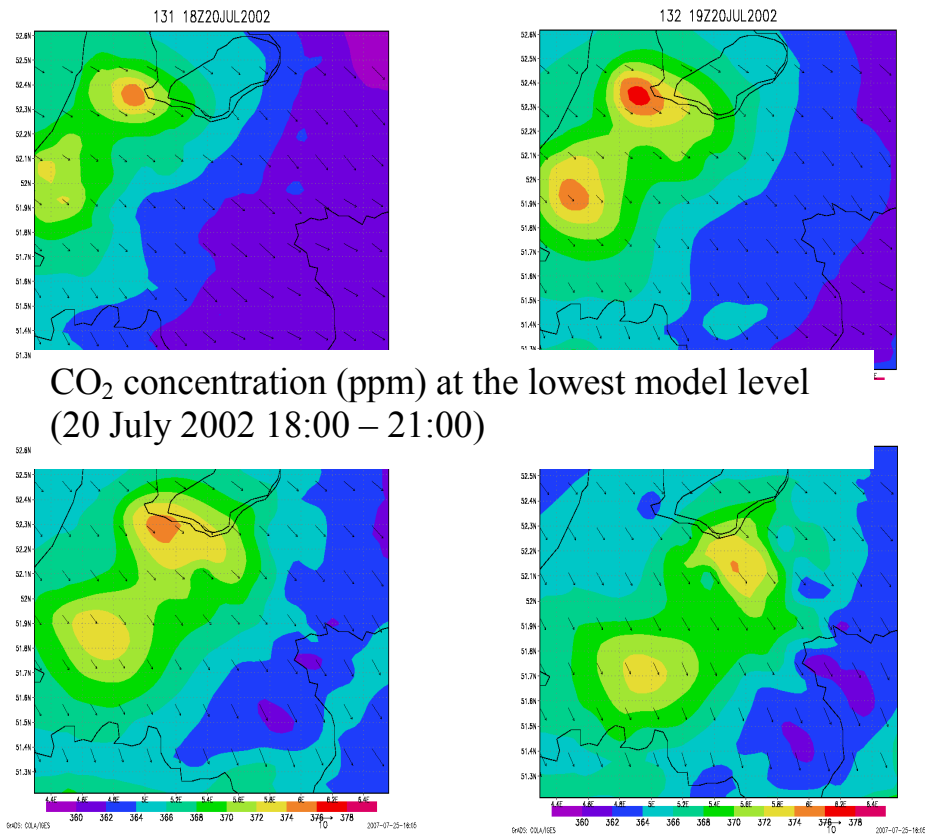
Figure 3.18: Example of CO_2 transport: snapshots of [CO_2] (ppm) at the lowest model level for 4 different times on 20 July 2002 (top left – bottom right: 18GMT – 21 GMT with hourly timesteps)

3.4 Discussion and conclusions

In a first attempt to simulate the carbon exchange on a regional scale for a heterogeneous area in The Netherlands, the coupled regional model (RAMS-SWAPS-C) is able to simulate results close to reality, but it also reveals some weaknesses requiring improvement. For the simulated period the comparison between station observations and model output looked very promising for the grass and forest sites. Latent heat flux for the agricultural site was simulated well but it appeared that the CO_2 flux, especially photosynthesis, was underestimated significantly due to underestimation of the shortwave radiation and the use of (generic) parameter values in the carbon

exchange sub model. The latter asks for observations above various land use types so that parameters that describe, amongst others, the carbon exchange of the vegetation (maize in this case) can be estimated better. This approach was taken during the CERES campaign, which was held in the early summer of 2005 (Dolman et al. (2006)), and campaigns which were set up within the framework of the The Netherlands research programme "Climate *changes* spatial planning" (Kabat et al. (2005)). These initiatives will provide the modelling community with a multitude of station observations for various land use types. In addition, land use maps should also account for this vegetation class if the difference with other vegetations is significantly large. During these campaigns observations were also taken in different parts of the year under varying meteorological conditions building on the experiences of the RECAB campaigns. This gives the modelling community an excellent opportunity to improve the calibration and validation of their models. It also helps in investigating the varying dynamics in CO_2 dispersion between summer (with active vegetation) and winter (increased importance of anthropogenic emission sources).

Another shortcoming in the comparison between the model and the observations is that the radiation at the surface is underestimated by the model especially in cloudy and unstable conditions. This in turn has its effect on the energy balance at the surface and the simulated CO_2 flux. The location and timing of cloud systems appeared to be important during the simulated period as this period of intense measurements was characterized by unstable, windy weather with a multitude of cloud systems of various scales passing over The Netherlands. As might be expected, the model is able to capture some of signal caused by the large-scale synoptic patterns, but has problems with the smaller scale features.

The model's performance is assessed given the databases that were ready to implement in the modelling environment. The simulations would be improved if a more realistic fine-resolution anthropogenic emissions map was available. Such data in principle are available (but no publicly) at very fine spatial resolutions from the basic inventories. Also for temporal downscaling more detailed approaches exist Friedrich et al. (2003).

Aircraft observed fluxes of latent heat across the same track during the observational campaign exhibited a very high variability, probably driven more by random errors and non stationary sampling conditions due to large scale turbulence, than by surface heterogeneity. The large scatter in aircraft observed fluxes makes it difficult to properly validate spatially simulated fields of latent heat flux. In this case spatial variations are

generally caused by clouds and are larger than variations that can be linked to known surface heterogeneities. Thus a proper simulation of cloud cover dynamic becomes crucial when conditions exhibit a high variability, like in the days of this campaign.

Spatially simulated carbon fluxes were compared against aircraft observations and the results showed that the simulated trends in carbon exchange generally followed the observed trends. However the point by point variation in the two correlated poorly. This is not strange when comparing simulated surface fluxes in the model with those measured higher up by the aircraft. Modelling the footprint area of the aircraft and then comparing the average simulated flux in the footprint to the aircraft observations might overcome this. Approaches in this direction have been developed by e.g. Ogunjemiyo et al. (2003), Hutjes et al. (2010), though Garten et al. (2003) point an important shortcoming in simple footprint models, that would certainly have complicated our study, that is "the inability to predict how quickly real clouds move and redistribute themselves vertically under particular meteorological conditions". In contrast we (and others, e.g. Sarrat et al. (2007)) meant to overcome this footprint mismatch by also comparing simulated fluxes at flight altitude to those observed. However, the simulated absence of turbulent diffusion is apparent as the CO_2 fluxes at flight level are close to zero even when a significant uptake at the surface is simulated. This asks for better vertical diffusion schemes in transport models, that simulate vertical flux divergence and entrainment near the boundary layer top more realistically.

The various profiles measured during the first period of the campaign showed that the model underestimates potential temperature especially in the morning. The boundary layer dynamics seem to be reproduced well, though the stable boundary layer in the early morning seems to be simulated too shallow and too cold. Fine scale structures in observed scalar profiles cannot be captured with the current vertical resolution of the model. From the station validation we can also see that during most mornings in the simulation the depletion of CO_2 at the lower levels, due to dilution and uptake at the surface, in the model occurs later than in the observations. These issues may all benefit from higher vertical resolution in lower part of the atmosphere in the model. The validation of the vertical profiles also indicates that the depth of the well-mixed day-time boundary layer is not well represented and is underestimated by 100-200 meter by the model. de Arellano et al. (2004) assessed the importance of the entrainment process for the distribution and evolution of carbon dioxide in the boundary layer. They also showed that the CO_2 concentration in the boundary layer is reduced much more effectively by the ventilation with entrained air than by CO_2 uptake by the vegetation.

In the turbulent parameterization (Mellor-Yamada) of the atmospheric model we found that the entrainment process is poorly represented leading to a higher simulated CO_2 concentration in most of the vertical profile. Also the building up and breaking down of the PBL seemed to be difficult to simulate by the present turbulent parameterization. Future model development should focus on turbulence and PBL parameterizations in general and on the entrainment processes in particular.

From the station validation of the CO_2 concentration (Figure 3.15) the influence of the sea might be an important factor for the concentrations simulated near the coastal strip of The Netherlands. One of the shortcomings of the present modelling system is the coarse resolution of the partial pressure of CO_2 within the sea and the values that were derived for the North Sea west and northwest of The Netherlands. According to Hoppema (1991) and Thomas et al. (2004) there is a strong gradient in the North Sea near the Dutch coastal strip with absolute values of the CO_2 partial pressure also being more dynamical in time than the values from Takahashi et al. (1997) suggest. Seasonal fields observations show that the North Sea acts as a sink for CO_2 throughout the year except for the summer months in the southern region of the North Sea. Figure 3.5 shows that the modelling system lacks these dynamics in δpCO_2. As a result in the case of strong winds blowing from west/northwestern directions air with relative low simulated $[CO_2]$ will penetrate inland compared to the seasonal fields observations in summer months.

The results of the sensitivity experiments showed that the response of $[CO_2]$ to these surface flux variations is larger at Cabauw than at Loobos and in both cases well above detection limits. However, we also show that the signal is strongest at low levels. We also conclude that it is possible to determine the cause of an observed change in CO_2 concentration in terms of sources and sinks in the vicinity of an observational site. This is complementary to the work of Vermeulen et al. (2006) who concluded that "inverse methods (…) are suitable to be applied in deriving independent estimates of greenhouse gas emissions using Source-Receptor relationships." Given this approach an observed change in $[CO_2]$ can be related to a certain greenhouse gas emission from a certain land use in the vicinity of the observational site. The present study also confirms the recommendations given by Geels et al. (2004) for future modeling work of improved high temporal resolution (at least daily) surface biosphere, oceanic and anthropogenic flux estimates as well as high vertical and horizontal spatiotemporal resolution of the driving meteorology. This study suggests that to

resolve 20 % flux difference you either need to measure concentrations close to the surface or very precise.

In this paper we tried to analyse some of the factors that control the carbon dioxide concentration for a region covering a large part of The Netherlands. Useful conclusions have been drawn from the use of a regional model coupled to a detailed land-surface model and comparing simulations to various observations ranging from station to aircraft measurements. The region used for this study is characterized by a strongly heterogeneous rural land use alternated with cities/villages of various sizes. The forests at the Veluwe decrease the atmospheric carbon dioxide whereas the emissions from the urbanized areas in The Netherlands increased $[CO_2]$ transported in plumes. At a larger scale, the influence of the cleaning effect of the sea seemed to be important to simulate the $[CO_2]$ more realistically. The effect of better representations of the partial pressure-fields of CO_2 for the North Sea on the simulated $[CO_2]$ inland remains a subject needing further research.

The aforementioned campaigns (CERES and "Climate *changes* spatial planning") will provide an excellent platform for further research, from both observational and modelling perspectives. These initiatives address the uncertainties in the input datasets and model structure and parameters. In part, results will be specific to the region under study but also progress on more general issues is significant, as this special issue demonstrates.

Regional atmospheric feedbacks over land and coastal areas

Chapter 4

The impact of high resolution model physics and North Sea surface temperatures on intense coastal precipitation in the Netherlands

abstract

This paper shows the influence of fine-scale and high SST values on precipitation in coastal areas in the Netherlands. Earlier analysis showed that about 30% of the rainfall in the coastal area in August 2006 was due to the high SST resulting from the warm July month before. In this paper, a regional atmospheric model (RAMS) has been implemented to investigate the impact of high resolution model physics and North Sea surface temperatures on intense coastal precipitation in the Netherlands. The precipitation in the model is simulated by the microphysics package and convective parameterizations have been switched off, assuming convection is fully resolved.

To analyse the effect of SST on precipitation several prescribed SST-fields are fed into the model. The prescribed SST-configurations are (1) SST observed with the NOAA satellite (weekly, 0.1°) and (2) SST values from the Met Office Hadley Centre's Sea Ice and Sea Surface Temperature dataset (HadISST1, monthly 1°). In a sensitivity experiment we assesses the impact of lower SSTs on coastal precipitation. The impact is significant with monthly precipitation sums that are 50 mm (west coast) to 150 mm (northern part of the Netherlands) lower .

This study shows that a good simulation of precipitation in convective circumstances depends on better representation of small SST gradients and that high spatial resolutions are unavoidable.

4.1 Introduction

More detailed information, on the way our climate is changing, is asked for by decision makers in (non-) governmental organizations and the general public. This level of detail is necessary to first assess the threats and opportunities that a changing climate will generate and to formulate realistic adaptation and mitigation strategies.

One of the shortcomings in current climate projections is that the scale of the smallest atmosphere phenomena simulated is on the order of 100km. This is a result of the model resolution on which state-of-the-art regional climate models are executed. As processes on scales which cannot be resolved by Global Climate Models (GCMs) are important, several initiatives have been taken to dynamically or statistically climate information to the more regional scale (Christensen et al. (2007), Jacob et al. (2007), Haylock et al. (2006), Maurer et al. (2008)). The Fourth Assessment Report of the IPCC (IPCC AR4) states that "Global Climate Models remain the primary source of regional information on the range of possible future climates" (Christensen et al. (2007)). Higher resolution climate models are thought to provide more regionally detailed climate predictions and better information on extreme events as spatial and temporal details are better resolved. However, an increased understanding of climate processes and feedbacks is necessary to reduce the uncertainty in climate projections.

For a country of the size of the Netherlands (approximately 200 by 300 km) regional climate projections will give more spatial information than a global climate projection in which the Netherlands is covered by roughly only a single grid cell of a GCM. The Netherlands is, according to GCM projections, located in a transition area between North European regions (higher than average rise in winter temperature) and Southern European regions (warmer and drier summer conditions) (van den Hurk et al. (2007)). van den Hurk et al. (2006) developed a set of four climate scenarios for the Netherlands (KNMI '06 scenarios), based primarily on a set of simulations of five selected global climate models that participated in the IPCC AR4 (IPCC (2007)) and an ensemble of regional model simulations. One of their conclusions was that special attention should have to go to dry summer scenarios and increased intensity of extreme daily precipitation.

Increase in daily precipitation extremes in GCM and RCM simulations has been reported in many studies (e.g.Pall et al. (2007), Frei et al. (2006), Christensen et al. (2003)). Similar findings have been found in observations over half of the land area of the globe (Groisman et al. (2005)), and also more locally, e.g. in the Netherlands (Lenderink et al.

(2008)). This last paper showed that for the observational site of De Bilt "one-hour precipitation extremes increase twice as fast with rising temperatures as expected from the Clausius–Clapeyron relation when daily mean temperatures exceed 12 ºC".

From the aforementioned KNMI '06 scenarios, studies from Lenderink et al. (2007) and van Ulden et al. (2006), two types of scenarios for the summer can be characterized: (a) a "dry" scenario where circulation changes and soil drying limit precipitation forming process; and (b) a "wet" scenario with a small increase in summer precipitation and no limitations due to circulation changes and soil drying. The KNMI'06 scenarios are based on certain assumptions about the global temperature rise (1 and 2 degrees warming in 2050) and circulation changes over the Western Europe ('no change" and more westerly circulations in winter and more easterly in summer). However, the potential impacts of the North Sea on the future climate are likely not to be captured in such type of simulations.

This paper continues the work that has been started by Lenderink et al. (2009), who investigated intense coastal rainfall in response to high coastal sea surface temperatures (SSTs). Their analysis showed that about 30% of the rainfall in the coastal area in August 2006 was due to the high SST resulting from the warm July month before. The advection of cold air-masses from the Northwest over the warm sea water led to numerous convective showers and a record wet August in the Netherlands (see next section). The research of Lenderink et al. (2009)) was performed with a model of intermediate grid squares of 6km^2. One of the outcomes of their study was that on a more detailed level "...the model fails to reproduce the exact spatial distribution (too much rain too close to the coast) and tends to underestimate the strongest daily events." The grid increment of 6 km is too coarse to explicitly solve convective showers and these are expected to be better captured by (non-hydrostatic) meso-scale models which can be executed on a grid mesh as small as 1 km. Bernardet et al. (2000) concluded that "2 km was sufficient to capture convection explicitly, keeping in mind that this depend on the high spatial resolution of physiography (particularly topography and top soil moisture), efficient communication between grids of different scales, and initialization procedures."

Several studies have demonstrated that predictability limitations at these cloud-resolving resolutions are highly relevant for quantitative precipitation forecasting (Hohenegger et al. (2007), Richard et al. (2003), Walser et al. (2004)). Bennett et al. (2006) reviewed the processes which are of importance for initiating convection in the United Kingdom and recommended "to run at a very small grid scale of 1 km,

opening up the possibility of significantly improving predictions of severe weather across the UK." Mass et al. (2002) questioned whether decreasing grid spacing in mesoscale models to less than 10–15 km generally improves the realism of the results as the objectively scored accuracy of the forecasts did not significantly improve. This inconsistency between fine resolutions and model performance has also been discussed by Clark et al. (2007), who argued that small errors in timing and location of precipitation are penalized stronger using fine scale resolutions. In response to this, object oriented skill test are currently under development Gallus (2010).

In this paper, the Regional Atmospheric Modelling System (RAMS, Cotton et al. (2003), Pielke et al. (1992), Ter Maat et al. (2013)) has been implemented for the Netherlands to explore the impact of fine resolution simulations on coastal rainfall. The main question to be answered is: "Can intense coastal rainfall in the Netherlands be better simulated at a finer grid scale due to better representation of the model physics and North Sea surface temperatures?".

August 2006 is used as case study for this assessment. First, the output of the RAMS simulation of August 2006 is compared with the results from Lenderink's study (from now on referred to as L09) and the observations from the rainfall observation network of the Royal Netherlands Meteorological Institute (KNMI). Next, an analysis is given on the influence of grid resolution and differing SST products on precipitation and in particular on coastal rainfall. We conclude by a discussion of the model results and to consider how the results presented here will help the progress in regional climate projection

4.2   Description of the model experiment and set-up

This paper builds on the work of Lenderink et al. (2009) and thus the set-up of the experiments follow the line of their work.

August 2006 was a record wet month in the Netherlands with an average of 184 mm countrywide compared to the climatological average of 62 mm. The precipitation near the western coastline was even higher with an average just over 213 mm for a rectangular area bounded by 51.3°N, 52.8°N, 3.5°E and 5.3°N. This square is also used for the analysis of the model output. Even a couple of stations recorded 320 mm of rainfall for this month (Figure 4.2 b,c). The abnormal wet weather was caused by a northwesterly circulation bringing depressions

that produced many showers, especially in the coastal areas of the Netherlands. In addition, the warm coastal sea water acted as an extra stimulus .

Simulations consist of a simulation performed with prescribed SST observed with the NOAA satellite (weekly, 0.1°) and one with prescribed SST values from the Met Office Hadley Centre's Sea Ice and Sea Surface Temperature dataset (HadISST1, monthly 1°) (Rayner et al. (2003)). The raw data of the NOAA satellite measurements are on a 1 x 1 km grid mesh, and have been aggregated to 0.1° by 0.1° and have a weekly time resolution. Both SST fields are linearly interpolated in time for the simulation period. The advantage of the NOAA SST dataset is the higher spatial and temporal resolution. Especially, the strong temperature gradient near the western coastline of the Netherlands is represented very well in this dataset. The coarse resolution of HadISST1 clearly cannot resolve this gradient. To validate the control simulation meteorological observations are taken from the database of KNMI.

RAMS (version 6.1) is used in this study to investigate the influence of high resolution modelling on coastal rainfall. The model is a 3D, non-hydrostatic model based on fundamental equations of fluid dynamics and includes a terrain following vertical coordinate system (Gal-chen et al. (1975)). The resolution in the vertical was fine enough to allow for modeling of the planetary boundary layer (PBL). RAMS was set-up to use two-way interactive grid nesting allowing us to zoom in from synoptic scale features to scales which allow for the explicit representation of moist convection.

Table 4.1: Configuration of RAMS 6.1

grids	1	2	3	4
dx, dy	18 km (80x84)	6 km (80x137)	2 km (191x242)	1 km (144x200)
dt	20 s	20 s	6.7 s	6.7 s
dz	50 – 1250 m (35 levels)			
Radiation	Chen & Cotton (Chen et al. (1983))			
Topography	GTOPO30 (~1 km grid increment)			
Land cover	GLCC USGS (~1 km grid mesh (Loveland et al. (2000))			
Land surface	LEAF-3 (Walko et al. (2000))			
Diffusion	MRF (Hong et al. (1996))			
Microphysics	Full microphysics package (Meyers et al. (1997))			
Forcing	ECMWF			
Nudging time	lateral: 1800 s (only on grid 1)			
Period	1 August 2006 – 31 August 2006 (+ preceeding spinup of 15 days)			

Table 4.1 shows the various details about the model setup. A two-way nested configuration was used (Walko et al. (1995)) in all four grids, covering a large part of Western Europe (grid 1, 18 km), Belgium, the Netherlands and Luxemburg (grid 2, 6 km), The Netherlands (grid 3, 2 km) and the western part of the Netherlands (grid 4, 1 km). The whole modeling domain and its topography is displayed in Figure 4.1. RAMS is initialized and nudged by reanalysis data from the European Centre for Medium-Range Weather Forecasts (ECMWF, ERA-interim) every 6 hours. The grid spacing of the forcing data is on a 0.5° by 0.5°. The nudging extends 10 gridpoints into the domain from the boundaries and has no center domain nudging. The simulation has a spin-up period of two weeks covering the period of warm and dry weather which preceded the very wet August 2006.

The precipitation is controlled by the microphysics package and convective parameterizations have been switched off, assuming convection is fully resolved on the high resolution grids 3 and 4. Earlier work by Ter Maat et al. (2013) showed the importance of choosing the appropriate parameterization of the planetary boundary layer (PBL) to
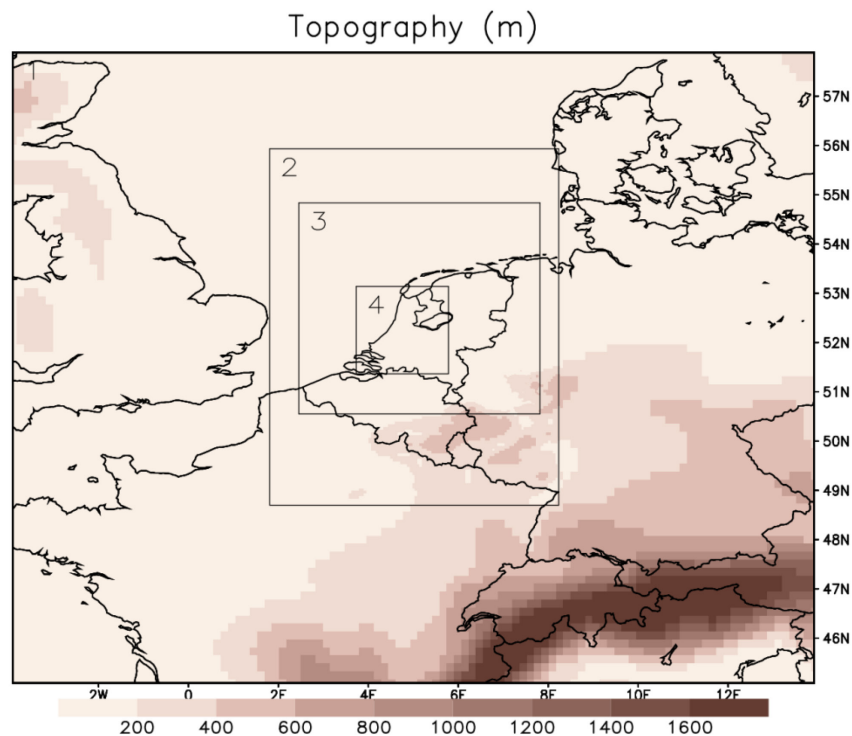
Figure 4.1: Topography of the modelling domain

use for the Netherlands. Following their results, the MRF scheme (Hong et al. (1996)) has been chosen as the PBL parameterization.
Soil properties were extracted from the Global Soil Data Task Group of the International Geosphere–Biosphere Programme Data and Information System (IGBP-DIS) soil properties database (Global Soil Data Task Group (2000)), which has a grid increment of approximately 10 km. Landcover classes were derived from the USGS database (Loveland et al. (2000)) with a grid mesh of around 1 km which is standard within the RAMS framework, just like the soil properties database.

4.3 Results

The control run is compared against observations of precipitation, temperature, wind speed and wind direction. For the control simulation the NOAA SST database has been implemented. All reference observations are taken from the KNMI database (http://www.knmi.nl/klimatologie/). The validation of the temperature and wind variables is performed on the observations at Schiphol Airport (the location of Schiphol is displayed in Figure 4.2). The validation of the precipitation is performed in a spatial setting. The dense network of precipitation observations is very suitable for this, although only daily values are stored. To a certain extent, this limits the analysis and validation of convective showers which typically have a shorter life time. Unfortunately, for this period precipitation radar fields are not available on hourly time scale, but monthly radar observations field are available to cover possible areas where the rainfall observation network was lacking, like over the sea and/or neighbouring countries.

To evaluate the added value of simulating precipitation on a finer spatial resolution, the simulated precipitation fields from L09 are also used. First, the spatial patterns of the simulated precipitation are compared against the station observations. The upper panel of Figure 4.2 shows the simulated precipitation for August 2006 for the NOAA-SST configuration. To compare the RAMS simulation with L09 the same color scheme is adapted and their results are also included in this Figure 4.2. The observations from the KNMI are also included in Figure 4.2 as well as the radar observed precipitation and the RAMS simulation in the HadISST-SST configuration.

One of the objectives of this paper is to show the added value of higher spatial resolution. By comparing the RAMS results with L09 it can be seen in Figure 4.2 that the magnitude and distribution of precipitation have clearly improved. The simulated monthly precipitation sums reach values of more than 250 mm, not only in the western part of the
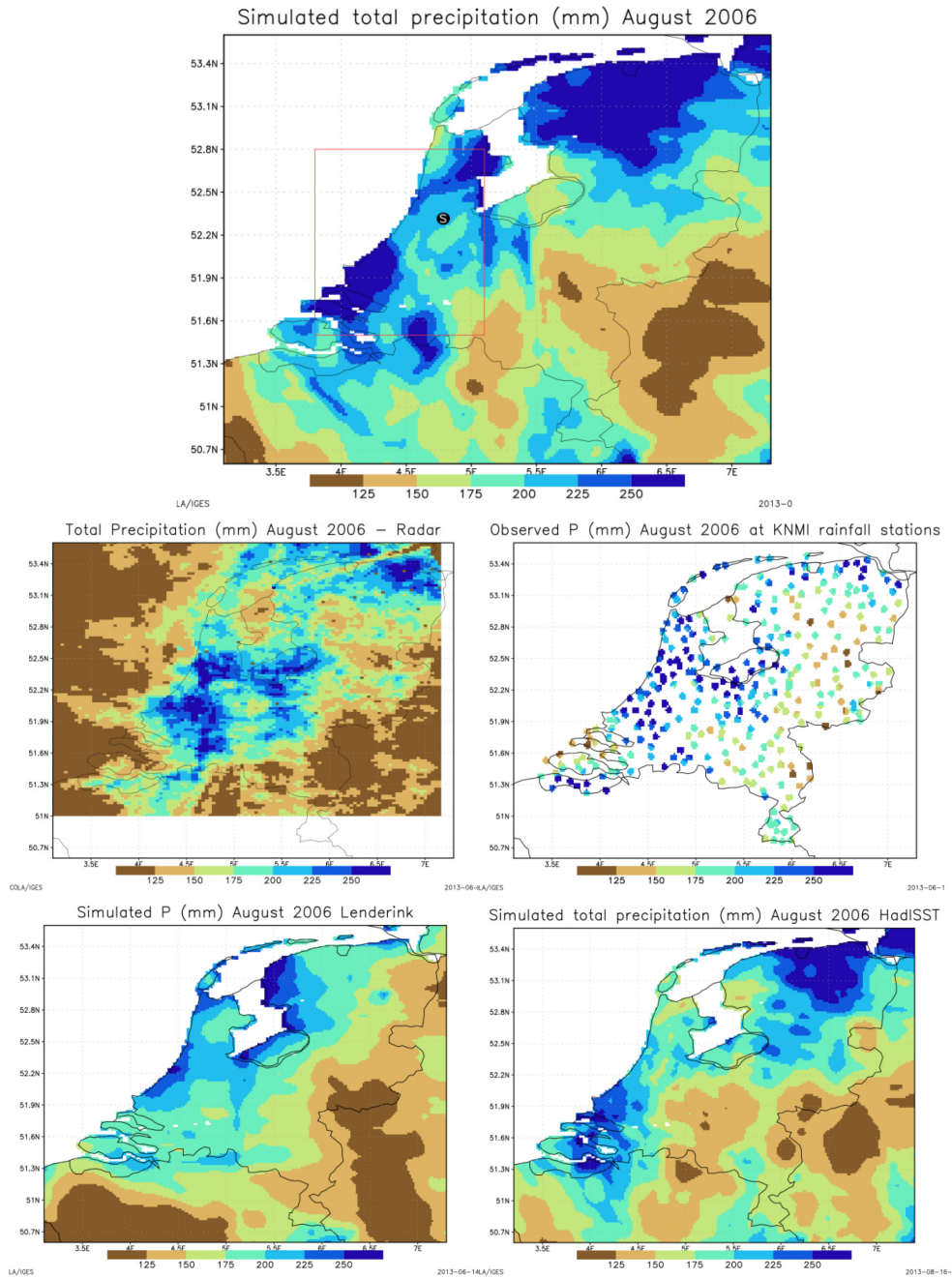
Figure 4.2: Spatial representations of the total precipitation (mm) in August 2006: upper panel: simulated by RAMS using NOAA SST, mid-left: radar observations, mid-right: observed precipitation at the KNMI rainfall stations, low-left: simulated by L09, low-right: simulated by RAMS using HadISST

Netherlands but also more inland. Compared with the radar, the model misses the high values in the vicinity, eastward and northward of Schiphol. However, the recordings from the KNMI precipitation gauge network shows that values above 250 mm were also recorded to the North of Schiphol. We conclude that the RAMS simulations show a spatial distribution of extreme rainfall that is more consistent with the observations than L09.

The model overestimates rainfall sums in the northern part of The Netherlands. Further research showed that the cause for this overestimation may be in the prescribed SST values. The Wadden Sea between the Dutch mainland and the islands to the north is influenced by a tidal regime. Analysis of the NOAA database showed that the SST values in the Wadden Sea were higher than the North Sea even though both are connected to each other and should mix well. We hypothesize that the NOAA satellite was looking at land which fell dry during low tide. Analysis of the satellite overpass times and the tidal records of the Wadden Sea show that this hypothesis may well be true. This tidal regime is not implemented in the modelling system. Therefore the combination of sea (source of vapor), extreme high SST values and a northwesterly flow leads, possibly, to an overestimation of rainfall in the northern provinces of the Netherlands.

The focus of the rest of the analysis is on the western coastal area of the Netherlands where most of the precipitation was observed in August
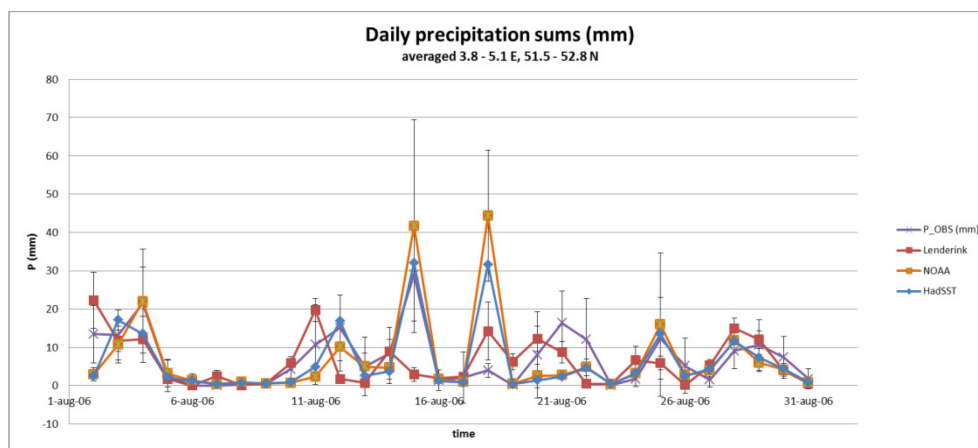
Figure 4.3: Areal averaged daily precipitation (mm) including the standard deviation, purple: observations, red: L09, orange: NOAA, blue: HadISST

Table 4.2: Averaged daily rainfall and standard deviation over the area enclosed by 3.5 E - 5.3 E, 51.3 N - 52.8 N .

Average daily rainfall	P (mm)	SD (mm)	Monthly P (mm)
Observations	7.051072	5.73006	217.2
RAMS_NOAA	6.837442	4.183426	212.3
RAMS_HadSST	6.14901	3.80083	188.7
Lenderink	6.055484	2.428752	186.1

2006. Figure 4.3 shows time series of the observed precipitation and the simulated precipitation. All values are averaged for a square enclosed by 51.5 N and 52.8 N and 3.8 E and 5.1 E (red square in Figure 4.2) and only values over land are included in the analysis. The results from L09 are also included as well as the simulated precipitation from the simulation with the prescribed HadISST-SST values. The daily sums of the simulated precipitation of L09 are based on a different interval if compared to the RAMS output and observations, i.e. the output from the RAMS simulations are summed from 8AM to 8AM the next day, which is according to the KNMI observations. L09 sums the rainfall from 0:00 to 0:00 the next day. This explains partly the discrepancies between L09 and the observations. The error bars show the standard deviation of the rainfall in the above mentioned square.

Figure 4.3 shows that the current set-up of the RAMS simulations nicely capture the various peaks in daily rainfall. The only 'miss' in the model is the peak simulated on 18 August 2006, which did not occur in reality. The rainfall showers which passes over the square are simulated just over land. As observations of rainfall are lacking over the North Sea it is hard to validate the hypothesis that the simulated precipitation is simulated too much to the east compared to the observations. Compared to L09 the RAMS simulations seem to capture the convective showers much better. This is also reflected in the monthly sums of precipitation (Table 4.2). Especially, the NOAA-SST as used by RAMS peforms good with a simulated sum of 212.3 mm. This is only 5 mm short of the observed value. The other configurations underestimate the precipitation by 30 mm.

The standard deviation is a measure to check the heterogeneity of the simulated results within the area of interest and thus is an indication to check whether the model is able to simulate convective showers. For the calculation of the standard deviation all grid points in the square are taken which are located on land. The standard deviation of RAMS-NOAA is also improving from L09, but still the model has difficulty to capture the heterogeneity which appears from the rainfall observations.
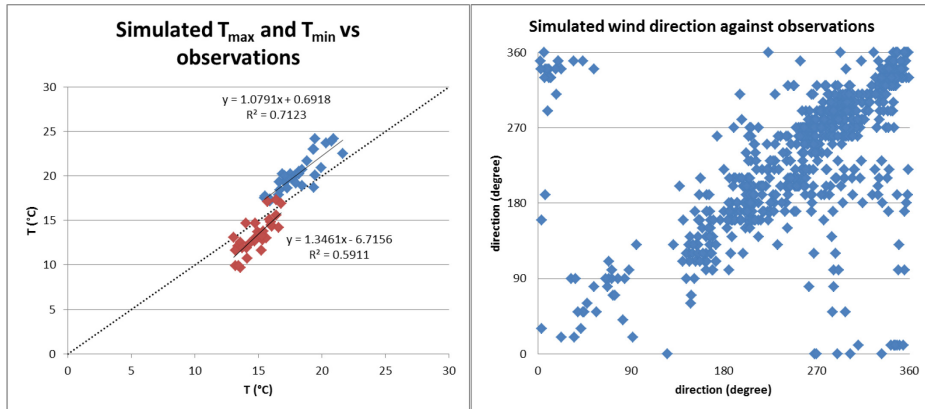
Figure 4.4: Comparison between simulated results and observations of the minimum (red) and maximum (blue) temperature (°C) (left panel) and hourly wind direction (right panel)

Figure 4.4 shows the validation of the control run (NOAA-SST) with regards to observations of temperature and wind direction at the surface. The maximum temperature is slightly overestimated by the model with a correlation coefficient of 0.71. The minimum temperature is most of the days captured by the model although there are some days where the model underestimates and some days where the model overestimated the minimum temperature. The wind direction is also displayed and the wind dynamics are, in general, well captured by the model.

Finally we perform a sensitivity simulation where 2 °C is subtracted from the NOAA SST fields. L09 hypothesized that the gradient near the coast may be a result of the warm period preceding August 2006. As observational records lack it is not possible to assess this effect. Therefore a sensitivity experiment is executed in which the gradient is retained, but the SST is lowered by 2 °C. With this experiment (NOAA-2), we assess the role of higher SST values on precipitation in the coastal areas.

Figure 4.5 shows the result in monthly precipitation between the NOAA simulation and the NOAA-2 simulation. This figure shows that the influence of a change in SST has a considerable effect on the precipitation. The impact of a lower SST on precipitation near the west coast is around 50 mm, but the effect is even higher near the northern coast and the Wadden Sea with areas where 150 mm less precipitation is simulated.
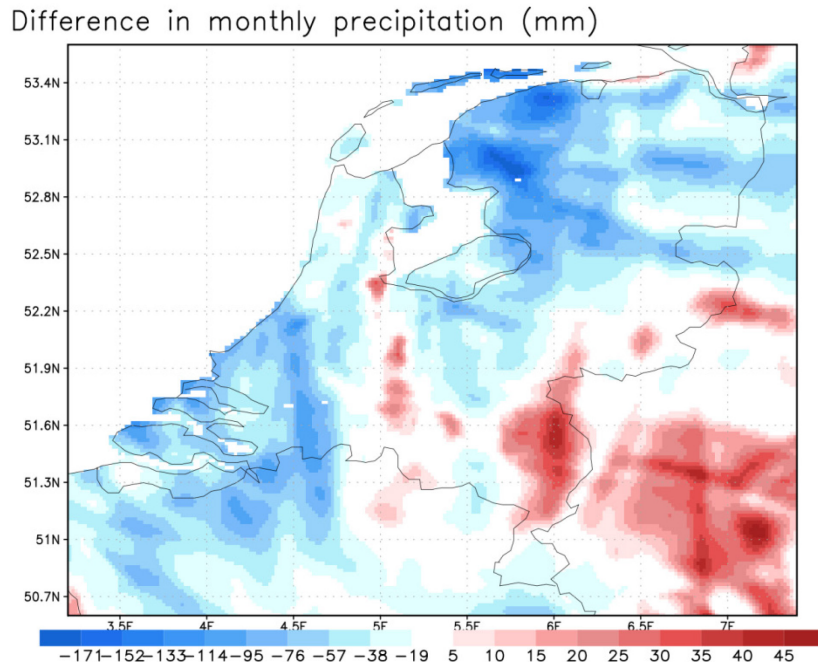
Figure 4.5: Difference in simulated monthly precipitation (mm) between the NOAA and NOAA-2 simulation (NOAA − NOAA-2)

4.4 Discussions and conclusions

The main question to be answered in this paper is whether intense rainfall is better simulated at a finer grid scale using a high resolution non-hydrostatic mesoscale model running at 1 km grid increment and with high resolution input SST fields. The results from the simulations performed with our set-up of RAMS show that to simulate precipitation with a convective origin a mesoscale model is necessary that resolves the convection. The inclusion of a SST database with a high resolution in the North Sea and a higher temporal resolution proved to have added value to the simulated precipitation compared to a monthly prescribed SST on a coarser spatial resolution. The monthly sum of the NOAA-configuration is 30 mm higher than the HadISST-configuration. The higher standard deviation of the NOAA and HadISST-configuration compared to the L09-study is a measure that the non-hydrostatic RAMS-configuration improves the simulations of small-scale precipitation features (e.g. convective showers).

Our results indicate that higher resolution NOAA-SST helps especially to improve the peak rainfall. A shortcoming of using satellite SST over the

tidal Wadden Sea has been identified and we recommend a better post-processing of satellite data over such areas and a better representation of this cyclic surface temperature variation (with a different period and phase than the diurnal cycle) is necessary in future simulations. The results from the sensitivity experiment shows the sensitivity in precipitation to the prescribed SST values of the Wadden Sea. Observations of SST in the Wadden Sea will be of great value to the atmospheric modelling community for a better impact assessment of the SST of the Wadden Sea on precipitation in the northern coastal provinces of the Netherlands.

The role of higher SST values on precipitation in coastal areas is present in RAMS, but peak rainfall needs further investigation. The inclusion of rainfall radar imagery, when available at e.g. hourly resolution, may be helpful with this. The comparison on daily values is valuable but, with convective showers passing over the area of interest, analysis on a shorter timescale will provide better statistical information. This will also give more understanding of the model and also where to improve the high resolution simulations.

This paper shows the influence of fine-scale and high SST values on precipitation in coastal areas in the Netherlands. As these values are expected to be more frequent in a future climate it provides insight in the possible impact on coastal precipitation. An alternative cause for extreme precipitation in the west of the Netherlands may be the dense urbanisation, e.g. heat island effects affecting convection. Presently we cannot separate this potential effect from the coastal warm sea waters. The inclusion of urban canopy models in mesoscale models to realistically simulate city-surroundings heat contrasts is needed to investigate the role of urban areas in the development of convective showers.

Regional atmospheric feedbacks over land and coastal areas

Chapter 5

Meteorological impact assessment of possible large scale irrigation in Southwest Saudi Arabia

abstract

On continental to regional scales feedbacks between landuse and landcover change and climate have been widely documented over the past 10-15 years. In the present study we explore the possibility that also vegetation changes over much smaller areas may affect local precipitation regimes. Large scale (~10^5 ha) irrigated plantations in semi-arid environments under particular conditions may affect local circulations and induce additional rainfall. Capturing this rainfall 'surplus' could then reduce the need for external irrigation sources and eventually lead to self sustained water cycling.

This concept is studied in the coastal plains in South West Saudi Arabia where the mountains of the Asir region exhibit the highest rainfall of the peninsula due to orographic lifting and condensation of moisture imported with the Indian Ocean monsoon and with disturbances from the Mediterranean Sea.

We use a regional atmospheric modeling system (RAMS) forced by ECMWF analysis data to resolve the effect of complex surface conditions in high resolution ($\Delta x=4$ km). After validation, these simulations are analysed with a focus on the role of local processes (sea breezes, orographic lifting and the formation of fog in the coastal mountains) in generating rainfall, and on how these will be affected by large scale irrigated plantations in the coastal desert.

The validation showed that the model simulates the regional and local weather reasonably well. The simulations exhibit a slightly larger diurnal temperature range than those captured by the observations, but seem to capture daily sea-breeze phenomena well. Monthly rainfall is well reproduced at coarse resolutions, but appears more localized at high resolutions. The hypothetical irrigated plantation (3.25 10^5 ha) has significant effects on atmospheric moisture, but due to weakened sea breezes this leads to limited increases of rainfall. In terms of recycling of irrigation gifts the rainfall enhancement in this particular setting is rather insignificant.

5.1   Introduction

Feedbacks between landuse and landcover change and weather and climate have been widely documented over the past 10-15 years, on both global and continental and regional scales (e.g. Kabat et al. (2004), Pielke et al. (2002)). A substantial subset of this literature focuses on landuse climate interactions in semi-arid regions often analyzing the relative role humans may have played in issues of desertification (e.g. Reynolds and Stafford-Smith (2002)). One of the more intensely studied systems is that of western Africa, where after the landmark paper of Charney (1975) a large number of (modelling) studies revealed linkages between (human induced) vegetation degradation and subsequent rainfall decreases in the Sahel (for a review see Xue et al. (2004)). Vice versa the very occurrence of vegetation may have contributed to a wetter climate that occurred in pre-historic times in that region (Claussen et al. (1999)), in turn starting-off studies into the potential regreening of the Sahara (Claussen et al. (2003)). More generalized, Koster et al. (2004) explored the sensitivity of regional climates around the world to land surface interactions and found profound feedback effect in areas in the Mid-US, Africa and India.

The basic mechanism is that a land cover or landuse change modifies the radiation balance and the subsequent partitioning of available energy over sensible or latent heat fluxes. These are first order effects and their relative importance may vary spatially and in time. Differences in latent and sensible heat input lead to altered heat and moisture content of the atmospheric boundary layer (ABL). ABL temperature and humidity feed back to the surface through stomatal behaviour of plants, creating a first potential loop. ABL temperature and humidity affect convective heating, total diabatic heating, subsidence, monsoon-flow strength and moisture convergence. These processes all affect cloud formation and as clouds strongly affect radiation a second potential feedback loop comes into play. If altered clouds also affect precipitation, additional feedback loops are activated through soil moisture stores, vegetation growth and phenology and eventually ecosystem changes / displacements. Each of these potential feedback loops (in the order discussed) acts on increasingly longer timescales.

Similar effects have been reported on smaller regional scales as a consequence of irrigation for agricultural purposes, and for a long time already the notion is prevalent that large scale irrigation may affect rainfall over or downwind of the irrigated area (Schickedanz and Ackermann (1977), Ben-Gai et al. (1993)). In broad lines the relationships between weather or climate and irrigation are similar as those outlined above but the generally smaller spatial scales bring

different mechanisms into play. The net effect is the sum of several opposing mechanisms. Obviously irrigated agriculture, through enhanced evaporation, will increase the vapor content of the (lower) atmosphere. However, at the same time the big thermal contrast between the cool, wet irrigated area and its hot, dry surroundings may create its own local circulation leading to downward motions over the area, thus decreasing the likelihood of precipitation. Whether this happens depends on the size of landscape patchiness that is needed before the boundary-layer structure is significantly affected and a mesoscale circulation produced, an issue explored by many authors Avissar et al. (1998). Conversely, in a coastal setting the cooling over the irrigated area may hinder the development of true sea breezes circulation preventing imported marine moisture to precipitate Lohar et al. (1995). Also, combined cooling and wetting of the atmosphere may increase low level instability, thereby triggering storms Moore et al. (2002). In these cases the main effect does not come from additional atmospheric moisture supplied by irrigation but rather through modification of local to regional dynamics that convert advected moisture into precipitation. For the same reason the rainfall enhancement may not occur over the irrigated area but some distance downwind, in the study by Van Der Molen (2002) up to 90km downwind.

The extent to which irrigation produces additional rainfall differs case by case. Moore and Rojstaczer (2002) found a 6-18% increase on a total of ~200mm in summer rainfall in the Texas High plains. Ben-Gai et al. (1993) found a 100-300% increase in October rainfall in Southwest Israel though absolute numbers were small 5-15mm). Miglietta (personal communication) reported a 90% (equivalent to16mm) increase in July-August rainfall for the Capitanata irrigation scheme in central Italy.

In the context of irrigation induced precipitation enhancement it is useful to invoke the concept of a recycling ratio: the fraction of evaporated water that is converted into precipitation. If this recycled water falls within the irrigated area or downwind but still within the catchment used to supply irrigation water it may reduce the need for irrigation water from other, more environmentally detrimental sources like deep wells or de-salinisation plants. Recycling, when sufficiently strong, may open up the possibility, after initial irrigation of a more self-sustained agriculture. Sud et al. (2001) found that the recycling ratio was more a function of background circulation than of local evaporation and remarkably robust for a large range of vegetation covers, soil types, and initial soil moistures. They found recycling ratios of 25 - 50% in wet conditions decreasing to <1 - 7% in dry synoptic conditions. In the study by Moore and Rojstaczer (2002) recycling amounted to about 10%.

In the present study we also explore the idea that large scale (~105 ha) irrigated plantations in semi-arid environments under particular conditions can modulate a patterning of the rainfall. As a case study area we focus on Southwest Saudi Arabia where plans are in exploratory stages of development to construct large scale irrigation works in its coastal plains, based on freshwater produced from sea water through sustainable de-salinisation techniques using solar or biomass energy. These plains are confined between the Red Sea in the west providing a lot of atmospheric moisture input, and the high Asir mountain range to the east which orographically force air to lift, potentially to condensation levels. These mountain ranges exhibit the highest rainfall of the Arabian Peninsula and sustain quite some traditional rainfed agriculture. In Koster et al. (2004; his figure 1) the southwest part of Arabia appears to have some potential strength in land-atmosphere coupling, even though not as profound as in the Mid-US, Africa and India.

The RAMS model (Regional Atmospheric Modelling System) has been implemented for the region and has been used to explore the impact of a hypothetical large scale irrigated plantation on the meteorology, in particular rainfall, of the region. The source of irrigation water and its application and distribution technicalities or societal impacts are of no concern in the present analysis, but are under study elsewhere. We will simply assume enough irrigation water will somehow be available to sustain more vegetation than is presently growing in a particular area. First we will validate the model using actual (little) vegetation and (low) soil moisture conditions in a control run. Next we will present results from runs with a large area with denser vegetation and higher soil moisture levels, followed by a discussion of these results, plausible causal mechanisms and broader implications. Finally, we will discuss to which extend capturing this rainfall 'surplus' could then reduce the need for external irrigation sources and eventually lead to self sustained water cycling.

5.2   Description of regional climate

Saudi Arabia is one of the hottest and driest countries in the world with precipitation ranging from 50 to 80 mm for most of the country. Our study area, the southwestern part of the country including the Asir Mountain range, records mean annual precipitation rates of 250 mm which is the country's highest rainfall. This is due to orographic lifting and condensation of moisture imported with the Indian Ocean monsoon and with disturbances originating from the Mediterranean Sea (Chakraborty et al. (2006)). From this mountain range, with elevations
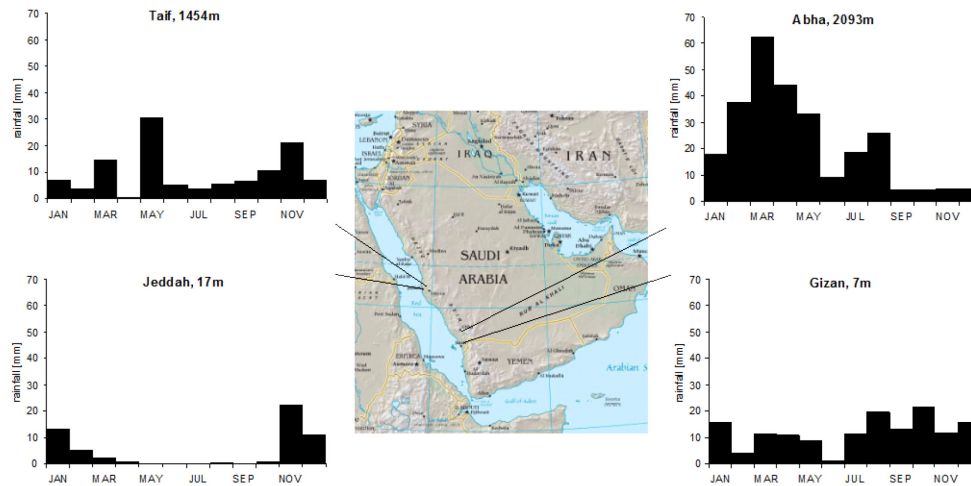
Figure 5.1: Averaged rainfall observations for stations in Southwest Saudi Arabia (Taif – upper left, Abha – upper right, Jeddah – lower left, Gizan – lower right). Taif data are averaged over 1961-1990 and the other station data over 1978 - 2001.

up to 3000 m above sea level, the dry interior plateau slopes gently to the Arabian Gulf east of the country. Between this mountain range and the Red Sea to the west lies a narrow coastal plain with a width of around 100 kilometers. As a result of the spatial distribution of rainfall, the agriculture in the mountains is mostly rainfed in contrast with the coastal plains where irrigation water is extracted from the ground.

The distribution of rainfall over the year and for different stations in Southwest Arabia is given in Figure 5.1. Two rainfall peaks can be distinguished for Abha and Gizan (cities in the mountains and coastal plain respectively) from March till May and in late summer. The first peak is a result of an unstable transition period from the Mediterranean to the monsoonal effect Bazuhair et al. (1997) and the second peak when the monsoon transports water vapor in Southwest Arabia. To the north (Taif and Jeddah), this monsoonal circulation is absent and the Mediterranean influence prevails with a period of heavy rainstorms between November and February. The influence of the monsoonal system is limited because of the strong continental air mass, which prevails over the Arabian Peninsula from June to September. Not shown here is the temporal distribution of temperature over the year, which is strongly seasonal.

5.3   Description of the experiment

To study the regional circulations and the meteorological impact of large scale irrigation combined with a landuse change, for the southwestern part of Saudi Arabia, the Regional Atmospheric Modelling System (RAMS version 4.4; Cotton et al. (2003), Pielke et al. (1992)). The model is 3D, non-hydrostatic based on fundamental equations of fluid dynamics and includes a terrain following vertical coordinate system. One of the advantages of RAMS is the possibility to perform simulations on high resolution meshes to model small-scale atmospheric systems.

In this study RAMS has been used in two configurations: a nested and a single grid configuration. The nested configuration had a large domain covering the Arabian Peninsula and part of the horn of Africa with two smaller domains (16 km and 4 km) zooming in on an area centered on Abha and Gizan. The smallest nested domain, as well as the stand alone domain had a horizontal grid spacing of 4 km covering Southwest Arabia, West Yemen and part of the Red Sea. Both simulations are executed for the period from 21 February until 15 May 2000 covering the wettest period of the year (Figure 5.1). Table 5.1 shows the various options/parameterizations which are used in RAMS for this study. Figure 5.2a shows the area which is used in the high resolution simulations and this figure also shows the details of the topography. The mountain range can clearly be distinguished together with the narrow coastal area between the mountains and the Red Sea.

Table 5.1: RAMS4.4 configuration

	Fine grid	Coarse grid
dx, dy	4 km (125x125)	80 km (60x62)
dt	10 sec	90 sec
Dz	100 stretching to 750 m (37 levels)	
Topography	GTOPO30 (~1 km increment)	
Radiation	Chen et al. (1983)	
land surface model	LEAF-2 (Walko et al. (2000))	
Diffusion	Mellor et al. (1982)	
nudging time scale	lateral 1800 s	lateral 1800 s, centre 7200 s
Convection	Full microphysics package (Meyers et al. (1997))	Modified Kuo convection scheme (Tremback, 1990)

a
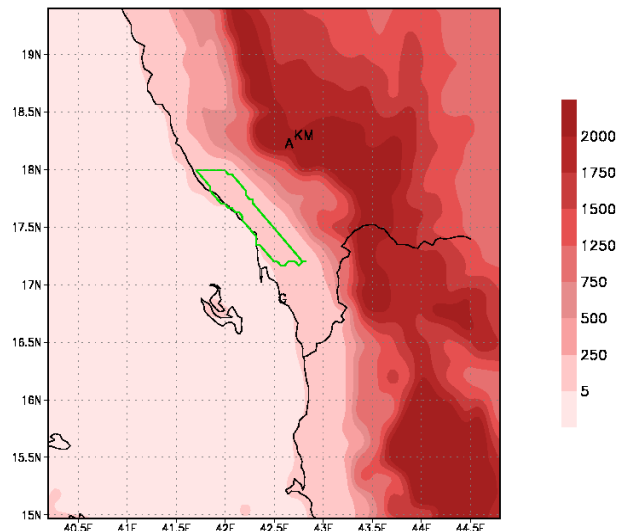
b
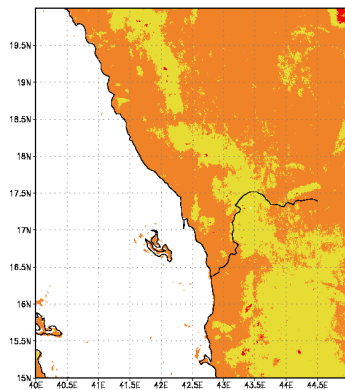
c
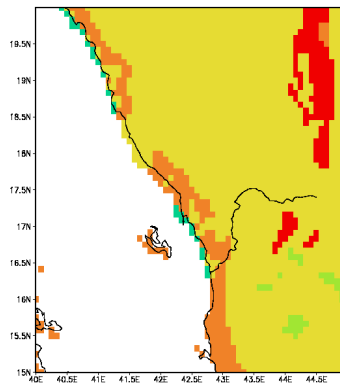
Figure 5.2: Study area Saudi Arabia: a) Topography (m) and location of the meteorological stations (A – Abha, KM – Khamis Mushayt, G- Gizan). The green line show the outline of the hypothetical irrigated plantation implemented in the 'green' simulation. b) Land cover classification (yellow: semi-desert, orange: desert, red: other landuse classes, mainly urban areas) c) Soil texture classification (yellow: loam, orange: silt loam, red: loamy sand, green: sandy clay loam)

Table 5.2: Weather stations used for validation. The stations are identified by WMO code.

Station	WMO code	Latitude (∘)	Longitude (∘)	Elevation (m)
Abha	41112	18.23N	42.65E	2093
Khamis Mushait	41114	18.3N	42.8E	2056
Gizan	41140	16.88N	42.58E	7

RAMS is forced by analysis data from the European Centre for Medium-Range Weather Forecasts (ECMWF) global model. The grid spacing of the forcing data is 0.5 by 0.5 degree and available every 6 hours.

Monthly sea surface temperatures have been extracted from the Met Office Hadley Centre's sea ice and sea surface temperature (SST) data set, HadISST1 Rayner et al. (2003).

The following databases have been used to prescribe the land cover and the soil texture in the area (Figures 5.2b, 5.2c). Landuse classes have been extracted from the USGS database Loveland et al. (2000) with a grid increment of around 1 kilometer which is standard within the RAMS framework. Soil properties (not standard in RAMS) were derived from the IGBP-DIS Soil Properties database (Global Soil Data Task Group (2000)) which has a grid mesh of approximately 10 kilometers.

To validate the results of the control simulation of RAMS surface observations and satellite products are used. Validating a regional model in an area where data availability at the surface is scarce is not trivial, and therefore satellite products are necessary in validating model output. The surface observations are extracted from the ECMWF observational archive at the main synoptic hours (0:00, 6:00, 12:00 and 18:00 UTC). The variables of interest from this database are dry bulb temperature (K), windspeed (m s-1) and wind direction (∘). Table 5.2 shows the surface stations used in the validation. The satellite data used in this paper are extracted from the Tropical Rainfall Measuring Mission (TRMM) satellite, which was launched 27 November 1997 (Huffman et al. (1995)). This satellite estimates among others rainfall rates and accumulated precipitation. We used the 3B43 data product, a merged product combining satellite derived estimates with ground observations. It is available (and used here) on two spatial grid meshes, on a 0.25º and a 1º grid mesh for the area bounded in the north and south by the 50 degrees latitude, in both cases on a monthly basis.

After validation of our control simulations, this paper will focus on meteorological effects caused by large scale irrigation in combination

with landuse change. The area designed for this landuse change is indicated as a green outline in Figure 5.2a. With regards to the location of the plantation, it is hypothesized that more moisture will be available above the irrigated plantation and that, subsequently, this moisture will be transported by the southwestern wind inland (sea breeze) and that, subsequently, orographic lifting might generate more rainfall in the Asir Mountains downwind of the plantation. The landuse of the irrigated plantation has been changed from desert into shrubland over an area of approximately 36 kilometers by 90 kilometers. This change leads to a change in albedo from 0.3 to 0.1 and in roughness length from 0.05 m to 0.14 m. These values are in LEAF defined from the BATS vegetation scheme (Dickinson et al. (1986)). The size of the plantation is equivalent to 9x22 gridpoints in the high resolution runs thus enabling its effects on the atmosphere to be resolved. The amount of irrigation given to the vegetation amounts 10 mm per day and this figure is based on irrigation projects in other parts of Saudi Arabia (Abderrahman (2001)). The initial soil moisture levels are also adjusted to account for a more realistic soil profile given the irrigation rate of 10 mm per day.

The simulations presented in this paper have been executed on the powerful supercomputer called the Earth Simulator, located at JAMSTEC in Yokohama, Japan (http://www.jamstec.go.jp/esc/) which can reach a theoretical peak performance of 40960 GFlops. The Earth Simulator provides a perfect scope to resolve complex terrain on a high resolution grid. To port RAMS to this supercomputer a couple of machine related changes had to be made to the original RAMS code. RAMS was set up using a message passing interface provided by the Earth Simulator Centre to execute RAMS in parallel mode. We used RAMS on in total 80 processors divided over 10 nodes. For this particular code and model configuration, using 80 processors led to a parallel efficiency of 60% while using 16 processors gave an efficiency of around 80%. This drop in efficiency for 80 processors is for the greatest part related to communication overhead.

Besides the machine related modifications mentioned above, a couple of model settings had to be adjusted as well to improve simulated results. During the model implementation phase we tested various setting (grid size and resolution, nesting configurations, nudging strengths) before a satisfactory control simulation was produced. One important setting for numerical stability was the representation of topography in the modelling environment. From Figure 5.2 one can see that the topography rises very steep from sea level to more than 2000 meters in hardly 100 kilometers. This asks for a conservative way of interpolating the raw topography fields in order to maintain a numerical stable model. The interpolation scheme used in this study uses a conventional mean

which smoothes the high peaks of the Asir Mountain range. To improve shortwave radiation at the surface, which at first was too much blocked by high altitude clouds, the 2nd moment shape parameters of the gamma distribution in the microphysics (Walko et al. (1995), Meyers et al. (1997)) had to be adjusted to narrow the distribution spectrum and let it peak at a larger diameter. This had a positive effect on the shortwave incoming radiation at the surface, which improved the simulations compared with radiation observations (NASA Remote Sensing Validation Data,
http://rredc.nrel.gov/solar/new_data/Saudi_Arabia/). To our knowledge no experimental microphysics data for this region are available to quantify the microphysics model parameters more objectively.

5.4 Results

The simulation results will be presented and discussed in two parts: validation and impact assessment. The first part deal with the validation of the model against surface observations and satellite data and the second part will focus on the meteorological impact assessment study of the landuse change described earlier.

5.4.1 Validation

The control run is compared against surface observations and satellite data to assess the performance of the model to simulate the regional climate of Southwest Arabia. In the validation against surface observations, the emphasis is on the three stations mentioned in Table 5.2 and indicated in Figure 5.2a with two stations located in the mountain range (Abha and Khamis Mushait) and the other station located at the coast (Gizan). The initial validation is based on temperature, wind speed and wind direction as these variables were available for most of the observations. Precipitation observations at the three stations were very limited and of uncertain quality and therefore we did not validate the precipitation simulated by RAMS against these observations. As mentioned before, the simulation extends from 21 February to 15 May 2000 with output generated every six hours in phase with the synoptic times of the surface observations. To obtain stationdata out of RAMS a bilinear interpolation is performed using the four gridpoints around the coordinates of the station.

One important step, to ensure proper validation, is to bring down temperature and windspeed from the lowest model level in RAMS (48 m above ground) to surface observation level, and to adjust for altitude

108

difference between model topography and station altitude. Similarity theory Louis (1979) is used to adjust model temperatures and wind speeds to the surface temperature observation level of 2 meter and the surface wind observation level of 10 meter. Altitude differences between station and model were used to correct simulated temperatures using the dry adiabatic lapse rate.

a
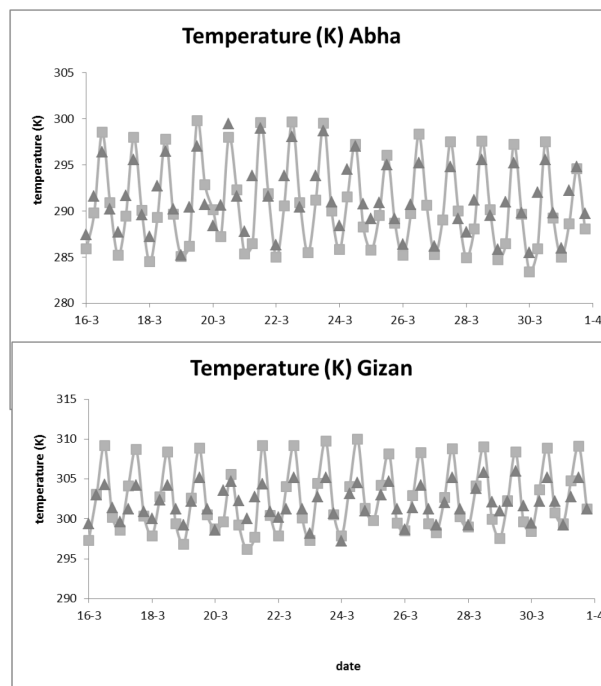
b
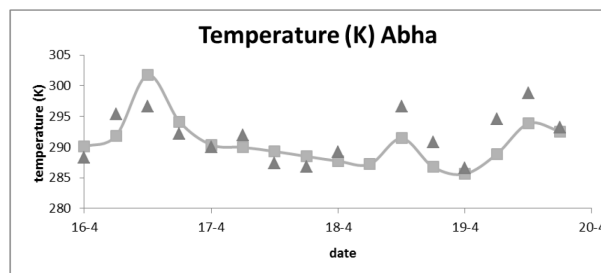
Figure 5.3: a) Time series of temperature for two sites from 16 March to 31 March. b) Time series of temperature (K) at Abha from 16 April 2000 until 19 April 2000. Line with squares: simulation, triangles: observations

Table 5.3: Simple statistical analysis for temperature (RMSE: root mean square error; bias defined as simulated-observed)

Month	Abha		Khamis Mushait		Gizan	
	RMSE	bias	RMSE	bias	RMSE	bias
February	2.25	-0.26	3.06	-1.06	2.22	0.32
March	2.68	-0.71	3.40	-1.64	2.67	-0.03
April	3.68	-1.61	4.28	-2.08	4.39	-2.25
May	3.42	0.28	3.79	-0.54	3.88	-2.36
Total	3.13	-0.81	3.74	-1.55	3.52	-1.18

Figure 5.3a shows the time series of temperature for the second half of March (as an example). The model is capable of simulating temperature at screen level reasonably well for this period. The agreement between model and observations is very good for Abha, however the maximum temperature is overestimated by RAMS for Gizan which may be a result of the limiting influence of the Red Sea as simulated by RAMS. During the simulation some events occur with a diurnal range of only a couple of degrees. This limited diurnal range is simulated by the model for all three stations, but the absolute temperature is underestimated by the model for Gizan. However, the mountain stations show a simulated temperature which is close to the observations as can be seen from Figure 5.3b which shows the simulated temperature and the observed temperature for a period with a small diurnal range.

Statistics of the temperature validation are given in Table 5.3. This table shows the monthly root mean square error (RMSE) and the bias for all three stations. The bias shows that the model in general underestimates temperature with only an overprediction for May in Abha and February in Gizan. For all three stations the RMSE peaks in April and is lowest in the first weeks of the simulation.

Figure 5.4a shows an example of the evolution of wind speed for Abha and Gizan. From both graphs it can be seen that, in a qualitative way, the wind speed is simulated reasonably well by the model capturing the relative high wind speeds between 21 and 26 March. In general the model underestimates most mid-day peaks in the wind speed, and seems to overestimate night time wind speed and this applies to the whole simulation. This is more pronounced for Gizan and less for the mountain stations. Note that the values of wind speed extracted from the ECMWF archive are only archived as whole numbers.

One important local weather phenomenon in the area of interest is the occurrence of sea breeze events as observable in the record of the coastal station of Gizan. Figure 5.4b shows the development of sea

breezes in both observations and model output. In the course of a day the wind changes from an easterly wind to a southwesterly wind. Figure 5.4b also shows the probable influence of more synoptically driven wind from 24 March onward, obstructing the development of a sea breeze, which is partly simulated by RAMS.

a
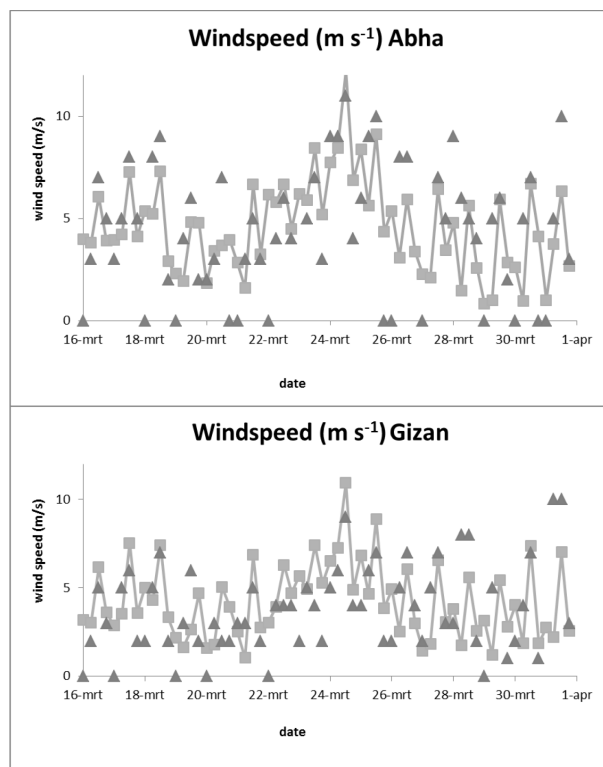
b
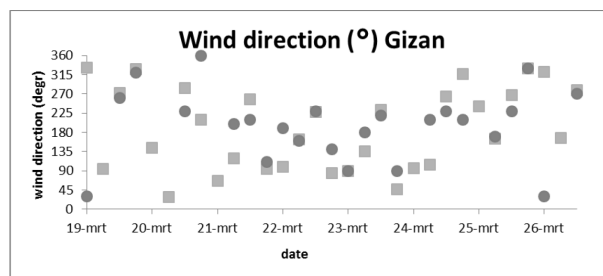
Figure 5.4: a) Windspeed (m s^{-1}) simulated and observed for Abha and Gizan, from 16 March to 31 March, line with squares: simulation, triangles: observations; b) Wind direction (º) for Gizan. squares: RAMS; dots: observations

Since only a few ground stations exist in our domain, the most important source for validation of magnitude and areal distribution of precipitation is the TRMM rainfall product 3B43. Figure 5.5 compares simulated and observed spatial patterns of monthly rainfall for the larger grid. It shows that in general patterns of precipitation are simulated well, though our model simulation gives more wide-spread rain over the Red Sea and Indian Ocean, especially in April and May. This is confirmed in Figure 5.6a which gives monthly rainfall areally averaged over entire domain of the coarse resolution grid (the extend is shown in Figure 5.5). It shows the average numbers do not differ significantly between model and observation. Figure 5.6b shows the same for the high resolution grid for the two full months that fall in the simulated period (21 February-15 May). It shows that the high resolution simulation seems to underestimate total rainfall in April, and it also simulates rain more localized than in reality. In March the opposite is true. Note the small absolute values of rain in both Figure 5.6 a and b. It further shows that the TRMM rainfall product gives different totals depending on the resolution of the 3b43 product. Since this latter phenomenon is more pronounced for individual gridboxes and the localized nature of actual and simulated rainfall we do not show a validation at station level as it is very inconclusive.
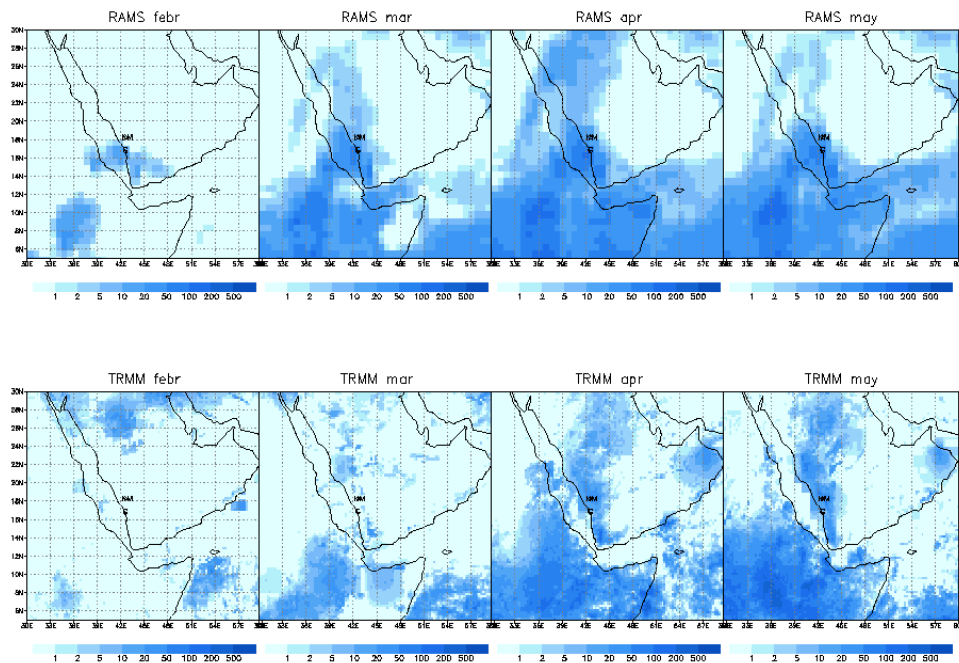
Figure 5.5: Comparison between simulated (upper panel) and observed (lower panel, TRMM 3b43 0.25° grid increment) spatial patterns of monthly rainfall for the coarse resolution grid.

112

a
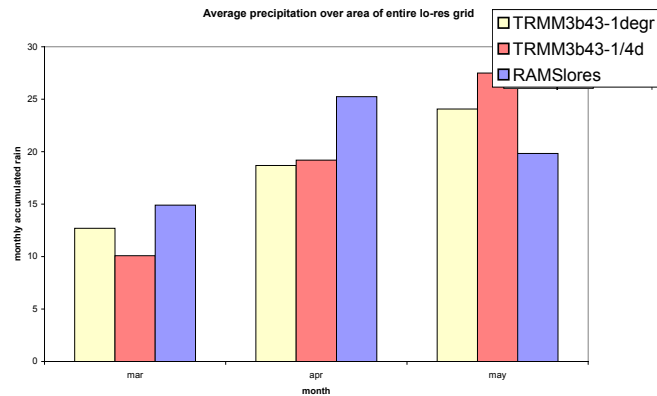
b
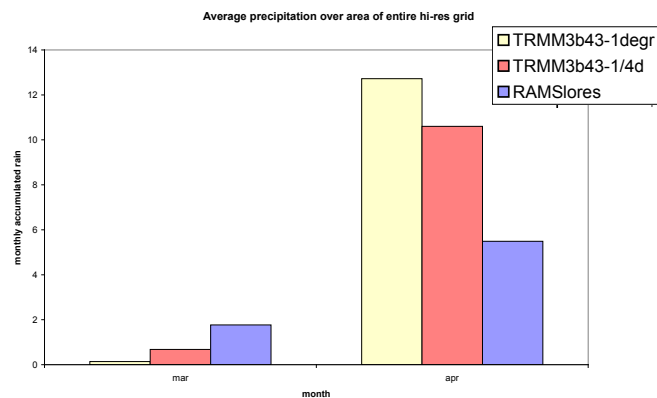
Figure 5.6: Comparison between simulated (blue) and observed monthly total rainfall areally averaged for the whole domain of a) the coarse resolution grid March, April and May(shown in Figure 5.5), and for b) the high-resolution grid March and April(shown in Figure 5.2). Observations are based on the merged (satellite-ground observations) TRMM product 3b43 available at 2 grid meshes: 0.25 degree (pink) and 1 degree (yellow).

5.4.2 Impact assessment

This section will deal with the difference between the control run and the green run, which is defined as the simulation where an irrigated plantation has been implemented in the model (see Figure 5.2a for the precise location of this plantation). Both simulations use the same meteorological boundary and initial conditions. Various analyses have
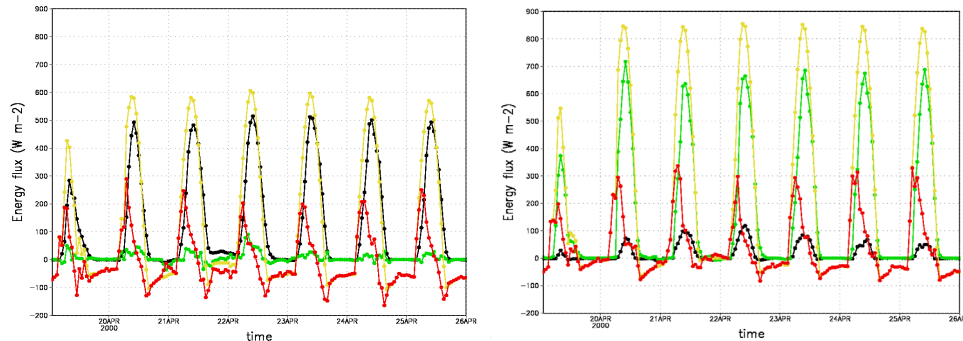
Figure 5.7: Energy balances for the control run (left panel) and the green run (right panel) from 19 April to 25 April. Yellow: Net radiation (W m^{-2}), green: latent heat flux (W m^{-2}), black: sensible heat flux (W m^{-2}), red: soil heat flux (W m^{-2})

been done to assess the differences but most of the analysis presented here focuses on the month of April 2000.

We start the impact assessment with the simulated effect of the irrigated plantation on the energy balance and the partitioning of energy over the various heat fluxes. Figure 5.7 shows the four important variables in the energy balance for the control simulation and the green simulation. The figure shows the balance for a week at the end of April with an hourly resolution. The biggest difference between both graphs is the change in latent heat flux which is for most of the days between 600 and 700 W m^{-2}, resulting in a change of evaporative fraction from 0.05 to about 0.9. The evaporative fraction (unitless) is defined as λ=LE/(H+LE), with LE latent heat flux (W m^{-2}) and H sensible heat flux (W m^{-2}). The irrigation rate of 10 mm per day results in a high transpiration as a result of high incoming radiation and low relative humidity, to. Another effect in the energy balance is the change of net radiation, which is raised in the green simulation by 25 %. This increase is a direct result of a change in albedo accompanied with the change in vegetation from desert to the irrigated plantation.

Figure 5.8a shows two time series of temperature (ºC) for April simulated for a location in the middle of the plantation (42.4 ºN and 17.5 ºE) that will be used in other graphs presented here as well. The simulated temperature is lower in the green run, which is a result of the cooling effect induced by the vegetation. The vegetation absorbs energy which is transformed into latent energy by plant transpiration, which leads to lower temperatures at the surface level. This cooling effect appeared to be higher on those days where the simulated vapor mixing

114

a)
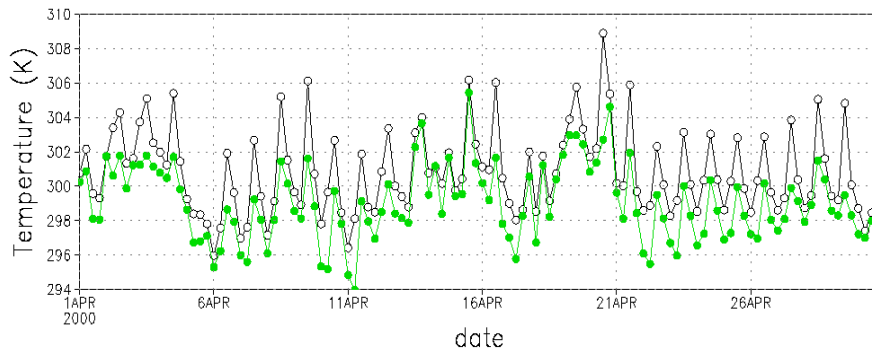
b)
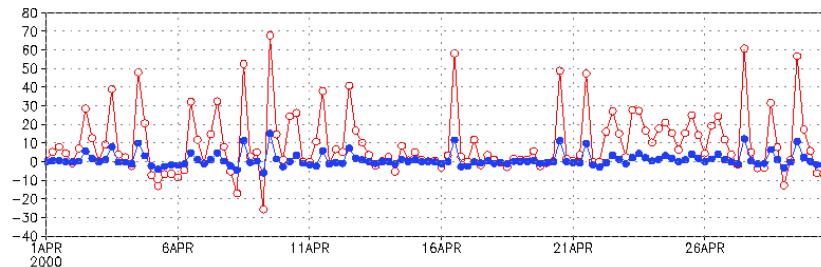
Figure 5.8: a) Simulated temperature (K; black line control run, green line 'green' run) and b) difference in relative humidity (%; red line and vapor mixing ratio (g kg^{-1}, blue line) in April at the centre of the irrigated plantation.

ratio was relatively high, most possibly triggering a higher rate of transpiration of the vegetation. The difference between the control and green simulation is most noticeable greater during midday but is even apparent at nighttime when the difference between both simulations is on average around 1 ºC. The cooling effect is mostly limited to the irrigation plantation (figure 5.9a) with a maximum cooling effect of 3.5 ºC at 12:00 UTC. During daytime a small area downwind (ie. inland) of the plantation also appeared to experience a small cooling effect. Model soundings show that the cooling effect of the plantation propagates upward until 700 m above ground level at daytime (figure 5.9b) and 200 m at nighttime (not shown).

Because of the transpiring vegetation, the humidity in the surrounding of the irrigated plantation is affected as well. Figure 5.8b shows the increase in relative humidity between the green and control simulations. Vapor mixing ratio is increased by a few g kg-1, occasionally up to more than 10 g kg-1. Due to simultaneous cooling the effect on relative

a
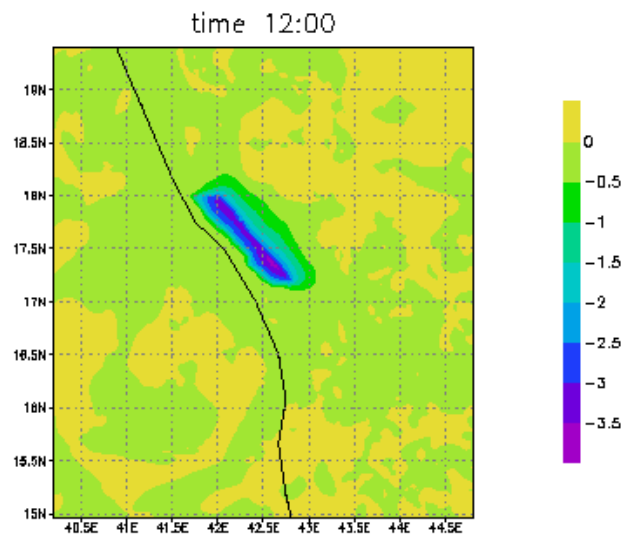
b
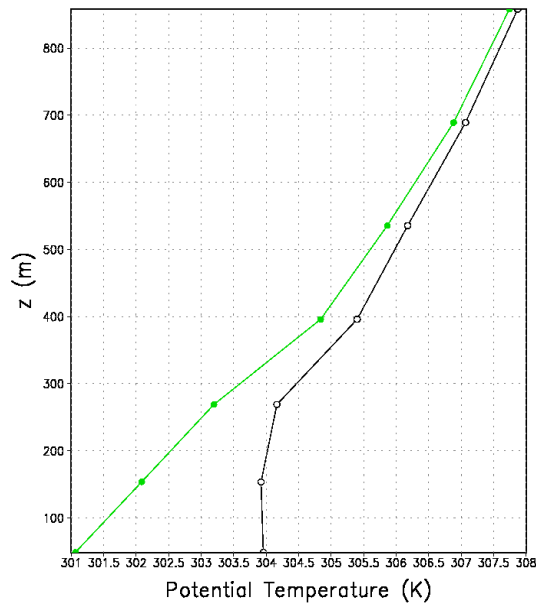
Figure 5.9: a) Spatial representation of the difference in temperature at 12:00 UTC averaged for April. The difference is calculated as green-control. b) Vertical profile of the potential temperature (K) at 12:00 UTC averaged for April at the reference point in the irrigation plantation. Black - control run; green - 'green' run.

116

a

b
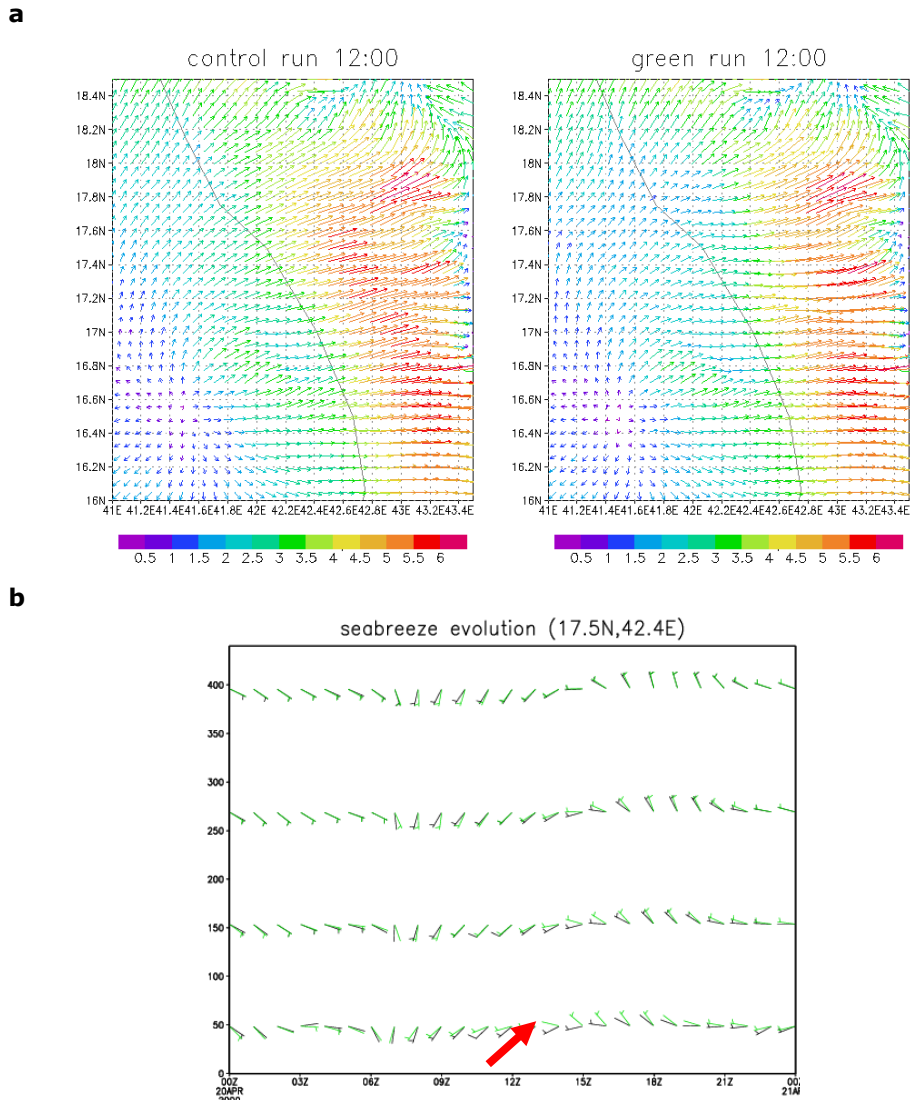
Figure 5.10: a) Spatial representation of wind vectors for the control simulation (left panel) and the green simulation (right panel) at 12:00 UTC (average for April). The color of the vectors represents the simulated wind speed in m s^{-1}. b) Vertical daily profile of the wind vectors simulated at centre of the plantation (17.5 ºN, 42.4 ºE) for 20 April 2000. Black - control run; green - 'green' run. The red arrow gives the direction orthogonal to the coast line at this latitude.

humidity is more pronounced. The increase is more profound in February and March (increase in relative humidity by >15% on average) than in April and May (~10% relative humidity increase).

In direct relation with the temperature change in the irrigated plantation changes in wind speed and wind direction occur. The strength of the sea breeze depends on the difference in temperature between the Red Sea and the land surface. The cooling effect in the green simulation therefore leads to a decrease in the strength of the sea breeze which is nicely simulated by the model (figure 5.10a). The velocity of the sea breeze is about one third smaller in the green simulation compared to the control simulation. Not only the velocity is affected by the change in vegetation but also the wind direction is shifted to a more (north) westerly flow compared to the southwest winds which are more perpendicular to the Arabian coastline. Figure 5.10b shows this clearly in a vertical profile for a certain day (20 April in this example) and at a higher time resolution (hourly) for the centre of the plantation.

Most interesting in this analysis is to see the impact of the vegetation change and change in soil moisture on precipitation. We analyse two effects: a local effect and a downwind effect. Figure 5.11 shows the local effect: the difference in precipitation between both simulations for an area directly over and around the irrigated plantation. The precipitation
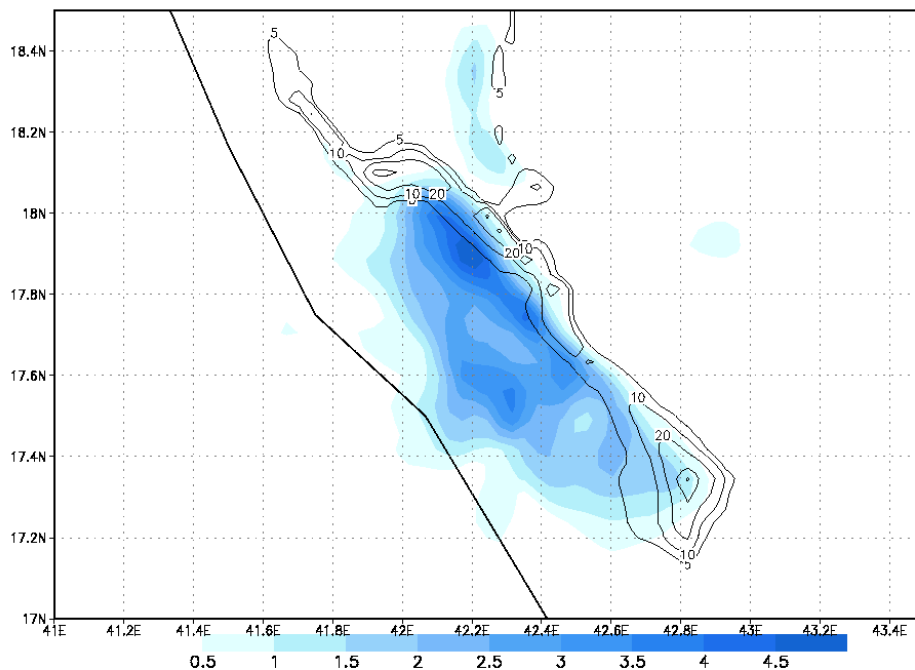
Figure 5.11: Spatial distribution of the difference in precipitation (mm) between green and control run for the whole February to May simulation. The thin black contours shows the relative increase (-), defined as (green-control)/control of precipitation (contour levels are at 5, 10, 20, 40 and 60%).

increase resulting from the irrigation plantation is apparent and is most visible over and just downwind of the plantation and concentrates at the northern part of the plantation. The increase is small in absolute numbers (averaged over the affected area from 1.5 to 3.7mm) but large in relative numbers. This local increase in precipitation is more pronounced in February and March, weakens in April and is almost zero in May.
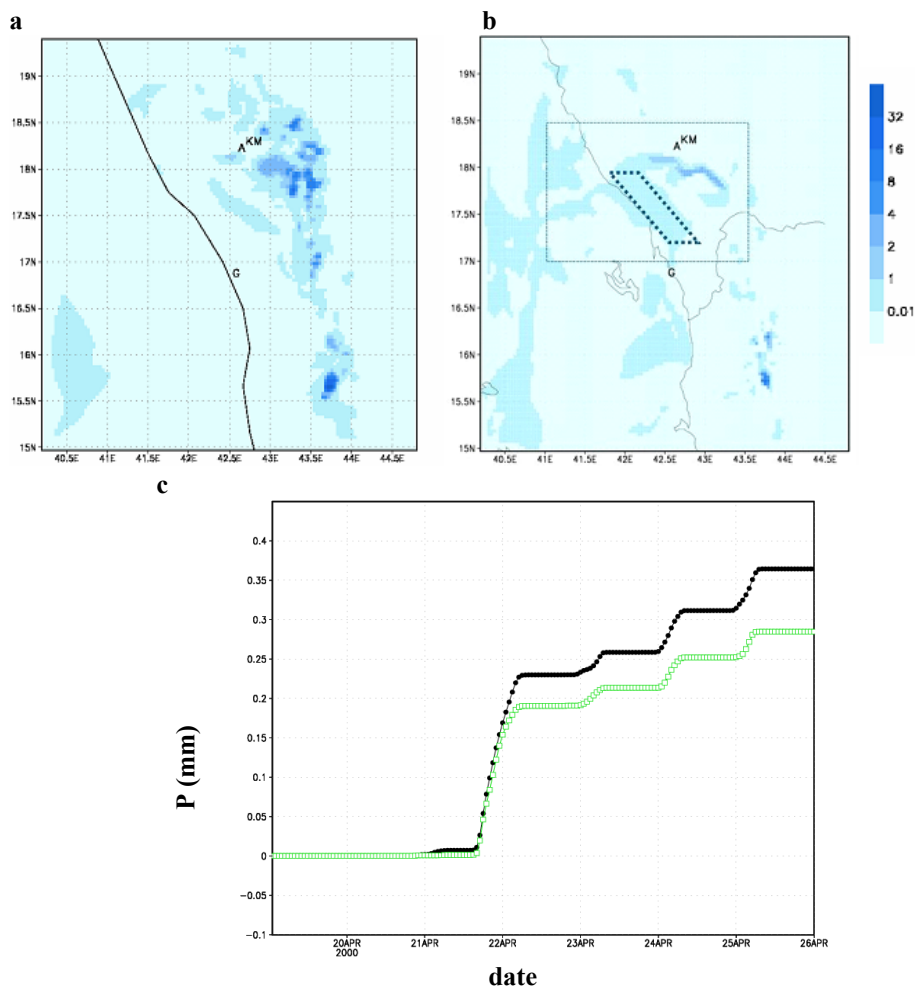
Figure 5.12: Case study of 1 week simulation for 19-26 April 2002. a) total rainfall (mm) for same period for control run. b) total rainfall difference (mm) for 'green' vs control runs. The skewed rectangle depicts the area of the irrigated plantation. The square outlines the area for which the fig 13c applies and for which numbers are given in the text. c) areal average rain (mm) for control (black filled circles) and green (green open circles) runs

For the downwind effect, we next present an analysis for one particular week in April. Started from history files we saved model output at higher temporal resolution. For this particular run Figure 5.12a shows that precipitation was well simulated: Khamis (KM in the figure) rainfall in this week was 31.7 mm and for Gizan 0 mm. Figure 5.12b shows the effect of the irrigated plantation which increases precipitation on the windward side of first mountain ridges (compare Figure 5.2). As the time series in Figure 5.12c show total rainfall (averaged over the square in 12b) increased by 34%. It also shows that most rainfall occurs at night. Detailed analyses using animation of the time series showed that the following process is responsible. During daytime a significant 'blob' of wet air develops over the irrigated plantation. With the onset of the sea-breeze this start being transported by the wind in easterly direction, uphill to the Asir Mountain range, where in the early evening fog starts to develop. Later at night then, light rains develop which stop as soon as the sun rises. The same mechanism occurs in the control run with moist air from the Red sea being blown by the sea breeze onto the mountains. Apparently, the extra moisture in the 'blob' originating from the plantation leads to the extra rain.

5.5   Discussion

We will discuss the validation and impact assessment parts separately.

5.5.1 Validation of control run

Our simulations seem to overestimate the diurnal range in temperature, especially for the coastal station of Gizan. One reason may be that in daytime our model overestimates sensible heat fluxes and underestimates latent heat flux. The only data on energy partitioning available to date have been measured at the old airport near Jeddah for most of 2004 (R. Ohba, personal communication). Though obtained outside our domain these data suggest (see Figure 5.7) that simulated net radiation is reasonable but that the simulated Bowen ratio is too high (~10 simulated vs ~4-5 observed). This may be related to the fact that in our model setup the 'desert' land use class has no vegetation at all, which may not be realistic. Night time sensible heat fluxes are remarkably small in both observations and model.
Wind speed and direction are well simulated, especially the occurrence of sea breeze phenomena. We consider this important because the hypothesized role sea breezes may play in advecting moist marine air to land.

Validation of precipitation in this particular area is complicated by a number of factors. As in semi-arid areas in general, any rain that occurs is highly intermittent and localized. The number of ground stations is limited (3 in our domain) and the quality of the observations is questionable. Also TRMM estimates differ with resolution. Therefore, a validation at local (station level) scales remains inconclusive. At larger scales validation is possible and it seems to reveal that RAMS in this particular setting over-estimates rainfall at coarse resolutions, that is, when using the convective parameterization. On the other hand RAMS seems to underestimate rainfall at higher, cloud resolving resolutions using its micro-physics parameterization. Also model performance seems to differ between long and short runs. We realize that these deficiencies do limit the robustness of the conclusions drawn later.

5.5.2 Impact of irrigated plantation

The effects of increased vegetation density and daily soil moisture repletion, as introduced by our hypothetical irrigated plantation, on the energy balance and partitioning are the expected ones. As a result the air passing over the 'oasis' is cooled (by 3-4K) and moistened (relative humidity increased by 10 to15%).

The wind climate of the coastal area of SW Saudi Arabia is amongst others characterised by daily occurrence of sea breezes. Since the irrigated plantation in that area decreases the thermal contrast between land and sea, the sea breeze weakens both in magnitude and directional change. This effect of coastal land cover changes in general (Pielke et al. (1999), Baker et al. (2001), Van der Molen (2002), Marshall et al. (2004)) and coastal irrigation in particular has been reported by others (Lohar et al. (1995)). It may be one of the reasons of the limited effect on rainfall. On the one hand because it limits the transport of the extra moisture land inward. On the other hand because it reduces the chance that the sea breeze triggers convective phenomena that may be more effective in rainfall generation, as discussed next.

Though we need to be cautious with respect to our conclusions on the effects of our hypothetical irrigated plantation on rainfall is seems justified to conclude that in a setting like the one discussed here rainfall increases are limited in absolute magnitude. Though our case study for late April suggested that the increase can be upto 34% in some periods, the overall effect is small. The reason for this is that in our simulations no extra triggering of convection occurs, as is the main cause for precipitation increases in other studies (De Ridder et al. (1998), Moore et al. (2002)). The total area of our irrigated plantation probably plays

some role. Total area of our oasis is $0.32.10^8$ m^2 as compared to e.g. about $1.5.10^8$ m^2 in De Ridder et al. (1998) for a case in SW Israel or more than 6.10^8 m^2 for a case in the US (Texas High plains) in Moore et al. (2002). Also the analysis in Pielke (2001) suggest that landscape variations have their largest influence on generating local wind circulations, which may act as triggers for deep convection, for horizontal spatial scales of the order of the Rossby radius which has a typical value of $\sim 10^5$m. However, we have to realize that these studies hypothesize a minimum area in order to generate local circulations, whereas in our case it is rather vice versa. Here a local circulation (sea breeze) is present which is weakened in response to the land cover change, and an increased irrigated area will rather suppress than enhance this circulation. The rainfall increase we do observe seems to originate in the extra moisture added to the air and not in triggering potentially larger atmospheric reservoirs. But since the sea breeze is weakened this moist air is only partially advected inland i.e. uphill to condensation levels.

5.6 Conclusions

The limited effects of the irrigated plantation on rainfall generation, in the particular setting reported here, seem to be caused by added moisture in an otherwise only little affected mesoscale flow. The reason for this is probably the limited size of the hypothetical oasis in the direction perpendicular to the main flow.

Finally some comments on the possibility of recycling of irrigation water, through evapotranspiration and subsequent rainfall enhancement. When we analyse the case study for the last week of April (figure 5.12c) and compute numbers for the square area delineated in Figure 5.12b the following picture emerges. The total prescribed irrigation gift in that period was $193 .10^6$ m^3. This led to an increase of evapotranspiration of $115 .10^6$ m^3. The extra atmospheric moisture resulting from this increased rainfall by $2.3 .10^6$ m^3. This occurred downwind but still on the same side of the water divide in the mountains, theoretically (but by no means practically) allowing capture of this rain and feeding it back to the irrigated area. Two conclusions can be drawn from these numbers. The first is that irrigation of 10 mm per day is too much. Potentially transpiring shrub vegetation in our simulation uses about 5-6mm per day. Secondly, recycling of this water is limited to just 2%. On one hand this is additional rain is too limited and too dispersed to re-capture and return to the irrigated area itself. On the other hand it falls in an area where rain fed agriculture occurs. There, though small in absolute numbers but big in relative numbers ($\sim 30\%$), the extra rain may

increase crop productivity or reduce the risk of crop failures and thus be important to local agriculture (Otterman et al. (1990)).

To strengthen such conclusions better statistics on more rainfall events are needed. We therefore are currently extending our simulations to cover at least a full year and have plans to repeat these for climatologically more wet or more dry years.

Regional atmospheric feedbacks over land and coastal areas

Chapter 6

Synthesis and outlook

In this thesis the most important feedbacks between the earth surface and the atmosphere are investigated. From all cases it is clear that a regional atmospheric model is a useful tool to study the meso-scale processes and the different feedbacks between the earth surface and the atmosphere. The case studies also show that a generic regional atmospheric model, which can be applied to any part of the world, is often more virtuality than reality. In all cases an adjustment was necessary to be able to correctly represent the regional atmosphere at the location and timespan of study. For all four cases the spatial resolution of the model enables the use of the microphysics package in RAMS and precipitation is not only simulated using convective parameterization.

Next to the choices of parameterizations and parameter values in a regional model , Weaver et al. (2002) also pointed out, correctly, that a regional atmospheric model "critically depends on informed choices of aspects of model configuration. These include horizontal resolution, strength of nudging, and atmospheric initialization." This line of thought has also been applied to the results of the case studies so that simulated results are not biased resulting from wrong grid configurations.

The regional atmospheric feedbacks will be addressed following the questions that were posed in the introduction of this thesis.

What is the regional atmospheric climate effect of land cover on precipitation and carbon dynamics in a heterogeneous environment in a temperate climate?

To answer this question the case studies from chapters 2 and 3 are used and referred to. The Netherlands are thought to be representative for a country in a temperate climate. The choice of a regional atmospheric model is justified in the Dutch cases while looking at the high degree of heterogeneity in the Netherlands with rural land use alternated with urban areas of various sizes.

Precipitation
The effect of land cover and even topography has a clear effect on the precipitation. The precipitation maximum at the Veluwe can only be explained by taking into account both land cover and topography. The effect of land cover on precipitation appears to be larger in winter periods than in summer periods. This difference results from synoptic conditions which favour the regional atmospheric feedbacks from forests more in winter than in summer. The main process, responsible for the positive feedback of land cover on precipitation, are the convergence of vapour at the edges of the forest and a higher availability of vapour in the atmosphere through the evaporation of the forest.

126

One of the important issues while executing regional atmospheric simulations for a country like the Netherlands is a well described planetary boundary layer. The land surface is coupled to the PBL as it integrates surface fluxes over regional and diurnal scales The main conclusion from the sensitivity tests with the changing turbulence parameterization in chapter 2 is that the choice for turbulence parameterization should be based on the event that is subject of the study. In chapter 2 the effect of turbulent parameterizations on simulated precipitation is shown. This effect can be 15-20 mm as was shown in figure 2.8. The Mellor-Yamada parameterization (MY) is giving a better performance in simulating precipitation in wintertime (frontal situation) but the configuration with MRF is performing better in simulating precipitation in convective circumstances. Further research is necessary to develop a parameterization that combines the properties and skill for winter and summer. This complements the conclusion from the study by Steeneveld et al. (2011) in which MRF and MY where compared in two different regional atmospheric models, with a focus on the representation of the physical processes in the planetary boundary layer.

Carbon dynamics
Chapter 3 shows the importance of a correct representation of surface fluxes on carbon dynamics and latent heat fluxes. Not all parameters of land cover classes were derived using optimizations because of a lack of observational data on certain fluxes. The priority of observations on the land cover classes has been described in Table 5.3 of chapter 3: coniferous forest, grassland and maize. Only the coniferous forest at Loobos and the grassland site of Cabauw were used for optimization as these sites have an extensive time series of observations to optimize the parameters for both the evaporation and the carbon exchange. This is justified by the fact that both forest and grassland are the most dominant types of land use in the area of interest of chapter 3. The simulated fluxes with the optimized parameters agree well compared to the site where no optimization was possible. Over the past years, initiatives have surfaced to provide the modelling community with a multitude of station observations for various land cover types that can help parameterising these accordingly.

The effect that a forest has on the CO_2 concentration ($[CO_2]$) is quite apparent. The forested area of the Veluwe is consistently resolved in both model and aircraft observations and in both latent heat and CO2 fluxes. The forests at the Veluwe in daytime decrease the atmospheric carbon dioxide whereas the emissions from the urbanized areas in The Netherlands increased $[CO_2]$ transported in plumes. The interaction

between urban areas and the atmosphere is only in one direction with the CO_2 emissions from the city influencing the $[CO_2]$ in the vicinity of the urban areas.

A regional atmospheric model is a very useful tool to assess the influence that the various land cover types (including urban areas) have on the regional $[CO_2]$-balance. This has also been confirmed in a more recent modelling study in a boreal environment (Kvon et al. (2012)). Earlier studies (e.g. Geels et al. (2007)) already recommended to use higher resolution models for interpretation of continental CO_2 data. The necessity to use high resolution data generated by a regional atmospheric model is essential in atmospheric inversion studies. In combination with estimates of surface fluxes, originating from land surface models, oceanic and anthropogenic databases, these atmospheric inversion studies are used to quantify the distribution of carbon sources and sinks at the global continental scale. Meesters et al. (2012) show the potential of high resolution inverse carbon dioxide flux estimates for the Netherlands.

Two parts of a regional atmospheric model certainly need attention for this, namely (1) a correct representation of the carbon fluxes at the surface by optimizing the parameters in the carbon submodel, and (2) a realistic representation of the boundary layer. The intensive experimental campaign described in chapter 3 was a good way to study the regional atmospheric feedbacks which are important in estimating $[CO_2]$ in the atmosphere and near the surface. The gaps in both the modelling strategy and measurement campaign show up in the analysis in chapter 3. The underlying land surface model, SWAPS-C, is able to correctly simulate the various fluxes if the correct parameters for the carbon submodel are used. The submodel which calculates the evaporation is not too sensitive for the choice of parameters. The same set of parameter values are used in chapters 2 and 3.

In chapter 3 the vertical profiles of potential temperature and CO_2 concentration show that boundary layer dynamics seem to be reproduced well, though the stable boundary layer in the early morning is simulated too shallow and too cold. The validation of the vertical profiles also indicates that the depth of the well-mixed day-time boundary layer is not well represented and is underestimated by 100–200m by the model. This has its effect of the mixing of CO_2 throughout the atmosphere. de Arellano et al. (2004) showed that the CO_2 concentration in the boundary layer is reduced much more effectively by the ventilation with entrained air than by CO_2 uptake by the vegetation. In the turbulent parameterization by Mellor-Yamada this entrainment process is poorly represented in the atmospheric model leading to a

128

higher simulated CO_2 concentration in most of the vertical profiles. The sensitivity of simulated CO_2 mixing ratios to the parameterization of the PBL is also assessed by Tolk et al. (2009).

For the Netherlands, it is shown from chapters 2 and 3 that land use and topography are boundary conditions that should be well validated before they can be implemented in a regional atmospheric model. This not only means that land cover classes are located correctly, but also that parameterization of these land cover classes within the modelling system should be well validated. This conclusion is also valid for the representation of soils and soil moisture content within the Netherlands or, even broader, on a European scale.

What role plays the sea surface temperature (SST) on precipitation in coastal areas in temperate and desert environments?
Chapters 4 and 5 deal with the impact of SST on precipitating processes in coastal areas. In chapter 4 the effect of a warmer than normal sea is explored, while in chapter 5 the sea is part of the modeling domain. Chapter 4 also deals with the effect of a higher resolution SST database on precipitation, both in time and space. In this case study it appears that a strong gradient in SST was observed near the western coastline of the Netherlands in the high resolution NOAA SST dataset. These small scale features are not visible in the coarse resolution dataset of HadISST1. This led to a significant improvement in the simulated precipitation with the simulated monthly precipitation sum for a box near the west coast in the Netherlands being almost identical to the observations. However, in the daily totals some differences are apparent between the model and the observations. This can be attributed for a large part to the fact that some heavy precipitation showers are simulated over the area of averaging, while in reality these showers are located more to the west.

Chapter 4 also focusses on the added value of a regional atmospheric model in non-hydrostatic mode at a high grid increment (1 kilometer). The results are compared with a study performed by Lenderink et al. (2009) who used a regional model in hydrostatic mode with a coarser resolution. The results in chapter 4 show that a regional atmospheric model improves the precipitation totals. To analyze if a regional atmospheric model really does a better job in simulating convective precipitation, a comparison has to be made with hourly rainfall radar data. Unfortunately, this data was not available at the moment of our research.

129

The last part of chapter 4 deals with the effect that higher SST has on the formation of precipitation near the coast. The sensitivity experiment showed that an overall decrease of 2 degrees of SST leads to a decrease in total amount of precipitation decreases for an area near the west coast of just over 60 mm (212 mm against 151 mm). This is still a high number, but not as extreme as was the case in August 2006. With climate change affecting the temperature of the North Sea, the possibility of extreme convective showers is higher in a changing climate.

The focus in chapter 5 has been on land use change, but because the projected area of land use change is located next to the sea, the sea certainly plays a role in influencing the regional climate.
Analysis of the observational records for the Saudi Arabian coastline, however, shows that the observed precipitation in this case is not directly influenced by SST values but is mostly driven by larger synoptic systems like the Mediterranean low pressure systems and the monsoon. According to studies by Evans (2010) and Almazroui (2013), the southwestern part of the Arabian peninsula will in future climate be more influenced by the ITCZ and, as a result, will experience more extreme rain events. Almazroui et al. (2013) made a first assessment to link a rise in SST values over the last two decades to observed values of temperature at the Arabian peninsula.

The wind climate of the coastal area of Saudi Arabia is characterized by daily occurrence of sea breezes. Since the irrigated plantation in that area decreases the thermal contrast between land and sea, the sea breeze weakens both in magnitude and directional change. The regional atmospheric model captures these aspects of the sea breeze nicely in the simulations of chapter 5.

Next to the effect that the sea has on precipitation in temperate and desert environments, the sea also plays a role in the $[CO_2]$ near the coast. Seasonal fields observations show that the North Sea acts as a sink for CO2 throughout the year except for the summer months in the southern region of the North Sea. As a result in the case of strong winds blowing from west/northwestern directions air with relative low [CO2] will penetrate inland.

What are the differences in impacts of land use change on the regional climate between a temperate and a desert environment?
Chapters 2 and 5 deal with idealized land use changes which are incorporated in the regional atmospheric model. The land use change in chapter 2 is defined by changing the forest at the Veluwe into grassland

which is most frequent in the area around the Veluwe. In chapter 5 a part of the desert is changed into shrubland. In this case study an irrigation gift of 10 mm per day is given to support the vegetation. The difference between both cases is that observations at the Veluwe measure a reasonable amount of precipitation per month throughout the year, while in Saudi Arabia this is limited to certain periods. Even in those periods only some rainfall stations (e.g. Abha, located in the mountains) observe values of over 50 mm per month.

The effect of land use change in the Netherlands differs between summer and winter. In winter the maximum change in precipitation is 18.6 %, while this is only 6.4 % in the summertime. The energy balance shows the largest differences in summertime when the latent heat flux clearly decreases as the forest is not apparent anymore. In both wintertime and summertime the incoming direct radiation is higher when the forest is not there. The atmosphere above the forest is more favourable to clouds which block the direct radiation. With the change into grassland also the outgoing longwave radiation is also affected with a different signal in winter and summertime due to respectively the faster cooling of the surface and the heating of the surface. The differences in the energy balance have its impact on the local temperature as well. In the summertime, the monthly averaged temperature at 11UTC increases by almost 0.5 degrees when the forest is removed.

The basic hypothesis for the irrigation case study in Saudi Arabia in chapter 5 was that more moisture will be available above the foreseen irrigated plantation and that, subsequently, this moisture will be transported by the southwestern wind inland (sea breeze) and that orographic lifting might generate more rainfall in the mountain range downwind of the plantation. However, this hypothesis was not confirmed by the present model study. The temperature signal was found stronger in Saudi Arabia with the air passing over the irrigated plantation being 3-4 degrees colder. The air is also 10 to 15 % more moist. This extra moisture is transported inland but it only adds up to an increase in precipitation inland of 1.5 to 3.7 mm. This extra rainfall originates from a mass of wet air being transported from the plantation uphill to the mountain range inland. The precipitation falls as light rain during the evening and night time.

The impact of land use changes does depend on the studied climate zone. The added value of 'greening' an area in a semi-arid environment is, in the case study presented in chapter 5, not reflected in the precipitation. This is supported by one of the outcomes of the recent study by Taylor et al. (2012), who concluded that drier surface

conditions in semi-arid environments favour afternoon precipitation better than more moist conditions due to suppression of the sensible heat flux which is the main driver for moist convection. The direct effect of an irrigated plantation is clear as the temperature in the plantation drops by almost 4 degrees. This is different in a temperate climate, but the effect of land use change on precipitation in an already moist surrounding is quite substantial in absolute values. This strong coupling between land and atmosphere cannot be deduced from the map derived by Koster et al. (2004), but more recent work by Seneviratne et al. (2006) and Zeng et al. (2010) hint at the importance of land-atmosphere coupling in Europe.

Outlook
The work in this thesis showed the feedbacks between the surface and the regional atmosphere for different climate zones using four different case studies. To study these feedbacks a regional atmospheric model has been introduced, utilised and modified to be able to explore these feedbacks. The feedbacks between the surface (land and sea) and the atmosphere are apparent from the presented cases. The positive effect of simulations at higher resolution has been discussed. One of the issues with simulations at a higher simulations is that the underlying databases should have at least the same resolutions, but preferably higher.

In this thesis recommendations have been made to improve regional atmospheric models. One important issue deals with the planetary boundary layer which strongly influences the feedbacks through redistributing vapour and carbon in the vertical in particular. Within this thesis the PBL scheme had to be adapted to the specific application and location. Thus we recommend to further develop a PBL scheme that is able to cover all relevant conditions with proper interactions of surface conditions, lower level clouds and atmospheric convection.

Validation of a regional atmospheric model is, of course, one of the most important parts of the models. As the resolution increases, the chance increases that the model produces convective showers or clouds but at a slightly different location from reality causing a double penalty. As this influences the score of the model, it is recommended to validate the model not only with point observations but in a more area wide setting. This holds especially true for precipitation and for clouds that prevent incoming shortwave radiation to reach the surface.

With the emergence of regional climate models, better knowledge of local-to-regional feedbacks is unavoidable. The relatively fine resolution on which regional atmospheric models can be executed also means that land use and topography can be represented on this fine resolution. This

means that the regional atmospheric models are a perfect platform to develop and test descriptions of processes, which are not currently well described in regional climate models. This is necessary as there is a growing need to have climate data information on the local level. To downscale the requested data to the local level a regional atmospheric model (RAM) in non-hydrostatic setting is complementary to climate data from the RCM. The whole modelling suite of GCM – RCM – RAM is a way forward to investigate the regional atmospheric feedbacks in a changing climate, although there might be a chance of introducing extra uncertainty while going to finer resolutions. However, following this chain of dynamical downscaling the feedbacks between the surface and the atmosphere are maintained and local conditions are better preserved.

Regional atmospheric feedbacks over land and coastal areas

Chapter 7

References

Abderrahman, W. A. (2001). "Energy and water in arid developing countries: Saudi Arabia, a case-study." <u>International Journal Of Water Resources Development</u> **17**(2): 247-255.

Almazroui, M. (2013). "Simulation of present and future climate of Saudi Arabia using a regional climate model (PRECIS)." <u>International Journal of Climatology</u> **33**(9): 2247-2259.

Almazroui, M., M. N. Islam and P. D. Jones (2013). "Urbanization effects on the air temperature rise in Saudi Arabia." 1-14.

Andre, J. C., P. Bougeault, J. F. Mahfouf, P. Mascart, J. Noilhan and J. P. Pinty (1989). "Impact of forests on mesoscale meteorology." <u>Philosophical Transactions of the Royal Society of London Series B-Biological Sciences</u> **324**(1223): 407-422.

Ashby, M. (1999). "Modelling the water and energy balances of Amazonian rainforest and pasture using Anglo-Brazilian Amazonian climate observation study data." <u>Agricultural and forest meteorology</u> **94**(2): 79-101.

Avissar, R. and T. Schmidt (1998). "An evaluation of the scale at which ground-surface heat flux patchiness affects the convective boundary layer using large-eddy simulations." <u>Journal Of The Atmospheric Sciences</u> **55**(16): 2666-2689.

Baker, R. D., B. H. Lynn, A. Boone, W. K. Tao and J. Simpson (2001). "The influence of soil moisture, coastline curvature, and land-breeze circulations on sea-breeze-initiated precipitation." <u>Journal of Hydrometeorology</u> **2**(2): 193-211.

Bakwin, P. S., P. P. Tans, C. L. Zhao, W. Ussler and E. Quesnell (1995). "Measurements of Carbon-Dioxide on a Very Tall Tower." <u>Tellus Series B-Chemical and Physical Meteorology</u> **47**(5): 535-549.

Bazuhair, A. S., A. AlGohani and Z. Sen (1997). "Determination of monthly wet and dry periods in Saudi Arabia." <u>International Journal Of Climatology</u> **17**(3): 303-311.

Ben-Gai, T., Bitan, A., Manes, A., Alpert, P. (1993). "Long term October rainfall patterns in S Israel." <u>Theoretical and Applied Climatology</u> **46**, 209–217.

Bennett, L. J., K. A. Browning, A. M. Blyth, D. J. Parker and P. A. Clark (2006). "A review of the initiation of precipitating convection in the United Kingdom." <u>Quarterly Journal of the Royal Meteorological Society</u> **132**(617): 1001-1020.

Bernardet, L. R., L. D. Grasso, J. E. Nachamkin, C. A. Finley and W. R. Cotton (2000). "Simulating convective events using a high-resolution mesoscale model." <u>Journal of Geophysical Research-Atmospheres</u> **105**(D11): 14963-14982.

Betts, A. K., R. L. Desjardins and J. I. Macpherson (1992). "Budget Analysis of the Boundary-Layer Grid Flights During Fife 1987." <u>Journal of Geophysical Research-Atmospheres</u> **97**(D17): 18533-18546.

Chakraborty, A., S. K. Behera, M. Mujumdar, R. Ohba and T. Yamagata (2006). "Diagnosis of tropospheric moisture over Saudi Arabia and influences of IOD and ENSO." Monthly Weather Review **134**(2): 598-617.

Charney, J. G. (1975). "Dynamics Of Deserts And Drought In Sahel." Quarterly Journal Of The Royal Meteorological Society **101**(428): 193-202.

Chen, C. and W. R. Cotton (1983). "A one-dimensional simulation of the stratocumulus-capped mixed layer." Boundary Layer Meteorology **25**: 289-321.

Christensen, J. H., T. R. Carter, M. Rummukainen and G. Amanatidis (2007). "Evaluating the performance and utility of regional climate models: the PRUDENCE project." Climatic Change **81**: 1-6.

Christensen, J. H. and O. B. Christensen (2003). "Climate modelling: Severe summertime flooding in Europe." Nature **421**(6925): 805-806.

Christensen, J. H., B. Hewitson, A. Busuioc, A. Chen, X. Gao, I. Held, R. Jones, R. K. Kolli, W.-T. Kwon, R. Laprise, V. M. Rueda, L. Mearns, C. G. Menéndez, J. Räisänen, A. Rinke, A. Sarr and P. Whetton (2007). "Regional climate projections." In: Solomon S, Qin D, Manning M, Chen Z, Marquis M, Averyt KB, Tignor M, Miller HL (eds) Climate change 2007: the physical science basis.Contribution of Working Group I to the fourth assessment report of the Intergovernmental Panel on Climate Change. Cambridge University Press, Cambridge.

Clark, A. J., W. A. Gallus and T. C. Chen (2007). "Comparison of the diurnal precipitation cycle in convection-resolving and non-convection-resolving mesoscale models." Monthly Weather Review **135**(10): 3456-3473.

Claussen, M., V. Brovkin, A. Ganopolski, C. Kubatzki and V. Petoukhov (2003). "Climate change in northern Africa: The past is not the future." Climatic Change **57**(1-2): 99-118.

Claussen, M., C. Kubatzki, V. Brovkin, A. Ganopolski, P. Hoelzmann and H. J. Pachur (1999). "Simulation of an abrupt change in Saharan vegetation in the mid-Holocene." Geophysical Research Letters **26**(14): 2037-2040.

Collatz, G. J., M. Ribas Carbo and J. A. Berry (1992). "Coupled photosynthesis-stomatal conductance model for leaves of C4 plants." Aust J Plant Physiol. East Melbourne : Commonwealth Scientific and Industrial Research Organization. 1992 **19**(5): 519-539.

Cotton, W. R., R. A. Pielke, R. L. Walko, G. E. Liston, C. J. Tremback, H. Jiang, R. L. McAnelly, J. Y. Harrington, M. E. Nicholls, G. G. Carrio and J. P. McFadden (2003). "RAMS 2001: Current status and

future directions." <u>Meteorology and Atmospheric Physics</u> **82**(1-4): 5-29.

Culf, A. D., G. Fisch, Y. Malhi and C. A. Nobre (1997). "The influence of the atmospheric boundary layer on carbon dioxide concentrations over a tropical forest." <u>Agricultural and Forest Meteorology</u> **85**(3-4): 149-158.

de Arellano, J. V. G., B. Gioli, F. Miglietta, H. J. J. Jonker, H. K. Baltink, R. W. A. Hutjes and A. A. M. Holtslag (2004). "Entrainment process of carbon dioxide in the atmospheric boundary layer." <u>Journal of Geophysical Research-Atmospheres</u> **109**(D18).

De Ridder, K. and H. Gallee (1998). "Land surface-induced regional climate change in southern Israel." <u>Journal of Applied Meteorology</u> **37**(11): 1470-1485.

Denning, A. S., I. Y. Fung and D. Randall (1995). "Latitudinal Gradient of Atmospheric CO_2 Due to Seasonal Exchange with Land Biota." <u>Nature</u> **376**(6537): 240-243.

Denning, A. S., T. Takahashi and P. Friedlingstein (1999). "Can a strong atmospheric CO2 rectifier effect be reconciled with a "reasonable" carbon budget?" <u>Tellus Series B-Chemical and Physical Meteorology</u> **51**(2): 249-253.

Derwent, R. G., D. B. Ryall, A. Manning, P. G. Simmonds, S. O'Doherty, S. Biraud, P. Ciais, M. Ramonet and S. G. Jennings (2002). "Continuous observations of carbon dioxide at Mace Head, Ireland from 1995 to 1999 and its net European ecosystem exchange." <u>Atmospheric Environment</u> **36**(17): 2799-2807.

Dickinson, R.E., Henderson-Sellers, A., Kennedy, P.J., Wilson, M.F. 1986). <u>Biosphere–Atmosphere Transfer Scheme for the NCAR Community Climate Model.</u> NCAR Tech. Rep. NCAR/TN2751STR. 69 pp.

Dolman, A. J. (1993). "A Multiple-Source Land-Surface Energy-Balance Model for Use in General-Circulation Models." <u>Agricultural and Forest Meteorology</u> **65**(1-2): 21-45.

Dolman, A. J., E. J. Moors, J. A. Elbers and W. Snijders (1998). "Evaporation and surface conductance of three temperate forests in the Netherlands." <u>Annales Des Sciences Forestieres</u> **55**(1-2): 255-270.

Dolman, A. J., J. Noilhan, P. Durand, C. Sarrat, A. Brut, B. Piguet, A. Butet, N. Jarosz, Y. Brunet, D. Loustau, E. Lamaud, L. Tolk, R. Ronda, F. Miglietta, B. Gioli, V. Magliulo, M. Esposito, C. Gerbig, S. Korner, R. Glademard, M. Ramonet, P. Ciais, B. Neininger, R. W. A. Hutjes, J. A. Elbers, R. Macatangay, O. Schrems, G. Perez-Landa, M. J. Sanz, Y. Scholz, G. Facon, E. Ceschia and P. Beziat (2006). "The CarboEurope regional experiment strategy." <u>Bulletin of the American Meteorological Society</u> **87**(10): 1367-+.

Dyer, J. (2011). "Analysis of a Warm-Season Surface-Influenced Mesoscale Convective Boundary in Northwest Mississippi." Journal of Hydrometeorology **12**(5): 1007-1023.

Ek, M. B. and A. A. M. Holtslag (2004). "Influence of soil moisture on boundary layer cloud development." Journal of hydrometeorology **5**(1): 86-99.

Evans, J. P. (2010). "Global warming impact on the dominant precipitation processes in the Middle East." Theoretical and Applied Climatology **99**(3-4): 389-402.

Evers, P. W., W. Bouten and J. J. M. van Grinsven (1991). CORRELACI : identification of traditional and air pollution related stress factors in a douglas fir ecosystem : the aciforn stands : a correlative evaluation of monitoring data on the carbon, nutrient and water cycles. Wageningen, De Dorschkamp.

Flatau, P. J., G. J. Tripoli, J. Verlinde and W. R. Cotton (1989). The CSU-RAMS cloud microphysical module: General theory and code documentation. Fort Collins, Colorado, Colorado State Univ.**:** 88.

Fraedrich, K., A. Kleidon and F. Lunkeit (1999). "A green planet versus a desert world: Estimating the effect of vegetation extremes on the atmosphere." Journal of Climate **12**(10): 3156-3163.

Frei, C., R. Scholl, S. Fukutome, J. Schmidli and P. L. Vidale (2006). "Future change of precipitation extremes in Europe: Intercomparison of scenarios from regional climate models." Journal of Geophysical Research-Atmospheres **111**(D6): 22.

Friedrich, R., A. Freibauer, E. Gallmann, M. Giannouli, D. Koch, P. Peylin, S. Pye, E. Riviere, R. S. Jose, W. Winiwarter, P. Blank, J. Kühlwein, T. Pregger, S. Reis, Y. Scholz, J. Theloke and A. Vabitsch (2003). Temporal and Spatial Resolution of Greenhouse Gas Emissions in Europe. Jena, MPI fuer Biogeochemie**:** 36.

Gal-chen, T. and R. C. J. Somerville (1975). "On the use of a coordinate transformation for the solution of the Navier-Stokes equations " Journal of Computational Physics **17**(2): 209-228.

Gallus, W. A. (2010). "Application of Object-Based Verification Techniques to Ensemble Precipitation Forecasts." Weather and Forecasting **25**(1): 144-158.

Garten, J. F., C. E. Schemm and A. R. Croucher (2003). "Modeling the transport and dispersion of airborne contaminants: A review of techniques and approaches." Johns Hopkins Apl Technical Digest **24**(4): 368-375.

Geels, C., S. C. Doney, R. Dargaville, J. Brandt and J. H. Christensen (2004). "Investigating the sources of synoptic variability in atmospheric CO_2 measurements over the Northern Hemisphere continents: a regional model study." Tellus Series B-Chemical and Physical Meteorology **56**(1): 35-50.

Geels, C., M. Gloor, P. Ciais, P. Bousquet, P. Peylin, A. T. Vermeulen, R. Dargaville, T. Aalto, J. Brandt, J. H. Christensen, L. M. Frohn, L. Haszpra, U. Karstens, C. Rodenbeck, M. Ramonet, G. Carboni and R. Santaguida (2007). "Comparing atmospheric transport models for future regional inversions over Europe - Part 1: mapping the atmospheric CO2 signals." Atmospheric Chemistry and Physics **7**(13): 3461-3479.

Gerbig, C., J. C. Lin, S. C. Wofsy, B. C. Daube, A. E. Andrews, B. B. Stephens, P. S. Bakwin and C. A. Grainger (2003). "Toward constraining regional-scale fluxes of CO_2 with atmospheric observations over a continent: 2. Analysis of COBRA data using a receptor-oriented framework." Journal of Geophysical Research-Atmospheres **108**(D24).

Gioli, B., F. Miglietta, B. De Martino, R. W. A. Hutjes, H. A. J. Dolman, A. Lindroth, M. Schumacher, M. J. Sanz, G. Manca, A. Peressotti and E. J. Dumas (2004). "Comparison between tower and aircraft-based eddy covariance fluxes in five European regions." Agricultural and Forest Meteorology **127**(1-2): 1-16.

Global Soil Data Task Group (2000). Global Gridded Surfaces of Selected Soil Characteristics (IGBP-DIS). [Global Gridded Surfaces of Selected Soil Characteristics (International Geosphere-Biosphere Programme - Data and Information System)]. Data set. Available on-line [http://www.daac.ornl.gov] from Oak Ridge National Laboratory Distributed Active Archive Center, Oak Ridge, Tennessee, U.S.A.

Groisman, P. Y., R. W. Knight, D. R. Easterling, T. R. Karl, G. C. Hegerl and V. A. N. Razuvaev (2005). "Trends in intense precipitation in the climate record." Journal of Climate **18**(9): 1326-1350.

Gurney, K. R., R. M. Law, A. S. Denning, P. J. Rayner, D. Baker, P. Bousquet, L. Bruhwiler, Y. H. Chen, P. Ciais, S. Fan, I. Y. Fung, M. Gloor, M. Heimann, K. Higuchi, J. John, T. Maki, S. Maksyutov, K. Masarie, P. Peylin, M. Prather, B. C. Pak, J. Randerson, J. Sarmiento, S. Taguchi, T. Takahashi and C. W. Yuen (2002). "Towards robust regional estimates of CO_2 sources and sinks using atmospheric transport models." Nature **415**(6872): 626-630.

Hanan, N. P. (2001). "Enhanced two-layer radiative transfer scheme for a land surface model with a discontinuous upper canopy." Agric for meteorol. [Amsterdam] : Elsevier, [1984 . Sept 27, 2001 **109**(4): 265-281.

Hanan, N. P., P. Kabat, A. J. Dolman and J. A. Elbers (1998). "Photosynthesis and carbon balance of a Sahelian fallow savanna." Global change biology **4**(5): 523-538.

Harrington, J. Y. (1997). The effects of radiative and microphysical processes on simulated warm and transition season Arctic

stratus. <u>Department of Atmospheric Science</u>. Fort Collins, CO 80523, USA, Colorado State University. **PhD Diss.:** 289 pp.

Haylock, M. R., G. C. Cawley, C. Harpham, R. L. Wilby and C. M. Goodess (2006). "Downscaling heavy precipitation over the United Kingdom: A comparison of dynamical and statistical methods and their future scenarios." <u>International Journal of Climatology</u> **26**(10): 1397-1415.

Hohenegger, C. and C. Schar (2007). "Atmospheric predictability at synoptic versus cloud-resolving scales." <u>Bulletin of the American Meteorological Society</u> **88**(11): 1783-+.

Holtslag, A. A. M. and B. A. Boville (1993). "Local Versus Nonlocal Boundary-Layer Diffusion in a Global Climate Model." <u>Journal of Climate</u> **6**(10): 1825-1842.

Holtslag, A. A. M., G. Svensson, P. Baas, S. Basu, B. Beare, A. C. M. Beljaars, F. C. Bosveld, J. Cuxart, J. Lindvall, G. J. Steeneveld, M. Tjernström and B. J. H. Van De Wiel (2013). "Stable Atmospheric Boundary Layers and Diurnal Cycles – Challenges for Weather and Climate Models." <u>Bulletin of the American Meteorological Society</u>.

Hong, S. Y. and H. L. Pan (1996). "Nonlocal boundary layer vertical diffusion in a Medium-Range Forecast Model." <u>Monthly Weather Review</u> **124**(10): 2322-2339.

Hoppema, J. M. J. (1991). "The Seasonal Behavior of Carbon-Dioxide and Oxygen in the Coastal North-Sea Along the Netherlands." <u>Netherlands Journal of Sea Research</u> **28**(3): 167-179.

Huffman, G. J., R. F. Adler, B. Rudolf, U. Schneider and P. R. Keehn (1995). "Global Precipitation Estimates Based on a Technique for Combining Satellite-Based Estimates, Rain-Gauge Analysis, and Nwp Model Precipitation Information." <u>Journal of Climate</u> **8**(5): 1284-1295.

Hutjes, R. W. A., O. S. Vellinga, B. Gioli and F. Miglietta (2010). "Dis-aggregation of airborne flux measurements using footprint analysis." <u>Agricultural and Forest Meteorology</u> **150:** 966–983.

IPCC (2007). <u>Climate Change 2007: The Physical Science Basis. Contribution of Working Group I to the Fourth Assessment Report of the Intergovernmental Panel on Climate Change</u>, Cambridge University Press, Cambridge, United Kingdom and New York, NY, USA.

Jacob, D., L. Barring, O. B. Christensen, J. H. Christensen, M. de Castro, M. Deque, F. Giorgi, S. Hagemann, G. Lenderink, B. Rockel, E. Sanchez, C. Schar, S. I. Seneviratne, S. Somot, A. van Ulden and B. van den Hurk (2007). "An inter-comparison of regional climate models for Europe: model performance in present-day climate." <u>Climatic Change</u> **81**: 31-52.

Jacobs, A. F. G., B. G. Heusinkveld and A. A. M. Holtslag (2009). "Eighty years of meteorological observations at Wageningen, the Netherlands: precipitation and evapotranspiration." International Journal of Climatology **30**(9): 1315-1321.

Jacobs, C. M. J., B. vandenHurk and H. A. R. deBruin (1996). "Stomatal behaviour and photosynthetic rate of unstressed grapevines in semi-arid conditions." Agricultural and Forest Meteorology **80**(2-4): 111-134.

Janssens, I. A., A. Freibauer, P. Ciais, P. Smith, G. J. Nabuurs, G. Folberth, B. Schlamadinger, R. W. A. Hutjes, R. Ceulemans, E. D. Schulze, R. Valentini and A. J. Dolman (2003). "Europe's terrestrial biosphere absorbs 7 to 12% of European anthropogenic CO_2 emissions." Science **300**(5625): 1538-1542.

Jarvis, P. G. (1976). "Interpretation Of Variations In Leaf Water Potential And Stomatal Conductance Found In Canopies In Field." Philosophical Transactions Of The Royal Society Of London Series B-Biological Sciences **273**(927): 593-610.

Kabat, P., M. Claussen, P. A. Diemeyer, J. H. C. Gash, L. Bravo de Guenni, M. Meybeck, R. A. Pielke Sr., C. J. Vorosmarty, R. W. A. Hutjes and S. Lutkemeier (2004). Vegetation, Water, Humans and the Climate: A New Perspective on an Interactive System, Springer Verlag, Berlin/New York.

Kabat, P., R. W. A. Hutjes and R. A. Feddes (1997). "The scaling characteristics of soil parameters: From plot scale heterogeneity to subgrid parameterization." Journal of Hydrology **190**(3-4): 363-396.

Kabat, P., W. van Vierssen, J. Veraart, P. Vellinga and J. Aerts (2005). "Climate proofing the Netherlands." Nature **438**(7066): 283-284.

Kala, J., T. J. Lyons and U. S. Nair (2011). "Numerical Simulations of the Impacts of Land-Cover Change on Cold Fronts in South-West Western Australia." Boundary-Layer Meteorology **138**(1): 121-138.

Kjellstrom, E. and K. Ruosteenoja (2007). "Present-day and future precipitation in the Baltic Sea region as simulated in a suite of regional climate models." Climatic Change **81**: 281-291.

KNMI (2011). De bosatlas van het klimaat, Noordhoff Uitgevers B.V. .

Knorr, W. (2000). Annual and interannual CO_2 exchanges of the terrestrial biosphere: process-based simulations and uncertainties in: GTCE-LUCC Special Section: Papers resulting from the Joint Open Science Conference of the IGBP Global Change and Terrestrial Ecosystems Project and the IGBP-IHDP Land Use and Cover Change Project, held in Barcelona, Spain, March 1998, **224**: 225–252.

Koning, A. J. and P. H. Franses (2005). "Are precipitation levels getting higher? Statistical evidence for the Netherlands." Journal of Climate **18**(22): 4701-4714.

Koster, R. D., P. A. Dirmeyer, Z. C. Guo, G. Bonan, E. Chan, P. Cox, C. T. Gordon, S. Kanae, E. Kowalczyk, D. Lawrence, P. Liu, C. H. Lu, S. Malyshev, B. McAvaney, K. Mitchell, D. Mocko, T. Oki, K. Oleson, A. Pitman, Y. C. Sud, C. M. Taylor, D. Verseghy, R. Vasic, Y. K. Xue and T. Yamada (2004). "Regions of strong coupling between soil moisture and precipitation." Science **305**(5687): 1138-1140.

Kuhlwein, J., B. Wickert, A. Trukenmuller, J. Theloke and R. Friedrich (2002). "Emission-modelling in high spatial and temporal resolution and calculation of pollutant concentrations for comparisons with measured concentrations." Atmospheric Environment **36**: S7-S18.

Kvon, E. V., J. Tuulik, M. Molder and A. Lindroth (2012). "Modelling Regional Surface Energy Exchange and Boundary Layer Development in Boreal Sweden - Comparison of Mesoscale Model (RAMS) Simulations with Aircraft and Tower Observations." Atmosphere **3**(4): 537-556.

Lebeaupin, C., V. Ducrocq and H. Giordani (2006). "Sensitivity of torrential rain events to the sea surface temperature based on high-resolution numerical forecasts." Journal of Geophysical Research-Atmospheres **111**(D12).

Lenderink, G. and E. Van Meijgaard (2008). "Increase in hourly precipitation extremes beyond expectations from temperature changes." Nature Geoscience **1**(8): 511-514.

Lenderink, G., E. van Meijgaard and F. Selten (2009). "Intense coastal rainfall in the Netherlands in response to high sea surface temperatures: analysis of the event of August 2006 from the perspective of a changing climate." Climate Dynamics **32**(1): 19-33.

Lenderink, G., A. van Ulden, B. van den Hurk and F. Keller (2007). "A study on combining global and regional climate model results for generating climate scenarios of temperature and precipitation for the Netherlands." Climate Dynamics **29**(2-3): 157-176.

Lloyd, J., J. Grace, A. C. Miranda, P. Meir, S. C. Wong, H. S. Miranda, I. R. Wright, J. H. C. Gash and J. McIntyre (1995). "A simple calibrated model of Amazon rainforest productivity based on leaf biochemical properties." Plant cell environ. Oxford, Blackwell Scientific Publishers. Oct 1995 **18**(10): 1129-1145.

Lohar, D. and B. Pal (1995). "The Effect Of Irrigation On Premonsoon Season Precipitation Over South-West Bengal, India." Journal Of Climate **8**(10): 2567-2570.

Louis, J. F. (1979). "Parametric Model of Vertical Eddy Fluxes in the Atmosphere." Boundary-Layer Meteorology **17**(2): 187-202.

Loveland, T. R., B. C. Reed, J. F. Brown, D. O. Ohlen, Z. Zhu, L. Yang and J. W. Merchant (2000). "Development of a global land cover characteristics database and IGBP DISCover from 1 km AVHRR data." International Journal of Remote Sensing **21**(6-7): 1303-1330.

Mahmood, R., R.A. Pielke Sr., K. Hubbard, D. Niyogi, P. Dirmeyer, C. McAlpine, A. Carleton, R. Hale, S. Gameda, A. Beltrán-Przekurat, B. Baker, R. McNider, D. Legates, J. Shepherd, J. Du, P. Blanken, O. Frauenfeld, U. Nair, S. Fall, 2013: Land cover changes and their biogeophysical effects on climate. International Journal of Climatology, DOI: 10.1002/joc.3736.

Mahrt, L., D. Vickers and J. L. Sun (2001). "Spatial variations of surface moisture flux from aircraft data." Advances in Water Resources **24**(9-10): 1133-1141.

Marquardt, D. W. (1963). "An Algorithm For Least-Squares Estimation Of Nonlinear Parameters." Journal Of The Society For Industrial And Applied Mathematics **11**(2): 431-441.

Marshall, C. H., R. A. Pielke, L. T. Steyaert and D. A. Willard (2004). "The impact of anthropogenic land-cover change on the Florida peninsula sea breezes and warm season sensible weather." Monthly Weather Review **132**(1): 28-52.

Mass, C. F., D. Ovens, K. Westrick and B. A. Colle (2002). "Does increasing horizontal resolution produce more skillful forecasts? The results of two years of real-time numerical weather prediction over the Pacific northwest." Bulletin of the American Meteorological Society **83**(3): 407-+.

Maurer, E. P. and H. G. Hidalgo (2008). "Utility of daily vs. monthly large-scale climate data: an intercomparison of two statistical downscaling methods." Hydrology and Earth System Sciences **12**(2): 551-563.

Meesters, A., L. F. Tolk, W. Peters, R. W. A. Hutjes, O. S. Vellinga, J. A. Elbers, A. T. Vermeulen, S. van der Laan, R. E. M. Neubert, H. A. J. Meijer and A. J. Dolman (2012). "Inverse carbon dioxide flux estimates for the Netherlands." Journal of Geophysical Research-Atmospheres **117**.

Mellor, G. L. and T. Yamada (1982). "Development of a turbulence closure model for geophysical fluid problems." Reviews of geophysics and space physics **20**(4): 851-875.

Meyers, M. P., R. L. Walko, J. Y. Harrington and W. R. Cotton (1997). "New RAMS cloud microphysics parameterization. Part II: the two-moment scheme." Atmospheric Research. 1997; **45**(1): 3-39.

Moore, N. and S. Rojstaczer (2002). "Irrigation's influence on precipitation: Texas High Plains, USA." Geophysical Research Letters **29**(16).

Mücher, C. A., J. L. Champeaux, K. T. Steinnocher, S. Griguola, K. Wester, C. Heunks, W. Winiwater, F. P. Kressler, J. P. Goutorbe, B. Ten Brink, V. F. Van Katwijk, O. Furberg, V. Perdigao and G. J. A. Nieuwenhuis (2001). Development of a consistent methodology to derive land cover information on a European scale from Remote Sensing for environmental monitoring : the PELCOM report. Wageningen, Alterra Green World Research**:** 159 p;.

Nair, U. S., Y. Wu, J. Kala, T. J. Lyons, R. A. Pielke and J. M. Hacker (2011). "The role of land use change on the development and evolution of the west coast trough, convective clouds, and precipitation in southwest Australia." Journal of Geophysical Research-Atmospheres **116**.

Noilhan, J., P. Lacarrere and P. Bougeault (1991). "An experiment with an advanced surface parameterization in a mesobeta-scale model. Part III: comparison with the HAPEX-MOBILHY dataset." Monthly Weather Review **119**(10): 2393-2413.

Ogink-Hendriks, M. J. (1995). "Modeling surface conductance and transpiratio of an oak forest in The Netherlands." Agricultural and Forest Meteorology **74**(1-2): 99-118.

Ogunjemiyo, S. O., S. K. Kaharabata, P. H. Schuepp, I. J. MacPherson, R. L. Desjardins and D. A. Roberts (2003). "Methods of estimating CO2, latent heat and sensible heat fluxes from estimates of land cover fractions in the flux footprint." Agricultural and Forest Meteorology **117**(3-4): 125-144.

Olivier, J. G. J. and J. J. M. Berdowski (2001). Global emissions sources and sinks. The Climate System. J. J. M. Berdowski, R. Guicherit and B. J. Heij. Lisse, A.A. Balkema Publishers/Swets & Zeitlinger Publisher**:** 33-78.

Orlanski, I. (1975). "Rational subdivision of scales for atmospheric processes." Bulletin of the American Meteorological Society **56**(5): 527-530.

Otterman, J., A. Manes, S. Rubin, P. Alpert and D. O. Starr (1990). "An increase of early rains in Southern Israel following land-use change." Boundary-Layer Meteorology **53**(4): 333-351.

Pall, P., M. Allen and D. Stone (2007). "Testing the Clausius–Clapeyron constraint on changes in extreme precipitation under CO_2 warming." Climate Dynamics **28**(4): 351-363.

Perez-Landa, G., P. Ciais, G. Gangoiti, J. L. Palau, A. Carrara, B. Gioli, F. Miglietta, M. Schumacher, M. M. Millan and M. J. Sanz (2007). "Mesoscale circulations over complex terrain in the Valencia

coastal region, Spain - Part 2: Modeling CO_2 transport using idealized surface fluxes." Atmospheric Chemistry and Physics **7**(7): 1851-1868.

Perez-Landa, G., P. Ciais, M. J. Sanz, B. Gioli, F. Miglietta, J. L. Palau, G. Gangoiti and M. M. Millan (2007). "Mesoscale circulations over complex terrain in the Valencia coastal region, Spain - Part 1: Simulation of diurnal circulation regimes." Atmospheric Chemistry and Physics **7**(7): 1835-1849.

Pfister, L., J. Kwadijk, A. Musy, A. Bronstert and L. Hoffmann (2004). "Climate change, land use change and runoff prediction in the Rhine-Meuse basins." River Research and Applications **20**(3): 229-241.

Pielke, R. A. (2001). "Influence of the spatial distribution of vegetation and soils on the prediction of cumulus convective rainfall." Reviews Of Geophysics **39**(2): 151-177.

Pielke, R. A., J. Adegoke, A. Beltran-Przekurat, C. A. Hiemstra, J. Lin, U. S. Nair, D. Niyogi and T. E. Nobis (2007). "An overview of regional land-use and land-cover impacts on rainfall." Tellus Series B-Chemical and Physical Meteorology **59**(3): 587-601.

Pielke, R. A., W. R. Cotton, R. L. Walko, C. J. Tremback, W. A. Lyons, L. D. Grasso, M. E. Nicholls, M. D. Moran, D. A. Wesley, T. J. Lee and J. H. Copeland (1992). "A Comprehensive Meteorological Modeling System - Rams." Meteorology and Atmospheric Physics **49**(1-4): 69-91.

Pielke, R. A., G. A. Dalu, J. S. Snook, T. J. Lee and T. G. F. Kittel (1991). "Nonlinear Influence of Mesoscale Land-Use on Weather and Climate." Journal of Climate **4**(11): 1053-1069.

Pielke, R. A., G. Marland, R. A. Betts, T. N. Chase, J. L. Eastman, J. O. Niles, D. D. S. Niyogi and S. W. Running (2002). "The influence of land-use change and landscape dynamics on the climate system: relevance to climate-change policy beyond the radiative effect of greenhouse gases." Philosophical transactions of the royal society of london series a mathematical physical and engineering sciences **360**(1797): 1705-1719.

Pielke Sr., R.A., A. Pitman, D. Niyogi, R. Mahmood, C. McAlpine, F. Hossain, K. Goldewijk, U. Nair, R. Betts, S. Fall, M. Reichstein, P. Kabat, and N. de Noblet-Ducoudré, 2011: Land use/land cover changes and climate: Modeling analysis and observational evidence. WIREs Clim Change 2011, **2**:828–850. doi: 10.1002/wcc.144.

Pielke, R. A., R. L. Walko, L. T. Steyaert, P. L. Vidale, G. E. Liston, W. A. Lyons and T. N. Chase (1999). "The influence of anthropogenic landscape changes on weather in south Florida." Monthly Weather Review **127**(7): 1663-1673.

Pitman, A. J. (2003). "The evolution of, and revolution in, land surface schemes designed for climate models." Journal of Climatology **23**(5): 479-510.

Rayner, N. A., D. E. Parker, E. B. Horton, C. K. Folland, L. V. Alexander, D. P. Rowell, E. C. Kent and A. Kaplan (2003). "Global analyses of sea surface temperature, sea ice, and night marine air temperature since the late nineteenth century." Journal of Geophysical Research-Atmospheres **108**(D14).

Reynolds, J.F., Stafford-Smith, D.M. (2002). Global desertification, do humans cause deserts? Dahlem Workshop Report, vol. 88. Dahlem Univ Press, Berlin.

Richard, E., S. Cosma, P. Tabary, J. P. Pinty and M. Hagen (2003). "High-resolution numerical simulations of the convective system observed in the Lago Maggiore area on 17 September 1999 (MAP IOP 2a)." Quarterly Journal of the Royal Meteorological Society **129**(588): 543-563.

Sampaio, G., C. Nobre, M. H. Costa, P. Satyamurty, B. S. Soares and M. Cardoso (2007). "Regional climate change over eastern Amazonia caused by pasture and soybean cropland expansion." Geophysical Research Letters **34**(17).

Sarrat, C., J. Noilhan, P. Lacarrere, S. Donier, C. Lac, J. C. Calvet, A. J. Dolman, C. Gerbig, B. Neininger, P. Ciais, J. D. Paris, F. Boumard, M. Ramonet and A. Butet (2007). "Atmospheric CO_2 modeling at the regional scale: Application to the CarboEurope Regional Experiment." Journal of Geophysical Research-Atmospheres **112**(D12).

Schar, C., D. Luthi, U. Beyerle and E. Heise (1999). "The soil-precipitation feedback: A process study with a regional climate model." Journal of Climate **12**(3): 722-741.

Schickedanz, P.T., Ackermann, W.C. (1977). Influence of irrigation on precipitation in semi-arid climates. In: Worthington, E.B. (Ed.), Arid Land Irrigation in Developing Countries. Pergamon Press, pp. 185–196.

Seneviratne, S. I., D. Luthi, M. Litschi and C. Schar (2006). "Land-atmosphere coupling and climate change in Europe." Nature **443**(7108): 205-209.

Soet, M., R. J. Ronda, J. N. M. Stricker and A. J. Dolman (2000). "Land surface scheme conceptualisation and parameter values for three sites with contrasting soils and climate." Hydrology and Earth System Sciences **4**(2): 283-294.

Sogalla, M., A. Kruger and M. Kerschgens (2006). "Mesoscale modelling of interactions between rainfall and the land surface in West Africa." Meteorology and Atmospheric Physics **91**(1-4): 211-221.

Spieksma, J. F. M., E. J. Moors, A. J. Dolman and J. M. Schouwenaars (1997). "Modelling evaporation from a drained and rewetted peatland." Journal of hydrology **199**(3-4): 252-271.

Steeneveld, G. J., L. F. Tolk, A. F. Moene, O. K. Hartogensis, W. Peters and A. A. M. Holtslag (2011). "Confronting the WRF and RAMS mesoscale models with innovative observations in the Netherlands: Evaluating the boundary layer heat budget." J. Geophys. Res. **116**(D23): D23114.

Steeneveld, G. J., J. Vilà-Guerau de Arellano, A. A. M. Holtslag, T. Mauritsen, G. Svensson and E. I. F. de Bruijn (2008). "Evaluation of Limited-Area Models for the Representation of the Diurnal Cycle and Contrasting Nights in CASES-99." Journal of Applied Meteorology and Climatology **47**(3): 869-887.

Stuurgroep Grondwaterbeheer Midden, N. (1992). Een nieuw evenwicht : grondwaterbeheer midden Nederland : rapport van de stuurgroep [GMN]. [Arnhem], [Provincie Gelderland].

Sud, Y. C., D. M. Mocko, G. K. Walker and R. D. Kosgter (2001). "Influence of land surface fluxes on precipitation: Inferences from simulations forced with four ARM-CART SCM datasets." Journal Of Climate **14**(17): 3666-3691.

Sutton, R. T. and D. L. R. Hodson (2005). "Atlantic Ocean forcing of North American and European summer climate." Science **309**(5731): 115-118.

Takahashi, T., R. A. Feely, R. F. Weiss, R. H. Wanninkhof, D. W. Chipman, S. C. Sutherland and T. T. Takahashi (1997). "Global air-sea flux of CO2: An estimate based on measurements of sea-air pCO(2) difference." Proceedings Of The National Academy Of Sciences Of The United States Of America **94**(16): 8292-8299.

Taylor, C. M., R. A. M. de Jeu, F. Guichard, P. P. Harris and W. A. Dorigo (2012). "Afternoon rain more likely over drier soils." Nature **489**(7416): 423-426.

Ter Maat, H. W., R. W. A. Hutjes, F. Miglietta, B. Gioli, F. C. Bosveld, A. T. Vermeulen and H. Fritsch (2010). "Simulating carbon exchange using a regional atmospheric model coupled to an advanced land-surface model." Biogeosciences **7**(8): 2397-2417.

Ter Maat, H. W., R. W. A. Hutjes, R. Ohba, H. Ueda, B. Bisselink and T. Bauer (2006). "Meteorological impact assessment of possible large scale irrigation in Southwest Saudi Arabia." Global and Planetary Change **54**(1-2): 183-201.

Ter Maat, H. W., E. J. Moors, R. W. A. Hutjes, A. A. M. Holtslag and A. J. Dolman (2013). "Exploring the Impact of Land Cover and Topography on Rainfall Maxima in the Netherlands." Journal of Hydrometeorology **14**(2): 524-542.

Teuling, A. J., S. I. Seneviratne, R. Stockli, M. Reichstein, E. Moors, P. Ciais, S. Luyssaert, B. van den Hurk, C. Ammann, C. Bernhofer,

E. Dellwik, D. Gianelle, B. Gielen, T. Grunwald, K. Klumpp, L. Montagnani, C. Moureaux, M. Sottocornola and G. Wohlfahrt (2010). "Contrasting response of European forest and grassland energy exchange to heatwaves." Nature Geoscience **3**(10): 722-727.

Thomas, H., Y. Bozec, K. Elkalay and H. J. W. de Baar (2004). "Enhanced open ocean storage of CO_2 from shelf sea pumping." Science **304**(5673): 1005-1008.

Tolk, L. F., W. Peters, A. G. C. A. Meesters, M. Groenendijk, A. T. Vermeulen, G. J. Steeneveld and A. J. Dolman (2009). "Modelling regional scale surface fluxes, meteorology and CO2 mixing ratios for the Cabauw tower in the Netherlands." Biogeosciences **6**(10): 2265-2280.

Tremback, C.J. (1990). Numerical simulation of a mesoscale convective complex: model development and numerical results. PhD Diss., Atmos Sci Paper No 465, Colorado State University, Department of Atmospheric Science, Fort Collins, CO 80523.

Valentini, R., G. Matteucci, A. J. Dolman, E. D. Schulze, C. Rebmann, E. J. Moors, A. Granier, P. Gross, N. O. Jensen, K. Pilegaard, A. Lindroth, A. Grelle, C. Bernhofer, T. Grunwald, M. Aubinet, R. Ceulemans, A. S. Kowalski, T. Vesala, Ü. Rannik, P. Berbigier, D. Loustau, J. Guomundsson, H. Thorgeirsson, A. Ibrom, K. Morgenstern, R. Clement, J. Moncrieff, L. Montagnani, S. Minerbi and P. G. Jarvis (2000). "Respiration as the main determinant of carbon balance in European forests." Nature **404**(6780): 861-865.

van den Hurk, B., A. K. Tank, G. Lenderink, A. v. Ulden, G. J. v. Oldenborgh, C. Katsman, H. v. d. Brink, F. Keller, J. Bessembinder, G. Burgers, G. Komen, W. Hazeleger and S. Drijfhout (2007). "New climate change scenarios for the Netherlands." Water Sci Technol **56**(4): 27-33.

van den Hurk, B., A. K. Tank, G. Lenderink, A. Van Ulden, G. J. Van Oldenborgh, C. Katsman, H. Van den Brink, F. Keller, J. Bessembinder, G. Burgers, G. Komen, W. Hazeleger and S. Drijfhout (2006). "KNMI Climate Change Scenarios 2006 for the Netherlands." (KNMI Scientific Report WR 2006-01): 82.

van der Molen, M.K. (2002). Meteorological impacts of land use change in the maritime tropics. Ph. D. Thesis. Vrije Universiteit, Amsterdam, The Netherlands.

van der Molen, M. K., A. J. Dolman, M. J. Waterloo and L. A. Bruijnzeel (2006). "Climate is affected more by maritime than by continental land use change: A multiple scale analysis." Global and Planetary Change **54**(1-2): 128-149.

van Heerwaarden, C. C., J. V. G. de Arellano, A. F. Moene and A. A. M. Holtslag (2009). "Interactions between dry-air entrainment,

surface evaporation and convective boundary-layer development." Quarterly Journal of the Royal Meteorological Society **135**(642): 1277-1291.

van Ulden, A. P. and G. J. van Oldenborgh (2006). "Large-scale atmospheric circulation biases and changes in global climate model simulations and their importance for climate change in Central Europe." Atmospheric Chemistry and Physics **6**: 863-881.

Van Wijk, M. T., S. C. Dekker, W. Bouten, F. C. Bosveld, W. Kohsiek, K. Kramer and G. M. J. Mohren (2000). "Modeling daily gas exchange of a Douglas-fir forest: comparison of three stomatal conductance models with and without a soil water stress function." Tree Physiology **20**(2): 115-122.

Vedel, H. and X. Y. Huang (2004). "Impact of ground based GPS data on numerical weather prediction." Journal of the Meteorological Society of Japan **82**(1B): 459-472.

Verburg, P. and K. Overmars (2009). "Combining top-down and bottom-up dynamics in land use modeling: exploring the future of abandoned farmlands in Europe with the Dyna-CLUE model." Landscape Ecology **24**(9): 1167-1181.

Vermeulen, A. T., G. Pieterse, A. Hensen, W. C. M. van Den Bulk and J. W. Erisman (2006). "COMET: a Lagrangian transport model for greenhouse gas emission estimation – forward model technique and performance for methane." Atmos. Chem. Phys. Discuss. **6**(5): 8727-8779.

Walko, R. L., L. E. Band, J. Baron, T. G. F. Kittel, R. Lammers, T. J. Lee, D. Ojima, R. A. Pielke, C. Taylor, C. Tague, C. J. Tremback and P. L. Vidale (2000). "Coupled atmosphere-biophysics-hydrology models for environmental modeling." Journal of applied meteorology **39**(6): 931-944.

Walko, R. L., W. R. Cotton, M. P. Meyers and J. Y. Harrington (1995). "New RAMS cloud microphysics parameterization. Part I: the single-moment scheme." Atmospheric Research. 1995; **38**(1): 29-62.

Walko, R. L., C. J. Tremback, R. A. Pielke and W. R. Cotton (1995). "An Interactive Nesting Algorithm for Stretched Grids and Variable Nesting Ratios." Journal of Applied Meteorology **34**(4): 994-999.

Walser, A., D. Luthi and C. Schar (2004). "Predictability of precipitation in a cloud-resolving model." Monthly Weather Review **132**(2): 560-577.

Wanninkhof, R. (1992). "Relationship between Wind-Speed and Gas-Exchange over the Ocean." Journal of Geophysical Research-Oceans **97**(C5): 7373-7382.

Weaver, C. P., S. B. Roy and R. Avissar (2002). "Sensitivity of simulated mesoscale atmospheric circulations resulting from landscape

heterogeneity to aspects of model configuration." Journal of Geophysical Research-Atmospheres **107**(D20).

Weiss, R. F. (1974). "Carbon dioxide in water and seawater: the solubility of a non-ideal gas." Marine Chemistry **2**(3): 203-215.

Wickert, B. (2001) Berechnung anthropogener Emissionen in Deutschland für Ozonsimulation – Modellentwicklung und Sensitivitätsstudien, PhD-thesis, Universität Stuttgart, Institut für Energiewirtschaft und Rationelle.

Wieringa, J. and P. J. Rijkoort (1983). Windklimaat van Nederland, Koninklijk Nederlands Meteorologisch Instituut.

Wu, Y. L., U. S. Nair, R. A. Pielke, R. T. McNider, S. A. Christopher and V. G. Anantharaj (2009). "Impact of Land Surface Heterogeneity on Mesoscale Atmospheric Dispersion." Boundary-Layer Meteorology **133**(3): 367-389.

Xue,Y.,Hutjes, R.W.A.,Harding,R.J., Claussen,M., Prince, S., Lambin, E.F., Alan, S.J., Dirmeyer, P. (2004). The Sahelian climate. In: Kabat, P., et al. (Eds.), Vegetation, Water, Humans and the Climate: a New Perspective on an Interactive System. Springer Verlag.

Zeng, X., M. Barlage, C. Castro and K. Fling (2010). "Comparison of Land-Precipitation Coupling Strength Using Observations and Models." Journal of Hydrometeorology **11**(4): 979-994.

Zhao, M., A. J. Pitman and T. Chase (2001). "The impact of land cover change on the atmospheric circulation." Climate Dynamics **17**(5-6): 467-477.

Regional atmospheric feedbacks over land and coastal areas

Chapter 8

Summary / Samenvatting

8.1   English summary

One of the challenges in present day atmospheric and climate sciences is to represent surface heterogeneity effectively and on the proper spatial and temporal scales. The need to derive meteorological data or climate data on a local level has increased over the last decades. Regional climate models are thought to provide more regionally detailed climate predictions and better information on extreme events as spatial and temporal details are better resolved. However, an increased understanding of climate processes and feedbacks is necessary to reduce the uncertainty in climate projections, as subtler heterogeneities in these must be resolved.

Non-hydrostatic atmospheric models have the ability to simulate physical processes on a very fine resolution (1-2 km). This level of detail is still not present in generally hydrostatic RCMs due to limitations in the equations used to describe all involved physical processes. In this thesis a fully, online coupled model, basically consisting of the Regional Atmospheric Modelling System (RAMS, Cotton et al. (2003), Pielke et al. (1992)) is used. RAMS is a 3D, non-hydrostatic model based on fundamental equations of fluid dynamics and includes a terrain following vertical coordinate system. One of the advantages of the model is the ability to perform simulations at high resolution and the subsequent representation of microphysics and precipitation processes. To study regional scale feedbacks it is important to use land surface descriptions of appropriate complexity, that include the main controlling mechanisms and capture the relevant dynamics of the system, and to represent the real-world spatial variability in soils and vegetation.

This thesis deals with the impact of feedbacks between the earth surface (both at land and sea) and the atmosphere. Especially, the feedbacks between the surface and the local-to-regional state of the atmosphere are studied and their importance assessed. Four different cases are presented in this thesis to increase our understanding of the processes and feedbacks in different settings.

All four cases are executed using RAMS coupled to a sophisticated land surface model that represents the surface in great detail. Three of the four cases deal with feedbacks between the surface and the atmosphere in the Netherlands (temperate climate). These cases deal with the feedbacks between land cover and atmosphere (chapter 2), the effect of surface heterogeneity on atmospheric carbon dynamics (chapter 3) and the effect of near-coastal sea surface temperature on coastal precipitation (chapter 4). The last case (chapter 5) deals with the impact

of a land cover change in the coastal area of a semi-arid/desert environments (Saudi Arabia).

To quantify the important feedbacks between the earth's surface and the atmosphere the following research questions are formulated:

- What is the regional atmospheric effect of land cover on precipitation and carbon dynamics in a heterogeneous environment in a temperate climate?

- What is the role of the sea surface temperature on precipitation in coastal areas in temperate and desert environments?

- What are the differences in impacts of land use change on the regional climate between a temperate and a desert environment?

Chapter 2 addresses the effect of land cover and topography on precipitation in the Netherlands. The effect of the forested area on the processes that influence precipitation is smaller in summertime conditions when the precipitation has a convective character. In frontal conditions the forest has a more pronounced effect on local precipitation through the roughness induced convergence of moisture. The effect of topography on monthly domain-averaged precipitation around the Veluwe is, in the winter 17 % increase and in summer 10% increase, which is quite remarkable for topography with a maximum elevation of just above 100 meter and moderate steepness. This is confirmed by observations.

In Chapter 3 the regional atmospheric model was set-up to simulate the carbon exchange on a regional scale for a heterogeneous area in The Netherlands. The simulations are in good qualitative agreement with the observations. Sensitivity experiments demonstrate the relevance of the urban emissions of carbon dioxide for the atmospheric carbon dioxide concentration dynamics in this particular region. The same experiments also show the relation between uncertainties in surface fluxes and those in atmospheric concentrations. To quantify the distribution of carbon sources and sinks it is important and feasible to use high resolution output from a regional atmospheric model, which can subsequently be fed into atmospheric inversions studies.

Chapter 4 assesses the effect that high resolution model physics and North Sea surface temperatures has on intense coastal precipitation in the Netherlands. The result from this experiment with a non-hydrostratic regional atmospheric model are compared with an earlier study using a

coarser resolution, hydrostatic model with a simpler land scheme. The precipitation sums have certainly improved by using a high resolution model. Another improvement in the simulations was that the resolution of the prescribed sea surface temperatures has also increased. This also helped to improve the results. The sensitivity experiment with 2 K lower SST values showed the effect of a colder sea surface. This effect is, on average, more than 60 mm for the selected period.

The geographical focus in chapter 5 shifts towards a semi-arid environment (Saudi Arabia). The simulations are analysed with a focus on the role of local processes (sea breezes, orographic lifting and the formation of fog in the coastal mountains) in generating rainfall, and on how these will be affected by large scale irrigated plantations in the coastal desert. The impact of an hypothetical irrigated plantation has significant effects on atmospheric moisture, but due to weakened sea breezes this leads to limited increases of rainfall inland. In terms of recycling of irrigation gifts the rainfall enhancement in this particular setting is rather insignificant.

The feedbacks between the surface (land and sea) and the atmosphere are apparent from the presented cases. The positive effect of simulations at higher resolution are discussed in all chapters. The high resolution takes better account of the surface heterogeneity and it gives the opportunity to use the microphysics package with the convective parameterizations switched off, assuming convection is sufficiently resolved on the high resolution. One of the issues with simulations at a higher simulations is that the underlying databases (e.g. land cover and soil maps, SST maps, etc) should have at least the same resolutions.

In this thesis recommendations have been made to improve regional atmospheric models. One important issue deals with the planetary boundary layer (see chapters 2 and 3) which strongly influences the feedbacks through redistributing vapour and carbon, in particular in the vertical. Within this thesis the PBL scheme had to be adapted to the specific application and location. Thus we recommend to further develop a PBL scheme that is able to cover all relevant conditions with proper interactions of surface conditions, lower level clouds and atmospheric convection. A second recommendation is that the surface fluxes of heat, vapour, momentum and carbon are well simulated in the modelling system. These fluxes influence the amount of heat, vapour and carbon in the planetary boundary layer, which subsequently have its effect on, for example, clouds, radiation and precipitation.

With the emergence of regional climate models, better knowledge of local-to-regional feedbacks is indispensable. The relatively fine

156

resolution on which regional atmospheric models can be executed also means that land use and topography must be represented on this fine resolution. This means that the regional atmospheric models are a perfect platform to develop and test descriptions of processes, which are not currently well described in regional climate models. This is necessary as there is a growing need to have present and future climate data information on the local level.

8.2   Nederlandse samenvatting

Eén van de grootste uitdagen in het huidige klimaatonderzoek is om een correcte beschrijving te hebben van een heterogeen aardoppervlak op de juiste ruimte- en tijdschaal. De afgelopen jaren is er een grotere vraag ontstaan naar klimaat- en weergegevens op lokaal niveau, nu en in de toekomst. Van regionale klimaatmodellen wordt verwacht dat zij dit kunnen geven met verbeterde informatie wat betreft extremen omdat ruimte- en tijdschalen beter worden opgelost. Dit noodzaakt echter tot meer heterogeniteit die moet worden opgelost. Hiervoor is een beter begrip nodig van processen en terugkoppelingen, die daarmee samenhangen, in het klimaatsysteem.

Met niet-hydrostatische atmosferische modellen kunnen fysische processen in de atmosfeer op een zeer fijne ruimtelijke schaal (1-2 km) worden gesimuleerd. Hydrostatische regionale klimaatmodellen kunnen niet op deze schaal worden gedraaid door de beperkingen in de vergelijkingen om fysische processen te beschrijven. In dit proefschrift wordt een volledig gekoppeld model, RAMS (Cotton et al. (2003), Pielke et al. (1992)) gebruikt. RAMS is een 3D, niet-hydrostatisch model, dat is gebaseerd op de fundamentele vergelijkingen van de stromingsleer. Het model bevat een reliëfvolgend verticaal coördinaatsysteem. Een groot voordeel van het model is dat simulaties op een fijne ruimtelijke schaal kunnen worden uitgevoerd zodat processen die de microfysica en de neerslag beïnvloeden correct kunnen worden beschreven. Om regionale terugkoppelingen te kunnen bestuderen is het belangrijk beschrijvingen van het aardoppervlak te gebruiken van geschikte complexiteit om de relevante dynamiek van het systeem te vatten, en om de juiste variabiliteit in bodem en vegetatie weer te geven.

Dit proefschrift behandelt de invloed van terugkoppelingen tussen het aardoppervlak (land én zee) en de atmosfeer. De terugkoppelingen tussen het oppervlak en de lokale/regionale toestand van de atmosfeer worden bestudeerd en het belang van deze terugkoppelingen wordt beoordeeld. Vier verschillende voorbeelden worden behandeld in dit proefschrift om het begrip te verbeteren van de processen en de terugkoppelingen op lokaal/regionaal niveau.

De vier voorbeelden zijn allen uitgevoerd met RAMS, dat gekoppeld is aan een gedetailleerd landoppervlak model. In drie van de vier voorbeelden worden de terugkoppelingen tussen het oppervlak en de atmosfeer onderzocht voor Nederland (gematigd klimaat). Het betreft hier terugkoppelingen tussen landgebruik en atmosfeer (hoofdstuk 2), het effect van heterogeniteit van het landschap op de dynamiek van kooldioxide in atmosfeer (hoofdstuk 3) en het effect van

158

zeewatertemperatuur op kustneerslag (hoofdstuk 4). Het laatste voorbeeld (hoofdstuk 5) behandelt de invloed van landgebruiksverandering in het kustgebied van een (semi-)aride omgeving in Saoedi Arabië.

Om de belangrijke terugkoppelingen tussen het aardoppervlak en de atmosfeer te kwantificeren, zijn de volgende vragen geformuleerd:

- Wat is het regionale atmosferische effect van landbedekking op neerslag en de dynamiek van kooldioxide in een heterogene omgeving in een gematigd klimaat?

- Welke rol speelt zeewatertemperatuur op kustneerslag in gematigde en aride omgevingen?

- Wat zijn de verschillen in invloed van landgebruiksverandering op het regionale klimaat tussen een gematigd en een aride omgeving?

Hoofdstuk 2 richt zich op het effect van landgebruiksverandering op neerslag in Nederland. Het effect van bebost gebied op processen die neerslag beïnvloeden is kleiner in de zomer als neerslag convectief van oorsprong is. In frontale omstandigheden heeft bos een uitgesprokener effect op neerslag als gevolg van vochtconvergentie. Het effect van reliëf op de maandelijks gemiddelde neerslag die valt op de Veluwe is in de winter een toename van 17% en in de zomer een toename van 10%. Dit is opmerkelijk voor een een gebied met een maximale hoogte van 100 meter en gematigd steile hellingen. Dit wordt bevestigd door waarnemingen.

Het regionale atmosferische model wordt in hoofdstuk 3 gebruikt om de uitwisseling van kooldioxide te simuleren voor een heterogene regio in Nederland. De resultaten van de simulaties komen kwalitatief goed overeen met de waarnemingen. Gevoeligheidsexperimenten laten het belang zien van stedelijke emissies van kooldioxide op de atmosferische kooldioxide concentratie voor een bepaalde regio. Deze experimenten laten ook het verband zien tussen onzekerheden in oppervlakte-fluxen en het gevolg daarvan in de concentratie van atmosferisch kooldioxide. Voor een correcte kwantificering van de bronnen en putten van kooldioxide is het dus mogelijk om de uitkomsten van een regionaal atmosferisch model te gebruiken als input voor atmosferische inversie studie.

Hoofdstuk 4 laat het effect zien van hoge resolutie model fysica en hoge resolutie zeewatertemperaturen van de Noordzee op kustneerslag in Nederland. De resultaten van de simulaties met een fijnmazig niet-

hydrostatisch model zijn vergeleken met een grofmazig hydrostatisch model. De neerslagsommen zijn verbeterd in de simulaties met een niet-hydrostatisch model. De hoge resolutie van zeewatertemperaturen hebben de simulaties van neerslag ook verbeterd. Het gevoeligheidsexperiment met lagere zeewatertemperaturen laat het effect zien van een koudere zee op neerslag. Dit scheelt gemiddeld meer dan 60 mm voor de gesimuleerde periode.

In hoofdstuk 5 verschuift de geografische focus naar een (semi)-aride omgeving (Saoedi Arabië). De simulaties zijn geanalyseerd om de rol van lokale processen (zeewind, hellingstijgwind en het ontstaan van mist in het kustgebergte) op neerslag te laten zien en hoe deze processen worden beïnvloed door grootschalige geïrrigeerde vergroening in de aride kuststrook. Deze vergroening heeft significant effect op de vochthuishouding in de atmosfeer, maar door het remmende effect van de vergroening op de zeewind leidt deze toename aan vocht in de atmosfeer niet tot meer neerslag landinwaarts. In verhouding tot de irrigatie giften is de toename van neerslag landinwaarts insignificant te noemen.

De terugkoppelingen tussen het aardoppervlak (land en zee) en de atmosfeer zijn zichtbaar in de vier gegeven voorbeelden. Het positieve effect van fijnmazige simulaties wordt in elk hoofdstuk behandeld. De heterogeniteit van het aardoppervlak komt beter tot zijn recht op deze hoge resolutie. Het geeft ook de mogelijkheid om de microfysica van het model te gebruiken zodat de neerslag niet via het convectieve schema geparameteriseerd hoeft te worden maar opgelost kan worden. Om op deze fijne resolutie te kunnen modelleren is het wel van belang dat de onderliggende datasets van bijvoorbeeld landbedekking, bodem en zeewatertemperatuur ook een fijne ruimtelijke resolutie hebben.

Dit proefschrift doet aanbevelingen om regionale atmosferische modellen te verbeteren. Een belangrijke verbetering heeft te maken met de grenslaag (zie hoofdstukken 2 en 3), die terugkoppelingen beïnvloedt door de verticale verdeling van vocht en kooldioxide. In dit proefschrift is het grenslaagschema steeds aangepast aan de toepassing en de locatie van de simulatie. Het is aan te bevelen dat er een generiek grenslaagschema wordt ontwikkeld waar de juiste wisselwerkingen tussen aardoppervlak, laaghangende bewolking en atmosferische convectie in aanwezig zijn. Een tweede aanbeveling is dat de uitwisselingen van warmte, vocht, impuls en kooldioxide goed gemodelleerd in het systeem komen. Deze uitwisseling beïnvloeden de hoeveelheid warmte, vocht en kooldioxide in de grenslaag met als gevolg dat, bijvoorbeeld wolken, straling en neerslag ook beter worden gemodelleerd.

Met de opkomst van regionale klimaatmodellen is betere kennis van wisselwerkingen (lokaal/regionaal) onontbeerlijk. De hoge ruimtelijke resolutie waarop regionale atmosferische modellen gedraaid kunnen worden vraagt ook een hoge ruimtelijke resolutie van landgebruik-, bodem- en reliëfdatasets. Regionale atmosferische modellen zijn een ideaal platform om processen te ontwikkelen en te testen die nog niet goed beschreven zijn in regionale klimaatmodellen. Dit is nodig als gevolg van een groeiende behoefte aan weer- en klimaatgegevens op lokaal niveau.

Regional atmospheric feedbacks over land and coastal areas

Dankwoord & Acknowledgements

Na vele jaren onderzoek is mijn proefschrift klaar. In de laatste periode is mij vaak gevraagd of mijn proefschrift al klaar was. Het resultaat ligt nu in jullie handen. De allereerste contacten om tot dit proefschrift te komen zijn 10 jaar geleden gelegd op een kamer aan de Duivendaal 2 in Wageningen. In de afgelopen jaren hebben verschillende mensen er aan bijgedragen dat dit proefschrift er is gekomen.

Ten eerste wil ik Bert Holtslag bedanken voor de eerste gesprekken die we ooit hebben gehad om een promotie-traject in te zetten. Dat je tot het eind van dit traject één van mijn promoteren bent gebleven, is een teken dat je altijd vertrouwen hebt gehad in de ingeslagen weg. Je was erg begripvol als er vertraging optrad door mijn werkzaamheden bij Alterra of door privé omstandigheden. Je pragmatisme in de discussies die we in de laatste periode hebben gehad hebben mij gemotiveerd om dit proefschrift versneld maar toch goed af te ronden.

Mijn tweede promotor, Pavel Kabat, wil ik ook bedanken. Jij kwam in beeld als promotor toen je professor van de vakgroep Aardsysteemkunde werd. De combinatie van meteorologie en aardsysteemkunde paste erg goed bij het onderwerp van mijn proefschrift. Je wist me altijd scherp te houden tijdens dit promotie-traject. Net zoals Bert was je altijd geïnteresseerd in de situatie thuis.

Mijn co-promotor en dagelijkse begeleider, Ronald Hutjes, moet ik wel het meest bedanken. Vanaf het moment dat ik, als jonge onderzoeker, bij het toenmalige Staring Centrum kwam te werken hebben we samen het modelleren op regionale schaal aangepakt. Vooral in de periode dat RAMS nog op de DEC-Alpha draaide, kon dit nog wel eens tot frustraties leiden. Ik heb van je geleerd om altijd tot een oplossing proberen te komen binnen de grenzen van de wetenschap.

Bart van den Hurk, Daniela Jacob, Roger Pielke sr. and Remko Uijlenhoet, I am happy that you are a member of the thesis committee. I hope that you enjoyed reading the thesis.

Dit proefschrift bevat onderzoeksresultaten die behaald zijn in projecten die ik bij Alterra heb uitgevoerd. De mogelijkheid om deze resultaten vast te leggen in dit proefschrift kon slechts gerealiseerd worden dankzij de mogelijkheden die hier door mijn teamleider, Eddy Moors, voor werden gegeven. Ook heb ik van jou geleerd hoe moeilijk het kan zijn om een proefschrift naast je 'normale' werk af te ronden. Daarnaast heb je de gave om altijd motiverend te zijn in welke omstandigheid dan ook.

Dit dankwoord is niet compleet zonder ook Leo Kroon te bedanken. Eén van mijn afstudeeronderwerpen had te maken met RAMS, het model

waarmee in dit proefschrift alle berekeningen zijn gemaakt. De eerste stappen in dit model hebben we ooit samen genomen. Mijn afstudeerverslag bij de vakgroep Meteorologie was het eerste waarin RAMS werd gebruikt en, voor zover ik kan nagaan, is dit ook het eerste proefschrift binnen de vakgroep Meteorologie waarin RAMS is gebruikt.

I want to thank Roger Pielke sr., Bob Walko, Joe Eastman, and, in particular, Craig Tremback. In the course of the past decade I could always ask you questions about RAMS. You were always helpful when I got stuck in the model. I really enjoyed the RAMS workshops which helped in bringing the users of the model together.

Running very complex models is limited by the amount of computer power which is available at the time. This thesis shows results which are obtained on various configurations of computers. I want to express my thanks to the helpdesk facilities of the Earth Simulator Computer (Yokohama, Japan) and SARA (Amsterdam, The Netherlands) which were always willing to assist. It was a privilege, but also a challenge, to compile and execute RAMS on these computers. Het past hier ook om Wietse te bedanken voor alle vragen, makkelijk en moeilijk, die betrekking hadden op het HPC. Je was altijd bereid om een helpende hand te bieden.

The opportunity to use the Earth Simulator Computer, at that time the number one supercomputer in the world, was very special. I want to thank dr. Ryoji Ohba and prof. Toshio Yamagata for giving me this opportunity within the scope of the Saudi Arabia-project. It also gave me the possibility to work in Japan for two stretches of three months and explore the fascinating Japanese culture. I know how hard it was for you to find an apartment for me with a reasonable sized-bed for a 2 meter tall 'giant'.

I had the privilege to work with various researchers in various research projects in the last decade. Special thanks to Gorka Perez Landa, Lieselotte Tolk and Antoon Meesters. It was great to interact with you concerning various modifications in the RAMS model. Geert Lenderink, thanks for your critical view regarding the use of a mesoscale model to simulate coastal showers. Han Dolman, thanks for your refreshing ideas.

To validate a model well-executed observations are essential. I want to thank the following persons who provided these: Fred Bosvelt, Jan Elbers, Holger Fritsch, Beniamino Gioli, Bert Heusinkveld, Wilma Jans, Franco Miglietta, Alex Vermeulen.

Bijzondere dank gaat ook uit naar mijn collega's in Wageningen. Tijdens dit promotie-traject heb ik aardig wat verhuizingen meegemaakt en mede daardoor ook verschillende kamergenoten gehad. Cor (kamergenoot Lumen), je hebt mij altijd scherp weten te houden niet alleen wetenschappelijk maar ook wat betreft het wel en wee van de snooker-wereld. Mijn kamergenoten in de hoekkamer van Atlas (Marleen, Maarten, Michelle, Olaf, Petra, Wietse), de sfeer in de kamer was erg goed, serieus, maar op zijn tijd ook over-gezellig. De laatste jaren was ik minder aanwezig in Wageningen (ouderschapsverlof) maar ben ik altijd met plezier naar Wageningen afgereisd vanuit Enschede. Bart, Jan, Meto, Wilma, Iwan, bedankt dat jullie altijd een luisterend oor zijn geweest, in het Aqua-gebouw en nu in Lumen. Kaj, jij hebt me laten zien dat voetbal toch wel de belangrijkste bijzaak in het leven is. De verschillende 'you tube'-filmpjes tijdens de schrijfweken maakten het schrijven nog leuker, ook dankzij de inbreng van 'mister GVC' Jeroen en Christian. Fulco, je was altijd geïnteresseerd en wist me goed advies te geven in, voor mij, lastig situaties.

Mijn promotie-traject is op te delen in een Wagenings deel en een Enschedees deel. Het Pool-cafe in Wageningen was een ideale plek om de wetenschap goed te bespreken samen met Bas, Roel en Wouter. De vraag was altijd of het spel met of zonder Slurfmans gespeeld zou worden. Samen met Roel en Wouter ook menig dinsdagavond meegedaan aan de pub quiz in, toen nog, café Tuck. Wat als een grapje begon, werd toch serieus. De meest lullige weetjes gingen mijn hersenen bevolken. Frank, de vele films die we hebben gekeken waren op zijn tijd een zeer welkome afwisseling. Inmiddels was ik al naar Enschede verhuisd en heb daar, ondanks de vele reistijd, wel de tijd weten te vinden om met vrienden door te brengen. Mark en Maarten, we moeten echt weer eens naar de Veste gaan of een filmpje te pakken. Reza ('jack in the box', elleboog op tafel), bedankt voor de nodige afleiding die van tijd tot tijd nodig was.

Kaj en Wouter, ik voel me vereerd dat jullie mijn paranymfen zijn.

Mijn schoonfamilie wil ik bedanken voor de interesse die ze altijd hebben getoond in mijn werk. Ook bedankt dat jullie iets vaker op de kinderen hebben kunnen en willen passen in de periode dat ik bezig was met de laatste loodjes van mijn proefschrift.

Dan kom ik aan bij de belangrijkste personen in mijn leven die me altijd gestimuleerd hebben om mijn ambities te verwezenlijken. Mijn ouders wil ik bedanken voor de mogelijkheden en vrijheden die ze me hebben gegeven voor het ontwikkelen van mijn persoonlijkheid. Helaas heeft mijn vader het niet meer mee kunnen maken om zijn zoon hier te zien

staan. Hij zou, net als mijn moeder nu, met trots vervuld zijn. Ook Hester, Arjan en Eljosha wil ik bedanken voor alle steun en interesse die ik van jullie heb gehad.

Als laatste wil ik mijn gezin bedanken. Lieve Jasmijn, bedankt voor de eerlijke en motiverende gesprekken die we gehad hebben. De tijd is nu weer aangebroken dat ik 's avonds weer gezellig bij je kan zitten. Je zult net zo blij zijn als ik dat ik mijn proefschrift nu heb volbracht. Het was niet altijd even makkelijk dat ik mijn vrije dagen moest opofferen. We kunnen nu samen met onze kinderen Marlinde, Romyrle en Silvan volop genieten van elkaar. De kinderen hebben me altijd doen beseffen dat er meer is dan 'alleen' een proefschrift. Ik hou van jullie!

Curriculum Vitae

Hendrikus Wicher (Herbert) ter Maat was born on the 4th of May 1974 in Brummen, The Netherlands. After finishing secondary school in 1993 (Baudartius College, Zutphen), he studied Soil, Water and Atmosphere (specialization Meteorology) at Wageningen University. During his study he started to specialize in land-atmosphere interactions. His MSc-theses dealt with modelling these interactions and how these interactions affect sea breeze development in the Netherlands. He concluded his study with an internship at the University of Idaho in Moscow, USA. Herbert was project researcher in the Columbia Plateau PM10 project (CP3-project) and his task was to simulate windvectors on a very high spatial grid mesh.

After his graduation in from university in 1998, he worked on several air quality projects at the National Institute of Public Health and Environment in Bilthoven, The Netherlands. From September 1999 onwards he has been working as a researcher on land-atmosphere interactions at Alterra in several modelling projects in the Sahel, Amazonia (Brazil), India (Haryana), Bangladesh (Khulna area) and Europe using RAMS, SWAP and SWAPS-C (land surface model with a carbon component). Main aim of these projects was to investigate the interaction between land use and atmosphere related to transport of water, momentum, non-reactive scalar (e.g. CO_2, ^{222}Rn, SF_6). More recent work deals with tailoring climate change scenarios for various sectors (e.g. infrastructure, agriculture). Herbert completed his dissertation in February 2014. He continues his work as researcher at Alterra in Wageningen, The Netherlands.

List of peer-reviewed publications

A.J. Dolman, M. K. van der Molen, **H.W. ter Maat** and R.W.A. Hutjes (2004) The effects of forests on mesoscale atmospheric processes. In Mencuccini, M., Grace J.C., Moncreiff, J.,and McNaughton, K. (eds) "Forest at the Land-Atmosphere Interface"

Ter Maat, H.W., Hutjes, R.W.A., Ohba, R., Ueda, H., Bisselink, B., Bauer, T. (2006) *Meteorological impact assessment of possible large scale irrigation in Southwest Saudi Arabia*. Global And Planetary Change. 54, pp. 183-201.

Sarrat, C., J. Noilhan, A. J. Dolman, C. Gerbig, R. Ahmadov, L. F. Tolk, A. Meesters, R. W. A. Hutjes, **H. W. Ter Maat**, G. Perez-Landa and S. Donier (2007). *Atmospheric CO2 modeling at the regional scale: an intercomparison of 5 meso-scale atmospheric models.* Biogeosciences, 4, pp. 1115-1126.

Jacobs, C.M.J., E.J. Moors, **H.W. Ter Maat**, A.J. Teuling, G. Balsamo, K. Bergaoui, J. Ettema, M. Lange, B.J.J.M. Van Den Hurk, P. Viterbo, W. Wergen (2008) *Evaluation of European Land Data Assimilation System (ELDAS) products using in situ observations*. Tellus A. 60, pp. 1023-1037

Van Pelt, S.C.; Kabat, P.; **Ter Maat, H.W.**; Van den Hurk, B.J.J.M.; Weerts, A.H. (2009) *Discharge simulations performed with a hydrological model using bias corrected regional climate model input*. Hydrology and Earth System Sciences Discussions, 6, 4589-4618

Ter Maat, H.W., R.W.A. Hutjes, F. Miglietta, B. Gioli, F.C. Bosveld, A.T. Vermeulen, H. Fritsch (2010) *Simulating carbon exchange using a regional atmospheric model coupled to an advanced land-surface model*. Biogeosciences, 7, pp. 2397-2417.

Schelhaas M.J., Hengeveld G., Moriondo M., Reinds, G.J., Kundzewicz Z.W., **ter Maat H.W.**, Bindi M., (2010). *Assessing risk and adaptation options to fires and windstorms in European forestry*. Mitigation and Adaptation Strategies for Global Change . DOI 10.1007/s11027-010-9243-0

Stipanovic, I., **H.W. ter Maat**, A. Hartmann, G. Dewulf (2011) *Climate Change and Infrastructure Performance: Should We Worry About?* Procedia - Social and Behavioral Sciences, Volume 48, 2012, Pages 1775-1784

Ter Maat, H.W., E.J. Moors, R.W.A. Hutjes, A.J. Dolman, A.A.M. Holtslag (2013) *Exploring the impact of land cover and topography on rainfall maxima in The Netherlands.* Journal of Hydrometeorology, 14 (2). - p. 524 - 542

Funding

Cover photo: Nationaal Park Dwingelderveld, The Netherlands (by Herbert ter Maat)